The Role of the Human Tau 3'-Untranslated Region in Regulating Tau Expression

Dissertation Advisor: Professor Michael Wolfe John Robert Dickson

The Role of the Human Tau 3'-Untranslated Region in Regulating Tau Expression

Abstract

The microtubule-associated protein tau forms pathological neuronal filaments in Alzheimer's disease (AD) and other neurodegenerative disorders, known collectively as tauopathies. Previous studies in transgenic mouse models of AD suggest that reducing tau expression may be safe and beneficial for the prevention or treatment of AD and possibly other tauopathies. As a first step toward identifying novel therapeutic strategies to reduce tau levels, the studies presented in this dissertation aim to investigate the role of the human tau 3'-untranslated region (3'-UTR) in regulating tau expression. Tau expresses two 3'-UTR isoforms, long and short, as a result of alternative polyadenylation. The exact sequence of these two 3'-UTR isoforms was determined by rapid amplification of cDNA 3'-ends (3'-RACE), and the two 3'-UTR isoforms were cloned into a luciferase reporter vector. Using these reporter constructs, the expression of these isoforms was found to be differentially controlled in human neuroblastoma cell lines M17D and SH-SY5Y by luciferase assays and quantitative PCR (qPCR). Through an unbiased screen of tau 3'-UTR deletions and fragments using luciferase reporter constructs, several regions in the long tau 3'-UTR isoform that contain regulatory *cis*-elements were identified. Additionally, several microRNAs were computationally identified as candidates that might bind the long tau 3'-UTR and thereby differentially control the expression of long versus short tau 3'-UTR isoforms. Screening these candidate microRNAs via luciferase reporter assay identified miR-34a, which was subsequently shown to repress the expression of endogenous tau protein and mRNA in M17D cells using Western blot and qPCR, respectively. Conversely, inhibition of endogenously expressed miR-34 family members leads to increased

endogenous tau expression. Taken together, these studies suggest that the expression of the two tau 3'-UTR isoforms is differentially regulated and that this differential regulation is due to the presence of regulatory *cis*-elements found only in the long tau 3'-UTR isoform, including a binding site for miR-34 family members. Improved understanding of the regulation of tau expression by its 3'-UTR may ultimately lead to the development of novel therapeutic strategies for the treatment of Alzheimer's disease and other tauopathies.

Table of Contents

Acknowledgements

I would like to thank the follow individuals, groups, and programs for their help, encouragement, support, and/or mentorship during the pursuit of my dissertation research:

Dr. Michael Wolfe, Dissertation Advisor

Dr. Stephen Buratowski, Dissertation Advisory Committee Chair

Dr. Paul Anderson, Dissertation Advisory Committee

Dr. Bruce Yankner, Dissertation Advisory Committee

Dr. Rosalind Segal, MD-PhD Advisor

Dr. Ronald Arky, Francis Weld Peabody Society Master

Dr. Mel Feany

Dr. Bradley Hyman

Dr. Matthew Frosch

Members of the Wolfe Lab

Members of the Center for Neurologic Disease

Division of Medical Sciences

Biological and Biomedical Science Program

MD-PhD Program

Dedication

I would like to dedicate this dissertation to the memory of my father, Larry Dean Dickson, whose life provided a great example to me and whose illness and death inspired me to pursue research on the topic of neurodegenerative diseases.

Chapter 1

Introduction

Introduction

The tau protein was initially reported in 1975 as an essential factor for the *in vitro* assembly of tubulin into microtubules (Weingarten, 1975). This protein was given the name of the Greek letter tau (τ) because it causes tubule assembly (Weingarten, 1975). Subsequently, the tau protein was found to form abnormal aggregates in several different neurodegenerative disease, known collectively as tauopathies (Lee et al., 2001). Because of its involvement in microtubule assembly and in neurodegenerative diseases, studying the biology of tau can provide insights into normal cellular physiology and disease pathophysiology.

The Normal Biology of Tau

Tau Gene Structure

Orthologs of the tau gene have been identified in species ranging from humans (*Homo sapiens*) to zebrafish (*Danio rerio*) (Chen et al., 2009); thus, tau is broadly conserved in bony vertebrates (Euteleostomi). The human tau gene, *MAPT* (microtubule-associated protein tau), is located on chromosome 17q21 (Neve et al., 1986) in an area of complete linkage disequilibrium (Baker et al., 1999). As a result, two haplotypes *MAPT* exist: H1 and H2, with H1 being the more common variant. These two haplotypes are defined by a series of single nucleotide polymorphisms (SNPs), as well as a 238 basepair (bp) deletion in intron 9 of the H2 haplotype (Baker et al., 1999). The existence of these two non-recombining haplotypes is explained by a 900 kilobase (kb) inversion polymorphism for chromosome 17q21.31, which contains the *MAPT* gene, as well as several other genes (Figure 1.1) (Stefansson et al., 2005).

The promoter of region of the *MAPT* gene is GC-rich; lacks TATA and CAAT boxes; and contains binding sites for Sp1, AP-2, and additional, as yet unidentified, transcription factors (Andreadis et al., 1996; Heicklen-Klein and Ginzburg, 2000; Sadot et al., 1996). The core

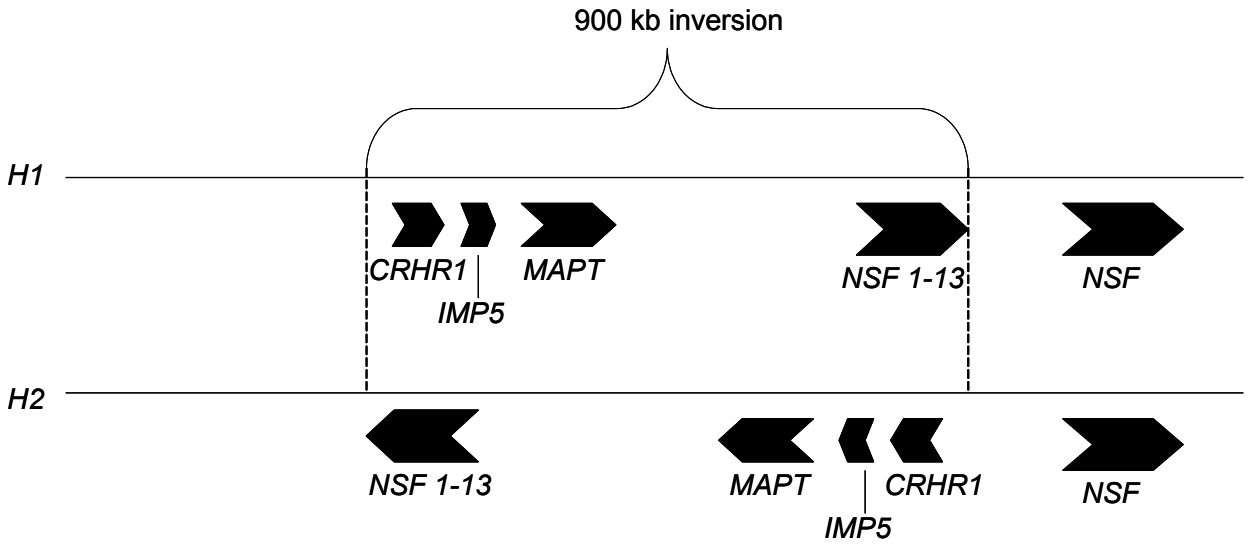

Figure 1.1. H1 and H2 Haplotypes. There is a 900 kb inversion of the H2 haplotype relative to the H1 haplotype. The *MAPT* gene is in this region, along with *CRHR1, IMP5*, and *NSF 1-13*. Adapted from Caffrey and Wade-Martins (Caffrey and Wade-Martins, 2007)66.

promoter, which is active in both neuronal and non-neuronal cell types, is located within nucleotides -302 to +4 relative to the +1 transcription start site (TSS) (Maloney and Lahiri, 2012). Distal regulatory sequences both upstream and downstream of the TSS conferred neuron-specific regulation of expression on the tau promoter (Maloney and Lahiri, 2012).

The *MAPT* gene consists of 16 exons, half of which are alternatively spliced (Figure 1.2), which is discussed in more detail below (Andreadis, 2005). The 5'-untranslated region (5'-UTR) is encoded by exon -1 (Andreadis et al., 1992), and it contains an internal ribosomal entry site (IRES), allowing for 5' cap-independent translation of tau mRNA (Veo and Krushel, 2009; 2012). The coding region is encoded by exons 1 to 13. In humans and rats (*Rattus norvegicus*), intron 13 is retained between exons 13 and 14; thus the 3'-untranslated region (3'-UTR) is comprised of exon 13, intron 13, and exon 14. In mice (*Mus musculus*) and cows (*Bos taurus*), some tau transcripts have been found to have intron 13 spliced out (Himmler, 1989; Poorkaj et al., 2001). The tau 3'-UTR will be discusses in more detail below.

It should be noted that Saitohin (*STH*), a small intronless gene, is encoded entirely within intron 9 of the human *MAPT* gene. The Saitohin protein is 128 amino acids in length and does not share clear homology with other proteins (Conrad et al., 2002). While the function of Saitohin remains an open question, it has been reported to bind tau, peroxiredoxin 6, and c-Abl (Gao et al., 2005; Wang et al., 2011).

Alternative Splicing of Tau

The extensive alternative splicing of tau mRNA allows for the generation of a diversity of tau transcripts. The alternative splicing of tau is spatially and temporally regulated, with (a) characteristic isoform(s) being expressed in a given tissue at a given developmental stage. In some cases, the alternative splicing also appears to be species-specific (Andreadis, 2005).

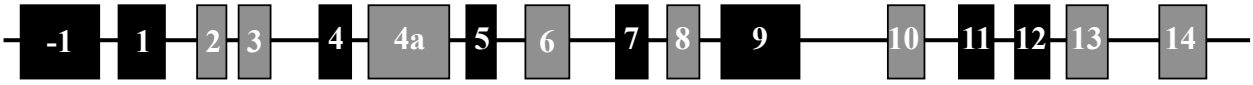

Figure 1.2. General Structure of the *MAPT* Gene. Exons are numbered. Black exons are constitutively expressed. Gray exons can undergo alternative splicing. Adapted from Andreadis (Andreadis, 2005).

The alternative splicing of exons 2 and 3 are related and fall into the category of "augmented combinatorial" alternative splicing (Andreadis, 2005). Exon 3 is only spliced into the transcript if it contains exon 2. Exon 2 may be spliced out (referred to as 0N), exon 2 may be spliced in without exon 3 (referred to as 1N), or exon 2 and exon 3 may be spliced in (referred to as 2N) (Andreadis, 2005; Andreadis et al., 1992). Both exon 2 and 3 are comprised of 87 nucleotides (nt) in humans (Andreadis et al., 1992).

Exon 4A is the largest of the tau exons, with a length of 753 in humans (Andreadis et al., 1992). It is included in tau mRNA in the peripheral nervous system (PNS), retina, and spinal cord, but it is spliced out of tau transcripts in other regions of the central nervous system (CNS) (Couchie et al., 1992; Georgieff et al., 1993). Exon 4A is thought to increase the spacing of microtubules in axons of neurons in which it is expressed (Georgieff et al., 1993)

Exon 6, which is 198 nt long in humans (Andreadis et al., 1992), is included in a minority of tau transcripts; however, it has been detected in fetal brain, skeletal muscle, and spinal cord (Wei and Andreadis, 1998). Inclusion of exon 6 has been found to inhibit neurite elongation in differentiated SH-SY5Y human neuroblastoma cells (Luo et al., 2004a). In addition to the canonical 3'-splice site of exon 6, two cryptic 3'-splice sites exist within exon. Utilization of either of these cryptic 3'-splice sites would result in a frame shift and introduction of premature stop codon in either exon 6 or exon 7, depending on which cryptic 3'-splice site were used (Wei and Andreadis, 1998). One of these truncated tau proteins has been identified *in vivo* (Luo et al., 2004b), and the truncated protein, which lacks the microtubule binding domain, has been found to inhibit polymerization of full-length tau protein *in vitro* (LaPointe et al., 2009).

Exon 8 has not been studied extensively. It is included in some transcripts from cow (Chen et al., 1994; Himmler, 1989) and rhesus macaques (*Macaca mulatta*) (Nelson et al., 1996). However, it has not been found in human tau (Chen et al., 1994).

Exon 10, which is 93 nt long in humans, is a cassette exon that encodes one of four imperfect repeats of the microtubule binding domain of tau; thus, exclusion of exon 10 from the tau transcript results in 3-repeat (3R) tau, whereas inclusion of exon 10 results in 4-repeat (4R) tau (Andreadis et al., 1992; Goedert et al., 1989a; 1989b). Dysregulation of exon 10 has been implicated in disease, which will be discussed in more detail below.

As noted above, in some species intron 13 is retained between exons 13 and 14, while in others it may be spliced out. In rodents, the 3'-splice site for exon 14 has the sequence acagGAA, whereas the corresponding sequence in humans is acaGAA. Thus, unlike rodents, humans lack the cagG consensus sequence of a 3'-splice site at the site where exon 14 should begin, which may explain why splicing out of intron 13 has not been observed in humans (Poorkaj et al., 2001). As a result, the generic mammalian sequences of exon 13, intron 13, and exon 14 all comprise the terminal exon of the human tau gene, which includes the 3'-end of the coding region, the stop codon, and the 3'-UTR. Additionally, multiple 5'-splice sites for exon 13 have been identified in mice and cows (Himmler, 1989; Lee et al., 1988).

Despite the diversity of possible tau transcripts resulting from alternative splicing, six isoforms are predominantly found in the human brain. These isoforms are produced by the alternative splicing of exons 2, 3, and 10, with the possible combinations being 0N3R, 1N3R, 2N3R, 0N4R, 1N4R, and 2N4R (Figure 1.3). The 0N3R isoform predominates in fetal human brain, while all six isoforms are found in adult human brain (Andreadis, 2005; Andreadis et al., 1992).

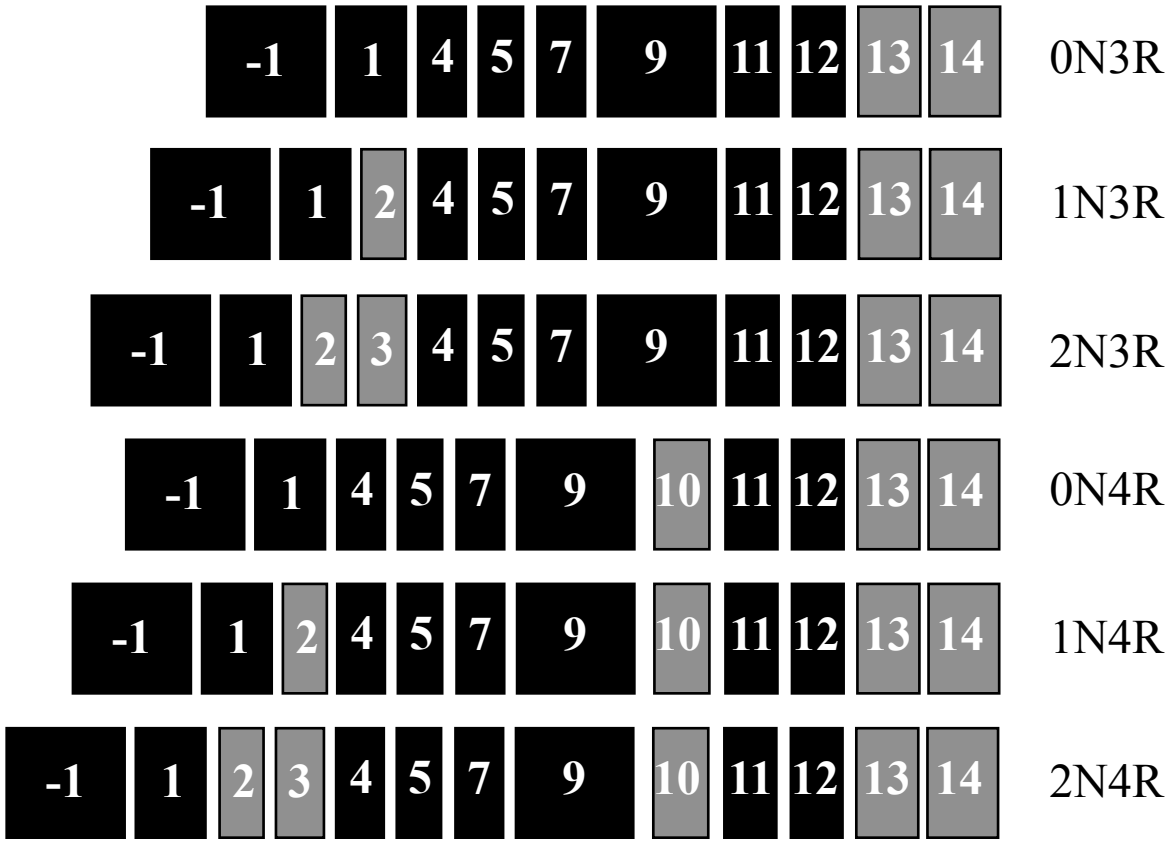

Figure 1.3. The 6 Major Tau mRNA Splice Isoforms in the Adult CNS.

General Tau Expression Patterns

While the expression pattern for some tau splice isoforms is mentioned in the previous section, the general expression patterns for tau will be discussed here. Tau is predominantly expressed in the nervous system; however, tau expression has been detected in several non-neural tissues (Drubin et al., 1986; Gu et al., 1996). In the CNS, two tau transcripts, approximately 2 and 6 kb in length, have been observed (Goedert et al., 1988; Neve et al., 1986; Wang et al., 1993). These transcripts are formed by alternative polyadenylation (APA) of tau mRNA, which produces two 3'-UTR isoforms. The 2 kb transcript corresponds to the short tau 3'-UTR isoform, and the 6 kb transcript corresponds to the long tau 3'-UTR isoform (Poorkaj et al., 2001). In the CNS, the 6 kb transcript tends to be the predominant isoform (Goedert et al., 1988; Wang et al., 1993). In neurons, the 6 kb tau transcript is localized to the axon and soma (Litman et al., 1993; Poorkaj et al., 2001), and tau protein is enriched in axons (Binder et al., 1985; Peng et al., 1986). Although tau is predominantly an axonal protein, it has been found in the nucleus, and it has been hypothesized that there is a link between the 2 kb transcript and nuclear tau (Wang et al., 1993), but no definitive evidence of this has been reported. It should be noted that an approximately 8 kb tau transcript is expressed in the PNS, and it corresponds to transcripts containing exon 4a (Couchie et al., 1992; Goedert et al., 1992).

The Tau 3'-UTR Isoforms

Although it has been known for decades that tau mRNA undergoes APA to produce two 3'-UTR isoform (Goedert et al., 1988; Poorkaj et al., 2001; Wang et al., 1993), no studies specifically addressing the functional consequences of the APA of tau have been reported. However, some regulatory functions of the long tau 3'-UTR isoform in rodents have been

reported. Before the functions of rodent tau 3'-UTR are discussed, a more general overview of 3'-UTR functions is provided.

In general, 3'-UTRs have a variety of functions in regulating gene expression, such as 3'-end processing, translational regulation, stability, and subcellular localization of the transcript (Figure 1.4) (Barrett et al., 2012). These regulatory roles are mediated by the interaction of *cis*-elements in the 3'-UTR and *trans*-factors, which include proteins and microRNAs (miRNAs), in the cell (Chen et al., 2006). An additional level of regulation results from APA, which can occur in transcripts that contain two or more polyadenylation signals (PASs). Transcripts that undergo APA express alternative 3'-UTR isoforms, which can be differentially regulated by either the inclusion or exclusion of regulatory *cis*-elements (Shi, 2012).

The rodent tau 3'-UTR has been shown to play a role in the stability, translational efficiency, and subcellular localization of tau mRNA. Aronov and colleagues identified a U-rich region of the rat tau 3'-UTR that increases the stability of tau mRNA (Aronov et al., 1999), which was later shown to bind the embryonic lethal abnormal vision (ELAV)-like protein HuD (Aranda-Abreu et al., 1999). The insulin-like growth factor mRNA binding protein 1 (IMP-1) and Ras-GTPase-activating protein SH3-domain-binding protein 1 (G3BP-1) were subsequently shown to bind mouse tau mRNA and HuD (Atlas et al., 2004). HuD, IMP-1, and G3BP-1 repress the translation of a luciferase reporter containing the mouse tau 3'-UTR (Atlas et al., 2007). While HuD binds the rat tau 3'-UTR at a U-rich sequence (Aranda-Abreu et al., 1999), IMP-1 binds the mouse tau 3'-UTR at a site distinct from HuD in a sequence-independent manner that may instead depend on a structural feature in the 3'-UTR (Atlas et al., 2007). This is possible, as a sequence-independent, stem-loop-containing regulatory *cis*-element, known as

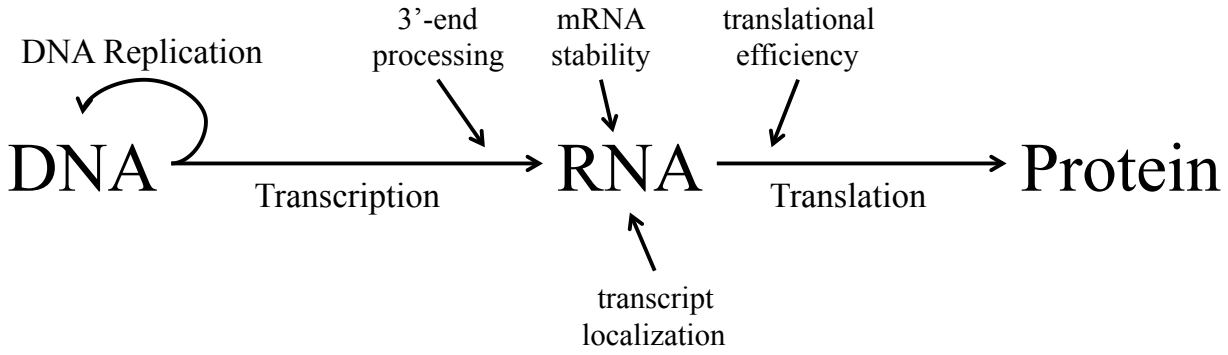

Figure 1.4. Central Dogma in Eukaryotes. Aspects regulated by 3'-UTRs are highlighted.

the stem-loop destabilizing element (SLDE), has been found in the 3'-UTR of interleukin (IL)-2, IL-6, and granulocyte colony-stimulating factor (G-CSF) (Brown et al., 1996).

The rodent tau 3'-UTR is also involved in directing the subcellular localization of tau mRNA. By transfecting primary neurons derived from rat embryos with a reporter plasmid containing different regions of the rat tau 3'-UTR downstream of a reporter gene, Behar and coworkers identified a region of the rat tau 3'-UTR involved in targeting the transcript to the axon (Behar et al., 1995). This region is the same one that stabilizes tau mRNA and binds HuD (Aranda-Abreu et al., 1999; Aronov et al., 1999). It was later shown that HuD and kinesin family member 3A (KIF3A) colocalize in axons of neuronally differentiated P19 rat embryonic carcinoma cell lines with the mRNA of a construct containing green fluorescent protein (GFP) fused to the tau coding region followed by a fragment of the rat tau 3'-UTR containing the axonal localization signal. This study also demonstrated that knocking down KIF3A resulted in neurite retraction and prevented the axonal targeting of tau mRNA (Aronov et al., 2002). Since KIF3A is a microtubule motor protein involved in anterograde axonal transport (Hirokawa, 2000), these data are consistent with the observation that tau mRNA is associated with microtubules in rat primary neuronal cell cultures (Litman et al., 1994).

While the studies discussed above provide insights into the function of the rodent tau 3'-UTR, it is difficult to extrapolate these findings to the human tau 3'-UTR. The U-rich region in the rodent tau 3'-UTR that binds HuD is not well-conserved in humans (Poorkaj et al., 2001). Since the IMP-1 binding site may be a sequence-independent structural feature of the rodent 3'-UTR (Atlas et al., 2007), this would prevent identification of an IMP-1 binding site in humans based on a comparative primary sequence analysis of human and rodent 3'-UTRs. Therefore,

further studies specifically on the human tau 3'-UTR are need to understand its role in regulating tau expression and to identify the *cis*-elements and *trans*-factors involved in this process.

Structure of the Tau Protein

In its native state, soluble tau protein has little, if any, secondary structural features, as determined by circular dichroism spectroscopy (Bergen et al., 2005; Cleveland et al., 1977; Schweers et al., 1994). The N-terminal region of the tau protein, known as the projection domain, mediates interactions between tau and components of the plasma membrane (Brandt et al., 1995) and between tau and Fyn, a Src family tyrosine kinase(Ittner et al., 2010; Lee et al., 1998; 2004). The proline-rich middle of the tau protein, known as the hinge region, has been implicated in influencing microtubule binding (Goode et al., 1997) and regulating neurite elongation (Luo et al., 2004a). The C-terminal region contains the microtubule binding repeats (Himmler et al., 1989; Lee et al., 1989).

Functions of the Tau Protein

Tau was identified as a factor that promoted the assembly of microtubules *in vitro* (Weingarten, 1975). It was later shown to increase microtubule assembly and stability in cells (Drubin and Kirschner, 1986). Since axonal transport occurs along microtubules and since tau bound to microtubules has been shown to block progression of kinesin and dynein along microtubules, tau has been implicated in regulating axonal transport (Dixit et al., 2008). The phosphorylation state of tau regulates its affinity for microtubules, with increased phosphorylation resulting in a decreased affinity (Biernat et al., 1993; Lindwall and Cole, 1984). Alternative splicing also regulates the affinity of tau for microtubules. Tau containing exon 10 (4R tau) has approximately 3-fold higher affinity for microtubules than tau lacking exon 10 (3R tau) (Goode, 2000).

Tau also plays a role in the function of Fyn. Fyn is a non-receptor tyrosine kinase of the Src family that is implicated in signaling processes in a variety of cell types, particularly in the nervous and immune systems (Saito et al., 2010). One notable function of Fyn signaling in the nervous system is the upregulation of *N*-methyl-D-aspartate (NMDA) receptors (NMDARs) (Trepanier et al., 2012). The N-terminus of tau binds Fyn via a PXXP motif in the tau projection domain (Lee et al., 1998), and Fyn phosphorylates tyrosine 18 in the N-terminal region of tau (Lee et al., 2004). Although the tau protein is enriched in axons (Binder et al., 1985; Peng et al., 1986), it has recently been found to play a role in dendrites, in which it targets Fyn to the postsynapse (Ittner et al., 2010). Tau and Fyn also interact in oligodendrocytes, and interrupting their interaction inhibits the outgrowth of oligodendrocyte processes (Klein et al., 2002).

Recently, it was reported that tau possesses intrinsic acetyltransferase activity and that it can catalyze autoacetylation. The catalytic cysteines are apparently located within the microtubule domains (Friedmann et al., 2013). Acetylation of tau has been found to inhibit its ability to promote the assembly and stability of microtubules (Cohen et al., 2011). As this is a new area of investigation, it is not yet clear if tau acetylates other proteins (Friedmann et al., 2013).

Tau in Disease

Alzheimer's Disease

Alzheimer's disease (AD) is a neurodegenerative disease characterized by progressive cognitive decline (Cummings, 2004). It is the most common form of dementia (Jones, 2003), with an estimated 5.2 million Americans suffering from the disease in 2013 (Alzheimer's Association, 2013). Amnestic memory impairment is the most common presenting symptom of AD, but other common symptoms include language deficits (e.g. word-finding difficulty),

visuospatial deficits (e.g. impaired object or face recognition), and executive function deficits (e.g. impaired reasoning or judgment) (McKhann et al., 2011). A possible or probable diagnosis of AD can be made based on the clinical presentation of symptoms; however, a definitive diagnosis of AD requires confirmatory histopathological findings in addition to the clinical diagnosis (Cummings, 2004).

Several neuropathological abnormalities can be found in the brain tissue from AD patients. Two types of abnormal protein aggregates are seen in AD brains: extracellular aggregates known as senile plaques and intracellular aggregates known as neurofibrillary tangles (NFTs) (Hyman et al., 2012). Characteristic patterns for the deposition of these aggregates over the course of the disease have been described (Braak and Braak, 1991). While there is some inter-individual variation, the progression of senile plaque deposition is classified according to three stages. In stage A, senile plaques are present at low density in the isocortex. In stage B, plaques are present at moderate density in the isocortex and at a low density in the hippocampus. In stage C, the isocortex has a high density of senile plaques, with a similar plaque burden in the hippocampus as in stage B. Also in stage C, senile plaques begin to be found in subcortical structures (Braak and Braak, 1991). A more consistent pattern of progression over the course of the disease is seen for NFTs, allowing for a delineation of six stages. However, these stages can be categorized into three groups, each containing two stages that share similar features. For simplicity, the stages will be presented in the three groups here. In the transentorhinal stages (stages I and II) the transentorhinal region, which is transition zone between the entorhinal cortex and the temporal isocortex, is preferentially affected with NFTs, with mild involvement of the hippocampus. In the limbic stages (stages III and IV), the involvement of the transentorhinal region and entorhinal cortex have progressed, a mild-to-moderate NFT burden is found in the

hippocampus, and the isocortex is mildly affected. The isocortical stages (stages V and VI) show marked involvement of the entorhinal cortex and hippocampus, isocortical NFTs are a prominent feature, and NFTs are found in subcortical structures (Braak and Braak, 1991). Interestingly, the burden of NFTs but not senile plaques is associated with AD severity (Bierer et al., 1995). In addition to these two protein aggregates, other pathological changes can been seen in the gross and histopathological examination of AD brains, including atrophy, neuron loss, synapse loss, and gliosis (Hyman et al., 2012).

Through the purification and sequencing of senile plaques, the major component of these protein aggregates was found to be a 4 kDa peptide that became known as the amyloid β (Aβ) peptide (Masters et al., 1985). It was later recognized that Aβ was a fragment of a larger transmembrane protein, which was called the amyloid precursor protein (APP), encoded by the *APP* gene on human chromosome 21 (Goldgaber et al., 1987; Kang et al., 1987; Robakis et al., 1987; Tanzi et al., 1987). Of note, individuals with trisomy 21, also known as Down's syndrome, are at an increased risk of developing AD (Visootsak and Sherman, 2007). Eventually, causative mutations in the *APP* gene were discovered in cases of familial AD (Goate et al., 1991; Hendriks et al., 1992; Mullan et al., 1992). Additional familial AD mutations were identified in members of the presenilin family, *PSEN1* and *PSEN2* (Levy-Lahad et al., 1995a; 1995b; Rogaev et al., 1995; Sherrington et al., 1995). Either PSEN1 or PSEN2 can serve as the catalytic subunit of the γ-secretase complex, which is involved in the proteolytic processing of APP to Aβ (Kimberly et al., 2000; Wolfe et al., 1999).

As with senile plaques, efforts were made to identify the components of NFTs, and these studies revealed tau to be the major protein in these aggregates (Delacourte and Defossez, 1986; Grundke-Iqbal et al., 1986; Kosik et al., 1986; Nukina and Ihara, 1986; Wood et al., 1986).

Another notable finding from examining NFTs, is that the tau contained within them is hyperphosphorylated (Morishima-Kawashima et al., 1995). Unlike the case with the Aβ, no mutations related to tau have been found in familial AD.

The fact that causative mutations in *APP*, *PSEN1*, and *PSEN2* were found in cases of familial AD and that individuals with trisomy 21, in which three copies of the *APP* gene are present, are at a higher risk for developing AD suggests a key role for Aβ in the development of AD. This led to the development of the amyloid cascade hypothesis, which states that the deposition of Aβ is the initial insult in the pathogenesis of AD. In this hypothesis, other events involved in AD, such as NFT formation and neuronal loss, occur downstream of Aβ deposition in the cascade (Hardy and Higgins, 1992). While the amyloid cascade hypothesis suggests that Aβ and tau participate in the same pathogenic pathway in AD, the precise molecular mechanisms that link the dysregulation of Aβ and tau have yet to be elucidated. However, some studies have shown that Aβ can induce hyperphosphorylation and/or proteolytic cleavage of tau, so these processes may be involved (Wolfe, 2012). Identifying the relationship between Aβ and tau in AD pathogenesis remains one of the key open questions in the field of neurodegeneration. In addition to the amyloid cascade hypothesis, other hypotheses for the pathogenesis of AD have been proposed, for example an axonal transport impairment hypothesis (Saper et al., 1987) or the tau axis hypothesis (Ittner and Götz, 2010). However, the amyloid cascade hypothesis is currently the most widely accepted hypothesis for AD pathogenesis.

Although alterations in tau are not considered to be an initial event in the pathogenesis of AD, mounting evidence suggests it is a key player in the pathophysiology of AD. Cultured hippocampal neurons from homozygous tau knockout mice failed to develop the Aβ-induced cytotoxicity (Rapoport et al., 2002) and axonal transport defects (Vossel et al., 2010) seen in

wild-type hippocampal neurons. Similarly, knock out of tau in APP/PSEN1 transgenic mouse models of AD results in improved learning and/or memory (Ittner et al., 2010; Leroy et al., 2012; Roberson et al., 2007), increased survival (Ittner et al., 2010; Leroy et al., 2012; Roberson et al., 2007), and reduced excitotoxicity (Ittner et al., 2010; Roberson et al., 2007) compared with littermates with wild-type tau. Ittner and colleagues provided mechanistic insights as to the reason for these findings by showing that loss of tau prevented tau from targeting Fyn to the postsynape, which decreased phosphorylation of NMDARs and reduced excitotoxicity (Ittner et al., 2010). Several tau knockout mouse strains have been generated, and they have a surprisingly normal phenotype (Ke et al., 2012). However, in one strain, aged tau knockout mice did develop muscle weakness, hyperactivity in a new environment, and impaired contextual fear conditioning (Ikegami et al., 2000). Since a reduction in tau levels can prevent Aβ-induced toxicity and since most tau knockout mouse strains have a normal phenotype, a reduction of tau expression may be an effective therapeutic strategy for treating AD.

Frontotemporal Lobar Degeneration

Frontotemporal lobar degeneration (FTLD) is a term that describes the heterogeneous clinical and neuropathological entities that possess the common phenotype of neurodegeneration in the frontal and temporal cortices of the brain. As a result of the brain regions affected, common symptoms include behavioral changes, impairment of executive function, and language deficits (Seltman and Matthews, 2012). FTLD can be subdivided into three main clinical syndromes based on the prominent early feature in that syndrome. The behavioral variant frontotemporal dementia (bvFTD) is characterized by changes in behavior and loss of executive function due to frontal lobe atrophy. Semantic dementia (SD) is characterized by deficits in semantic knowledge due to anterior temporal lobe atrophy (left-sided atrophy is more

pronounced than on the right). Progressive non-fluent aphasia (PNFA) is associated with left peri-sylvian atrophy, which results in deficits in expressive or motor speech (Neary et al., 1998; Seltman and Matthews, 2012). In addition to these "pure" cases of FTLD, there is significant clinical, neuropathological, and genetic overlap with other neurodegenerative diseases: amyotrophic lateral sclerosis (ALS), progressive supranuclear palsy (PSP), and cortiobasal degeneration (CBD) (Seltman and Matthews, 2012).

Neuropathological examination of the brain of a patient with FTLD typically shows neuronal loss in the affected area, which may be accompanied by white matter myelin loss and/or astrocytic gliosis. Abnormal intracellular protein aggregates are also a hallmark of FTLD, but the specific nature of the aggregate depends on the neuropathological subtype of FTLD (Cairns et al., 2007).

One of the intraneuronal pathological aggregates that occurs in FTLD is called a Pick body, which was first described by Alois Alzheimer and is named after Arnold Pick, the first to describe clinical cases of frontal and temporal lobe atrophy that are now considered in the FTLD spectrum. Pick's disease was a term that was formerly used to describe cases that are now included in the bvFTD category, and Pick bodies were seen in brains of patients with Pick's disease (Seltman and Matthews, 2012). Pick bodies were eventually shown to contain tau protein (Murayama et al., 1990), particularly 3R tau that lacks exon 10 (Delacourte et al., 1998). Thus, one of the main neuropathological subtypes of FTLD is classified as tau-positive FTLD (FTLD-tau) (Mackenzie et al., 2009).

In a familial subtype of FTLD known as frontotemporal dementia with parkinsonism linked to chromosome 17 (FTDP-17) (Foster et al., 1997), causative mutations in the *MAPT* gene were identified (Hutton et al., 1998; Poorkaj et al., 1998; Spillantini et al., 1998). Over three

dozen tau mutations have described, and they tend to cluster in the C-terminal microtubule binding region. Some of these mutations affect exon 10 splicing, some decrease the affinity of tau for microtubules, and others make tau more aggregation prone (Wolfe, 2008). The presence of tau mutations in cases of FTDP-17, together with the evidence discussed above for its role in AD, strongly suggests tau can play a critical, and sometimes even causative, role in neurodegeneration.

Besides tau, other protein aggregates are seen in FTLD. In some cases of FTLD and ALS, the aggregates are composed of TAR DNA-binding protein of 43 kDa (TDP-43) (Arai et al., 2006; Neumann et al., 2006). These cases are classified as TDP-43-positive FTDL (FTLD-TDP) (Mackenzie et al., 2009). TDP-43 is an RNA-binding protein that is implicated in a variety of RNA-related processes, including splicing, mRNA stability, and mRNA trafficking. A variety of mutations in TDP-43 have been described in cases of FTLD and ALS (Lee et al., 2011). In other cases of FTLD and ALS, aggregates are composed of the fused in sarcoma (FUS) protein (Kwiatkowski et al., 2009; Neumann et al., 2009). These cases are classified as FUS-positive FTLD (FTLD-FUS) (Seltman and Matthews, 2012). Like TDP-43, FUS is an RNA-binding protein involved in several aspects of RNA metabolism (Baloh, 2012). Together, FTLD-tau, -TDP, and -FUS, make up a majority of the FTLD cases. However, there are other cases of FTLD that are classified as ubiquitin proteasome system-positive (FTLD-UPS), type IV intermediate filament-positive (FTLD-IF), or no inclusion (FTLD-ni) (Mackenzie et al., 2009; Seltman and Matthews, 2012).

Progressive Supranuclear Palsy

Progressive supranucelar palsy (PSP) is a neurodegenerative tauopathy that can present as a heterogeneous set of clinical syndromes. The classic symptoms of PSP present in what is

known as Richardson's syndrome and include supranuclear gaze palsy, parkinsonism, and postural instability. PSP is named for the characteristic supranuclear gaze palsy finding, which prevents downward gaze. Unlike in Parkinson's disease, the parkinsonian symptoms in PSP respond minimally with levodopa therapy (Boeve, 2012). The neuropathological findings in PSP include tau-containing NFTs, neuronal loss, and gliosis primarily in the basal ganglia, diencephalon, and brain stem (Dickson et al., 2010). In PSP, an increase in the tau 4R/3R ratio has been noted (Takanashi et al., 2002). While no causative genetic mutations have been linked to PSP, the H1 haplotype of the *MAPT* gene confers an increased risk of developing PSP (Pittman, 2005).

Corticobasal Degeneration

Like PSP, corticobasal degeneration (CBD) is a neurodegenerative tauopathy that can have a variety of clinical presentations. It is also referred to as corticobasal syndrome (CBS) to reflect that fact. In addition to this heterogeneity within the disease, there is significant overlap in symptoms with other neurodegenerative diseases, such as FTLD and PSP. Common symptoms of CBD include parkinsonism with a mild-to-moderate response to levodopa, apraxia, alien limb phenomenon, language impairment, and cognitive impairment (Armstrong et al., 2013). Tau-positive inclusions are seen in neurons, oligodendricytes, and astrocytes in the frontal and parietal cortices, as well in as the basal ganglia (Dickson et al., 2002). Like PSP, an increased tau 4R/3R ratio is seen in CBD (Takanashi et al., 2002), and the H1 haplotype of the *MAPT* gene is associated with an increased risk of developing CBD (Pittman, 2005).

Other Tauopathies

There are a number of additional tauopathies, and it is impossible to adequately discuss all of them here. Instead, a few general principles will be mentioned. In some tauopathies, tau

aggregates are the predominant neuropathological feature, while in others, additional types of aggregates may be found. While tau's mechanistic role in the pathogenesis of some tauopathies, particularly AD and FTLD-tau, is becoming clearer, it is unclear if and how tau contributes to the development of other tauopathies. What is clear, however, is that tau aggregation is a commonality among a number of neurodegenerative disorders (Lee et al., 2001).

Summary

The microtubule associated protein tau has important physiological functions, including promoting microtubule assembly and stability (Drubin and Kirschner, 1986; Weingarten, 1975) and dendritic targeting of Fyn to the postsynapse (Ittner et al., 2010). Additionally, tau is implicated in a number of neurodegenerative diseases, which are known as tauopathies (Lee et al., 2001). Tau plays a critical role in the pathogenesis of AD (Ittner et al., 2010; Leroy et al., 2012; Roberson et al., 2007) and FTDP-17 (Hutton et al., 1998; Poorkaj et al., 1998; Spillantini et al., 1998). As a result, many aspects of tau biology have been studied extensively. One aspect of tau biology that has been relatively understudied, especially in humans, is the role of its 3'-UTR in regulating tau expression. A more complete understanding of the function of the human tau 3'-UTR will provide insights into the basic biology of tau. Additionally, it may aid in the identification of novel therapeutic strategies to reduce tau expression in AD and other tauopathies. Therefore, the studies presented in this dissertation aim to investigate the role of the human tau 3'-UTR in regulating tau expression.

Chapter 2

Alternative Polyadenylation of Tau mRNA Regulates Tau Expression

Experimental contributions to this chapter: John Dickson performed the 3'-RACE, cloning, transfections, dual luciferase assays, and qPCR. Rachel Moda, an undergraduate student at Harvard College, Cambridge, MA, assisted with performing site-directed mutagenesis under the supervision of John Dickson.

Introduction

The presence of multiple functional PASs at the 3'end of a gene allows for APA to occur, which produces alternative 3'-UTR isoforms. Since different 3'-UTR isoforms may include or exclude certain regulatory *cis*-elements, APA is a mechanism of regulating gene expression (Shi, 2012). The tau gene, *MAPT*, contains two PASs in tandem, separated by approximately 4,000 nt. Thus, tau can undergo APA to produce a short 3'-UTR isoform that is approximately 2 kb in length and a long 3'-UTR isoform that is approximately 6 kb in length (Poorkaj et al., 2001). Despite the recognition that APA of tau occurs, there are no reports of the functional significance of the APA of tau. The goals of the experiments presented in this chapter are to explore the role APA plays in regulating tau expression.

Methods

3'-RACE

Rapid Amplification of cDNA 3'-Ends (3'-RACE) was performed on human frontal cortex total RNA (Agilent Technologies) with the FirstChoice RLM-RACE Kit (Life Technologies) using primers targeting the short and long human tau 3'-UTR isoforms (Table 2.1). An overview of the 3'-RACE protocol is provided in Figure 2.1. The FirstChoice RLM-RACE Kit contains the reverse transcriptase, 3'-RACE adaptor, adaptor primer, heat-stable DNA polymerase, and buffers used in the 3'-RACE protocol. The 3'-RACE products were subjected to agarose gel electrophoresis and gel extraction as described below. The purified 3'-RACE products were sequenced and aligned with human *MAPT* using ClustalW (Larkin et al., 2007).

Cell Culture

All cells were cultured at 37 ºC in a 5% CO_2 atmosphere. Primary human neonatal dermal fibroblasts (ATCC) were cultured in Fibroblast Basal Medium (a proprietary formulation

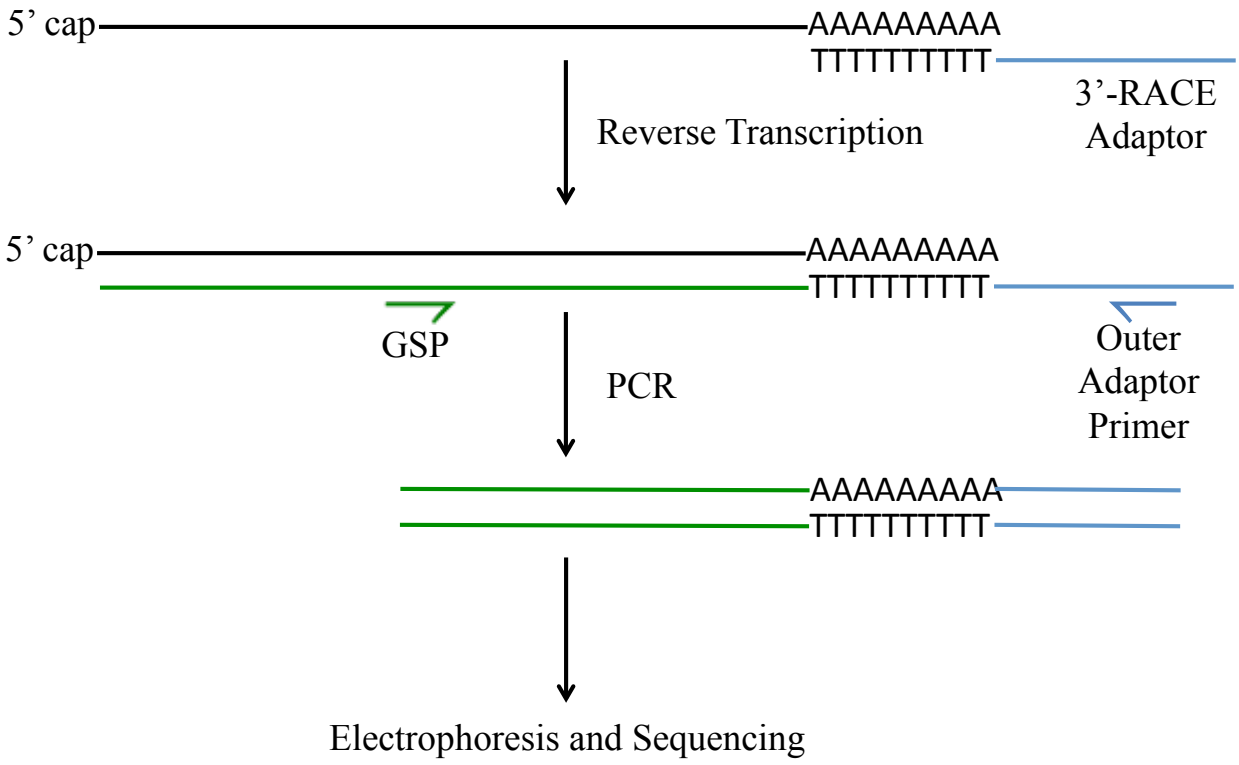

Figure 2.1. General Overview of the 3’-RACE Protocol. GSP stands for gene specific primer.

Table 2.1. Primers for 3'-RACE.

Purpose	*Location*	*Orientation*	*Sequence (5' to 3')*
3'-RACE Reverse Transcription Adaptor	Poly(A) Tail	Reverse	GCGAGCACAGAATTAATACGACTCACTATAGG-$(T)_{12}$-VN
3'-RACE Outer Primer	3'-RACE Adaptor	Reverse	GCTGATGGCGATGAATGAACACTG
Short Tau 3'-UTR Primer	Tau 3'-UTR 112-134	Forward	TCGGTTAATTGGTTAATCACTTA
Long Tau 3'-UTR Primer	Tau 3'-UTR 3531-3550	Forward	CCACTGACAGGCTTTCCCAG

of amino acids, vitamins, other organic compounds, trace minerals and inorganic salts designed to support fibroblast growth) supplemented with Fibroblast Growth Kit—Low Serum (ATCC). The Fibroblast Growth Kit—Low Serum adds the following components to the Fibroblast Basal Medium to achieve the final concentrations given: L-glutamine (7.5 mM), rh FGF beta (5 ng/mL), rh Insulin (5 µg/mL), hydrocortisone (1 µg/mL), ascorbic acid (50 µg/mL), fetal bovine serum (FBS, 2%). M17D human neuroblastoma cells (kind gift of Dennis Selkoe) and Human Embryonic Kidney (HEK) 293 cells (ATCC) were cultured in Dulbecco's Modified Eagle Medium (DMEM, Life Technologies) supplemented with 10% heat-inactivated FBS (Sigma-Aldrich) and L-glutamine (Life Technologies). SH-SY5Y human neuroblastoma cells were cultured in 1:1 Eagle's Minimal Essential Medium (EMEM): Ham's F-12 Medium (Sigma-Aldrich) supplemented with 10% FBS (ATCC). SH-SY5Y cells were differentiated using a modified version of a previously published protocol (Encinas et al., 2000). Briefly, SH-SY5Y cells were plated on fibronectin-coated plates (BD-Biosciences) and treated with 10 µM retinoic acid (Sigma-Aldrich) in 1:1 EMEM:Ham's F-12 Medium supplemented with 10% FBS for 7 days. The SH-SY5Y cells were then treated with 50 ng/mL brain-derived neurotrophic factor (BDNF, Life Technologies) in 1:1 EMEM:Ham's F-12 Medium (without FBS) for 3 days.

Isolation of genomic DNA

Genomic DNA was isolated from primary human neonatal dermal fibroblasts using the DNeasy Tissue Kit (Qiagen) according to the manufacturer's instructions. Briefly, cells are lysed with Proteinase K, and the lysate is added to a spin column containing a silica-based membrane that adsorbs DNA at high concentrations of chaotropic salts. The DNA can be conveniently washed to remove impurities while adsorbed to the membrane. The purified DNA is then eluted from the column in a low-salt buffer or water.

Polymerase Chain Reaction (PCR)

The wild-type human tau 3'-UTR sequence was amplified from genomic DNA derived from primary human neonatal dermal fibroblasts by PCR using KAPA HiFi HotStart ReadyMix (Kapa Biosystems) according to the manufacturer's instructions, with an annealing temperature of 65 ºC. KAPA HiFi HotStart ReadyMix is a high-fidelity heat-stable DNA polymerase that comes in a convenient format with the polymerase, buffer, and deoxyribonucleotide triphosphates (dNTPs) premixed into a master mix. Template DNA, forward and reverse primers, and water to bring the components to the final concentration are added to this master mix, which is then subjected to 25 cycles of PCR with denaturation, annealing, and extension steps. The resulting cloned construct from this DNA (described below) served as a template for PCR of the short tau 3'-UTR isoform. The primers used for PCR are listed in Table 2.2.

Restriction Digest of the pmirGLO Vector

The pmirGLO Dual-Luciferase miRNA Target Expression Vector (Promega) is a luciferase reporter vector that contains the firefly luciferase coding region, the expression of which is driven by the human phosphoglycerate kinase promoter. Located 3' of the stop codon of the firefly luciferase coding region is a multiple cloning site containing several unique

Table 2.2. Primers for PCR of Full-Length Wildtype and Short Tau 3'-UTR Sequences.

Construct	*Tau 3'-UTR Location*	*Orientation*	*Sequence (5' to 3')*
Tau3UTR_WT	1-15	Forward	GCTCGCTAGCCTCGAGTCAGGCCCCTGGGGC
Tau3UTR_WT	4451-4465	Reverse	ATGCCTGCAGGTCGACTGGTGCCGGTCTTGC
Tau3UTR_short	1-15	Forward	GCTCGCTAGCCTCGAGTCAGGCCCCTGGGGC
Tau3UTR_short	223-256	Reverse	ATGCCTGCAGGTCGACTGAATGTTTTTTTTTAAA TATTTTATTACTAGCC

restriction sites that can be used for cloning inserts into that region. Sequences cloned into the multiple cloning site are included in the 3'-UTR of the reporter gene. Thus, this luciferase reporter is useful in studying the function of 3'-UTRs from genes of interest. Also included in the pmirGLO vector is a completely different luciferase gene, that of the *Renilla* luciferase, the expression of which is driven by the SV40 early enhancer/promoter. The *Renilla* luciferase expression is not influenced by the sequence cloned into the multiple cloning site; thus, it serves as a normalization control for transfection efficiency. The vector also contains an ampicillin resistance gene for selection in bacteria.

The pmirGLO vector was subjected to a double digest by the restriction endonucleases *XhoI* and *SalI* (New England Biolabs) in 1X Buffer 3 (New England Biolabs) and 1X bovine serum albumin at 37ºC overnight.

Agarose Gel Electrophoresis

DNA was subjected to agarose gel electrophoresis using 0.8% (for large DNA fragments) to 2% (for small DNA fragments) agarose gel in 1X Tris-Acetate-EDTA (TAE) buffer (Life Technologies) at a constant voltage of 110V. DNA bands were stained with ethidium bromide

(Sigma-Aldrich) or SYBR Safe DNA Gel Stain (Life Technologies) and visualized under ultraviolet (UV) illumination.

Gel Extraction of DNA

DNA bands were cut out of the agarose gel and gel extracted using the NucleoSpin PCR Clean-Up and Gel Extraction kit (Macherey-Nagel) according to the manufacturer's instructions. This DNA purification kit works by a similar principle as the DNeasy Tissue Kit.

Cloning

The desired sequences were inserted into the pmirGLO vector between the *XhoI* and *SalI* restriction sites using the In-Fusion HD EcoDry Cloning Kit (Clontech) according to the manufacturer's instructions. The In-Fusion HD EcoDry Cloning Kit includes an enzyme that possesses 3'-to-5' exonuclease activity that generates approximately 15 bp of a ssDNA overhang at the 5'-end of linear dsDNA. If different strands of dsDNA have complementary ends, they can anneal at the 5'-overhangs. For In-Fusion cloning, inserts are amplified by primers that include 15 bp of homology with the desired sites in the multiple cloning site of the vector. The vector is linearized at these sites (e.g. by restriction digest), and the vector and insert are combined the presence of the In-Fusion enzyme. The DNA fragments are initially associated non-covalently by base-pairing interactions. The associated DNA fragments are ligated to form the final desired vector in bacteria following transformation of the bacteria with the DNA (Irwin et al., 2012).

Transformation of Bacteria

The In-Fusion cloning mixture (2.5 μL) was used to transform 20 μL of XL10-Gold Ultracompetent Cells (Agilent Technologies), which are bacteria that can be transformed with high efficiency, according to the manufacturer's instructions, except that 0.8 μL of β-

mercaptoethanol was used per 20 µL of cells. Briefly, XL10-Gold cells are incubated with β-mercaptoethanol and DNA from the In-Fusion reaction. The XL10-Gold cells are then heat-shocked at 42 ºC for 30 sec to induce them to take up the DNA. They are allowed to recover on ice for 2 min, and then they are incubated in SOC medium (Life Technologies) for 1 h at 37 ºC. Of the final transformation mixture, 200 µL was plated on imMedia Amp Agar (Life Technologies) ampicillin-containing LB-agar plates and incubated at 37 ºC overnight to allow for colony growth.

Plasmid Preparation

A transformed bacterial colony was used to inoculate 3 mL LB medium (MP Biomedicals) containing ampicillin (Sigma-Aldrich) at a concentration of 50 µg/mL. The miniprep culture was incubated at 37 ºC overnight while shacking at 250 rpm. Following the incubation, 1.5 mL of the culture was stored at 4 ºC for future use, and the other 1.5 mL of the culture was subjected to centrifugation at 11,000 × *g* for 30 s. A miniprep purification was performed on the cell pellet using the NucleoSpin Plasmid QuickPure kit (Macherey-Nagel), which purifies DNA in manner similar to the DNeasy Tissue Kit described above, according to the manufacturer's instructions. The purified plasmids were sequenced using the Genewiz sequencing service to confirm successful cloning. In order to obtain a larger quantity of plasmid DNA for future experiments, a midiprep culture of 80 mL LB medium containing ampicillin at a concentration of 50 µg/mL was inoculated with 1.5 mL of the reserved miniprep culture and incubated at 37 ºC overnight while shacking at 250 rpm. Following the incubation, the culture was subjected to centrifugation at 5,000 × *g* for 15 min at 4 ºC. A midiprep purification was performed on the cell pellet using the NucleoBond Xtra Midi Plus EF kit (Macherey-Nagel),

which purifies DNA in manner similar to the DNeasy Tissue Kit described above, according to the manufacturer's instructions.

Site-Directed Mutagenesis

Site-directed mutagenesis was performed using the QuikChange Lightning Site-Directed Mutagenesis Kit (Agilent Technologies), according to the manufacturer's instructions. Briefly, PCR is performed on the desired circular vector with primers containing the desired mutation. The PCR replicates both strands of the vector, except that the strands produced by PCR contain the desired mutation. The two strands can anneal, but contain a nick on each strand. Thus, a mutated circular piece of DNA with offset ssDNA nicks present on either strand is produced. The original (unmutated) template vector, which was originally purified by midiprep purification from bacteria, had undergone DNA methylation in the bacteria. However, the new mutated vector produced by PCR is not methylated. The original template vector can be digested by the restriction enzyme *DpnI*, which digests only methylated DNA, leaving the new mutated vector intact. The mutated vector is transformed into XL-10 Gold cells as described above, and the ssDNA nicks are ligated in the bacteria. Primers used for site-directed mutagenesis are listed in Table 2.3.

Table 2.3. Primers for Site-Directed Mutagenesis of the Proximal PAS in the Human Tau 3'-UTR.

Construct	*Orientation*	*Sequence (5' to 3')*
Tau3UTR_long	Forward	TTTCCAAATTGATGGGTGGGCTAGTAATCAAATATTTAAAAAA AAACATTCAAAAACA
Tau3UTR_long	Reverse	TGTTTTTGAATGTTTTTTTTTAAATATTTGATTACTAGCCCACC CATCAATTTGGAAA

Transfection of Cultured Cells

M17D and HEK 293 cells were transfected at 80-90% confluency using Lipofectamine 2000 (Life Technologies), and differentiated SH-SY5Y cells were transfected at 80-90%

confluency using Lipofectamine LTX (Life Technologies) according to the manufacturer's protocols. Plasmids were transfected at 1 μg per well of a 24-well plate.

Dual Luciferase Assay

Firefly and *Renilla* luciferase activity was determined using the Dual-Luciferase Reporter Assay System (Promega), which uses luciferin as a substrate for firefly luciferase, and coelenterazine as a substrate for *Renilla* luciferase, according to the manufacturer's instructions. Luminescence signal was measured using a Synergy H1 Hybrid Multi-mode Microplate Reader (BioTek).

Total RNA Isolation

Total RNA was isolated using the Nucleospin RNA II kit (Macherey-Nagel), according to the manufacturer's protocol. The RNA isolation by the Nucleospin RNA II kit works according to a similar principle to that of the DNeasy Tissue Kit described above, except that RNA is adsorbed to the membrane instead of DNA. The total RNA was DNaseI-treated using the TURBO DNA-free Kit (Life Technologies) to remove any contaminating DNA.

Quantitative PCR

RNA was reverse transcribed to cDNA using Double Primed RNA to cDNA EcoDry Premix (Clontech) according to the manufacturer's instructions. Quantitative PCR (qPCR) was performed using TaqMan chemistry (Life Technologies) using the absolute quantification method of analysis on the ViiA 7 Real-Time PCR System (Life Technologies). In qPCR using TaqMan chemistry, a modified PCR reaction is performed. In addition the forward and reverse primers used in traditional PCR, a third oligonucleotide, known as the TaqMan probe, is used. The TaqMan probe anneals to the target DNA sequence between the forward and reverse primers. A fluorophore is covalently attached to the 5'-end of the TaqMan probe, while a

quencher is attached to the 3'-end of the probe. The fluorphore and quencher are in close proximity while attached to the probe, and the quencher quenches the fluorescence of the fluorophore. The heat-stable Taq DNA polymerase used in the qPCR reaction has intrinsic 5'-to-3' exonuclease activity, and when it encounters the TaqMan probe annealed to the template as the polymerase is replicating the DNA in the 5'-to-3' direction, the 5'-to-3' exonuclease activity of the polymerase degrades the TaqMan probe, releasing the fluorophore and quencher into the solution. No longer covalently attached by the probe, the fluorophore and quencher are no longer in sufficient proximity for the fluorescence to be quenched. The fluorescence signal from the fluorphore can then be detected by the qPCR instrument. The fluorescence signal is proportional to the amount of DNA template present in the reaction. A variety of methods for analyzing the qPCR results have been developed. In these studies, the absolute quantification method was used. A serial dilution of a DNA standard of known copy number is included on the qPCR plate for each probe used. From this, a standard curve can be generated to allow the determination of the target copy number in the unknown samples. The pmirGLO vector was used as a standard for the firefly luciferase gene *luc2* and the *Renilla* luciferase gene *hRluc*. Custom TaqMan probes (Life Technologies) were designed for the *luc2* and *hRluc* genes in the pmirGLO vector (Table 2.4).

Statistical Analysis

Data are presented as a mean of biological replicates, and variation is indicated as the SEM. Comparisons were conducted using a one-way ANOVA followed by a Tukey test to correct for multiple comparisons.

Table 2.4. Custom TaqMan Gene Expression Assay Probes.

Target	*Oligonucleotide Type*	*Sequence (5' to 3')*
Firefly luciferase (*luc2*)	Forward Primer	GCGCAGCTTGCAAGACTATAAG
	Reverse Primer	TTGTCGATGAGAGTGCTCTTAGC
	TaqMan Probe	CTGGTGCCCACACTAT
Renilla luciferase *(hRluc*)	Forward Primer	CCTCCTGGATCACTACAAGTACCT
	Reverse Primer	GTGGCCCACAAAGATGATTTTCT
	TaqMan Probe	CAGCAGCTCGAACCAA

Results

In order to define the 3'-ends of the human tau 3'-UTR isoforms, total RNA from human frontal cortex was subjected to 3'-RACE. The 3'-RACE products were sequenced and aligned with the human *MAPT* gene to identify the site where cleavage and polyadenylation occur for each isoform. The short 3'-UTR isoform is 256 nt long beginning at the first nucleotide after the stop codon, has a canonical AATAAA PAS, and has a canonical CA cleavage site (Figure 2.2A). The long tau 3'-UTR isoforms is 4163 nt in length, has a canonical AATAAA PAS, and has a non-canonical TA cleavage site (Figure 2.2B). These data were used to clone the wild-type and short tau 3'-UTR sequences into the pmirGLO luciferase reporter construct. A construct that expresses the long only tau 3'-UTR was made by mutating the proximal tau PAS (A233C) in the wild-type tau 3'-UTR constructs so that cleavage and polyadenylation do not occur at this site. A schematic of these constructs is shown in Figure 2.2C.

These constructs were used to investigate the potential role of alternative polyadenylation in regulating tau expression. As a pilot experiment, the empty pmirGLO vector, the wild-type tau 3'-UTR construct (Tau3UTR_WT), the short tau 3'-UTR construct (Tau3UTR_short), or the long tau 3'-UTR construct (Tau3UTR_long) was transfected into HEK 293 cells because of their ease of transfection. After 48 h, the transfected cells were lysed, and the lysate was subjected to a dual luciferase assay for firefly luciferase and *Renilla* luciferase activity. Firefly luciferase

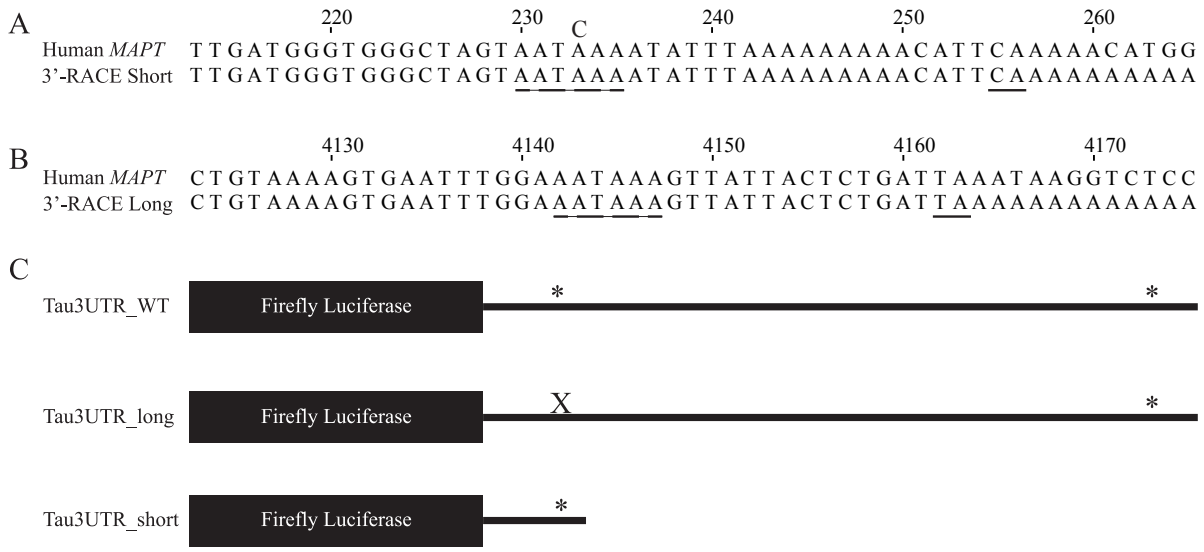

Figure 2.2. Human Tau 3'-UTR Isoforms. A and B. ClustalW alignment of the 3'-UTR of the human *MAPT* gene with (A) the short 3'-RACE product and (B) the long 3'-RACE product. The numbering begins at the first nucleotide of the human tau 3'-UTR. The PAS is indicated by a dashed line, and the cleavage site is indicated by a solid line. The "C" above position 233 in A. denotes the position mutated in the PAS to produce the Tau3UTR_long construct (A233C mutation). C. Diagram of the luciferase reporter constructs containing wild-type (WT), long, and short tau 3'-UTRs.

activity for a sample was normalized by dividing by the *Renilla* luciferase activity for that sample. The pilot experiment revealed a statistically significant difference in the expression of the Tau3UTR_short and Tau3UTR_long constructs (Figure 2.3), suggesting alternative polyadenylation may be a mechanism of regulating tau expression.

In order to study this phenomenon in a system more relevant to the nervous system, the experiment was repeated in two human neuroblastoma cells lines, M17D and differentiated SH-SY5Y cells. For these experiments, in addition to examining the expression of the luciferase reporters at the protein level by the dual luciferase assay, the mRNA expression level was determined by qPCR. In agreement with the results from HEK 293 cells, these experiments revealed that the expression of the short isoform construct is significantly higher than that of the long isoform construct in both neuroblastoma cell lines at the level of both protein and mRNA (Figure 2.4). In general, the wild-type tau 3'-UTR reporter, which contains both PASs, had intermediate expression levels (Figure 2.4).

Discussion

Tau transcripts approximately 2 kb and 6 kb in length, corresponding to the short and long tau 3'-UTR isoforms, respectively, have been described (Goedert et al., 1988; Poorkaj et al., 2001; Wang et al., 1993). Additionally, sequence analysis of the *MAPT* gene from human, mouse, and rat has revealed potential PASs in the tau 3'-UTR from these species (Poorkaj et al., 2001). However, the 3'-RACE data presented here represents the first report of the sequence of both human tau 3'-UTR isoforms at nucleotide resolution. The PAS for the short tau 3'-UTR identified by 3'-RACE (Figure 2.2A) corresponds to the PAS predicted by Poorkaj and colleagues (Poorkaj et al., 2001). Poorkaj and coworkers identified two possible PASs for the long tau 3'-UTR isoform, one being an AATAAA motif and the other being an ATTAAA motif

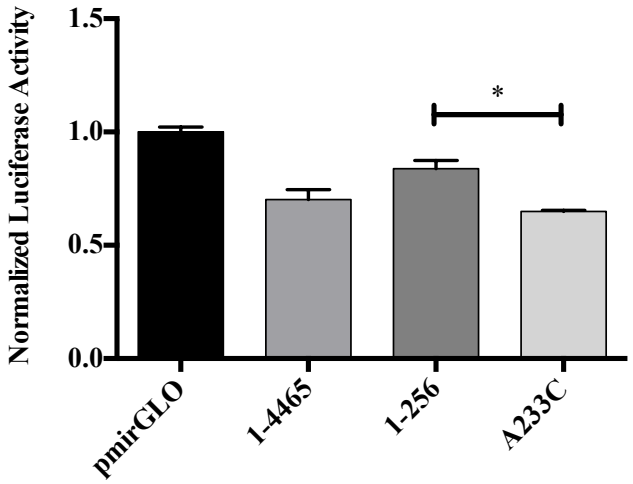

Figure 2.3. Expression of Human Tau 3'-UTR Isoforms is Differentially Regulated in HEK 293 Cells. The indicated constructs were transfected into HEK 293 cells. After 48 h, luciferase expression was determined by dual luciferase assay. n = 3 biological replicates. Error bars represent SEM. Data analyzed by one-way ANOVA followed by Tukey test. *, adjusted $p < 0.05$. Note that all comparisons with pmirGLO reached statistical significance, but this is not indicated on the graph for clarity.

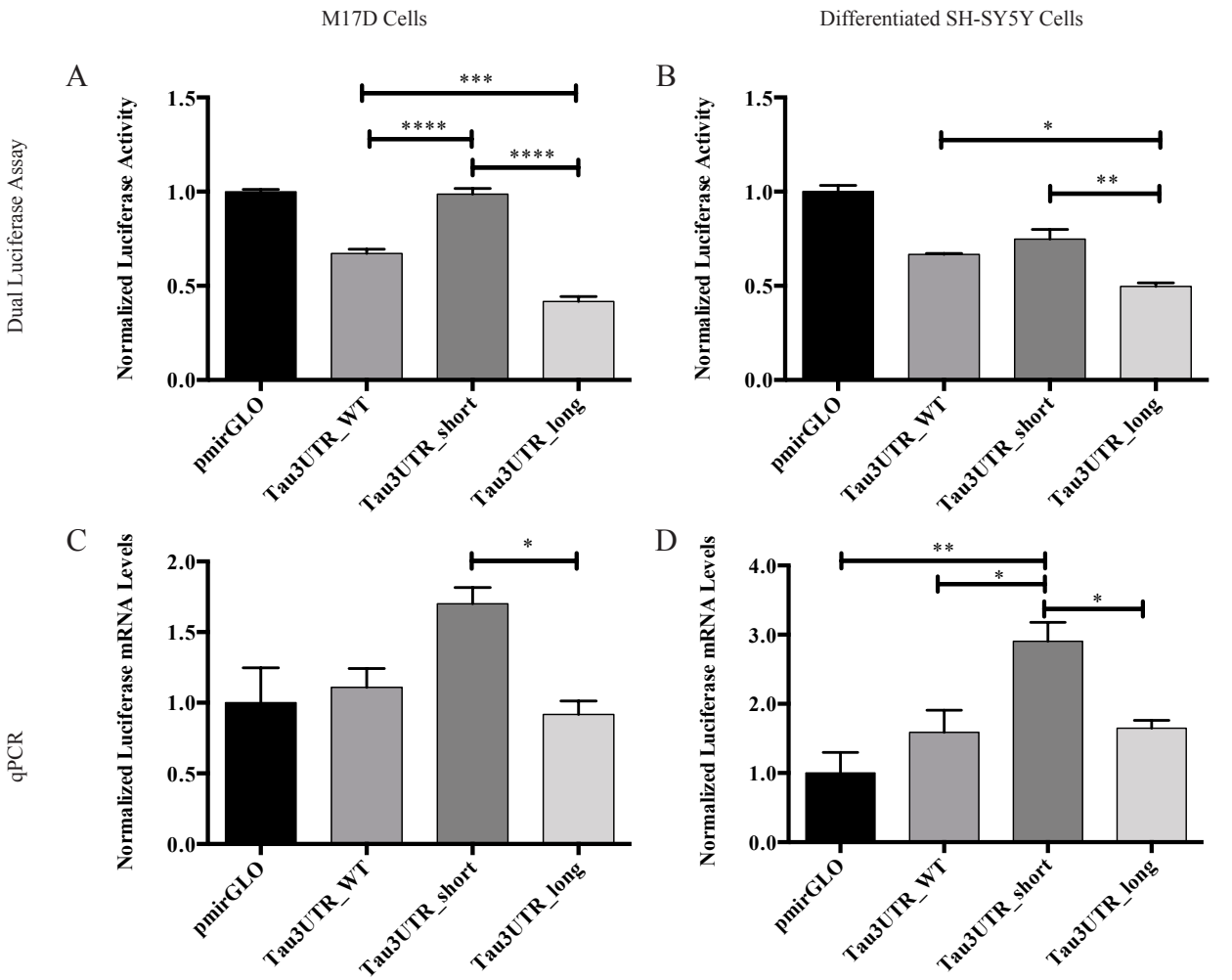

Figure 2.4. Expression of Human Tau 3'-UTR Isoforms is Differentially Regulated in Human Neuroblastoma Cells. The indicated constructs were transfected into (A and C) M17D cells or (B and D) differentiated SH-SY5Y cells. After 48 h, luciferase expression was determined by (A and B) dual luciferase assay or (C and D) qPCR. For each experiment, n = 3 biological replicates. Error bars represent SEM. Data analyzed by one-way ANOVA followed by Tukey test. *,**,***,**** adjusted $p < 0.05$, 0.01, 0.001, 0.0001, respectively. Note that in A, comparisons of pmirGLO with Tau3UTR_WT and Tau3UTR_long reached statistical significance and in B, all comparisons with pmirGLO reached statistical significance. These comparisons are not indicated on the graph for the sake of clarity.

in humans (Poorkaj et al., 2001). The 3'-RACE data unequivocally show that the PAS used for the long human tau 3'-UTR is the AATAAA motif, as the cleavage site is the TA of the ATTAAA motif (Figure 2.2B).

Alternative polyadenylation is an important mechanism of regulating gene expression. Alternative transcripts produced by APA may have different stabilities, translational efficiencies, and/or localizations (Shi, 2012). Despite the knowledge that tau undergoes APA (Goedert et al., 1988; Poorkaj et al., 2001; Wang et al., 1993) and the recognition that APA is a key regulator of gene expression (Shi, 2012), the functional consequences of the APA of tau has not previously been studied. The present study is the first to demonstrate that the expression of the two 3'-UTR isoforms resulting from the APA of tau is differentially regulated. In all three cell lines tested, the protein expression from the short tau 3'-UTR isoform construct is higher than that of the long tau 3'-URT construct (Figures 2.3 and 2.4). Similarly, in both cell lines in which mRNA expression was examined, the mRNAs were higher for the short tau 3'-UTR construct than the long tau 3'-UTR construct (Figure 2.4). These results are consistent with previous reports that short 3'-UTRs are associated with higher expression than their long 3'-UTR counterparts (Mayr and Bartel, 2009; Sandberg et al., 2008). The results presented here suggest that the APA of human tau plays a role in regulating its expression.

While these results provide valuable insights into an unexplored aspect of tau biology, there are some limitations of these studies. The functional studies were performed using luciferase reporter constructs, and while these constructs allow for easy experimental manipulation, they lack the endogenous tau promoter. If expression from the luciferase reporter construct is substantially higher than that of the endogenous tau gene, the overexpression of the constructs may produce transcripts in vast excess relative to the *trans*-factors responsible for the

regulation of endogenous tau expression via its 3'-UTR. If this were to occur, the expression pattern of the constructs may differ substantially from that of the endogenous tau 3'-UTR isoform transcripts. Another limitation of these experiments is that they do not examine the stability and translational efficiency of the two tau 3'-UTR isoforms. While differences in the levels of both mRNA and protein are seen when comparing the two isoforms (Figure 2.4), it is not possible with the experimental design employed here to determine if these differences are due solely to differences in stability or if differences in translational efficiency are also involved. Despite the limitations of the present study, the consistency among different cell types and at the protein and mRNA levels is reassuring, as is the fact that the results are in agreement with previously reported patterns of expression from other short and long 3'-UTR isoforms (Mayr and Bartel, 2009; Sandberg et al., 2008).

The results presented here provide a novel and fundamental insight into tau biology: APA is a mechanism of regulating tau expression. This observation suggests several avenues of follow up studies. The differential expression of the two tau 3'-UTR isoforms is most likely due to the presence of one or more *cis*-elements present in the long tau 3'-UTR isoform but absent in the short tau 3'-UTR. The effect of the regulatory *cis*-element(s) would be mediated by *trans*-factors. Chapters 3 and 4 of this dissertation are focused on the identification of some of these regulatory *cis*-elements and *trans*-factors, respectively.

The finding that APA can regulate tau expression also raises additional questions for future study. For example, in what contexts is the regulatory effect of APA on tau important? In general, APA is spatially and temporally regulated, reflecting the need for differential gene expression profiles during different physiological states (Shi, 2012). Examples of this that are particularly relevant for tau include a general trend toward expression of shorter 3'-UTR

isoforms following neuronal activity (Flavell et al., 2008) and a general trend toward expression of longer 3'-UTR isoforms during the process of development (Ji et al., 2009). In addition to physiological processes, such as those discussed above, changes in APA have been associated with diseased states. The most studied disease in which APA patterns change is cancer, in which there is a general upregulation of short 3'-UTR isoforms (Fu et al., 2011; Lin et al., 2012; Mayr and Bartel, 2009). A global trend toward increased expression of short 3'-UTR isoforms has also been described in cardiac hypertrophy (Park et al., 2011). One report describes an increase in the short tau 3'-UTR in the frontal cortex of AD patients (Goedert et al., 1988), but the identity of the isoform was unclear at the time. There have been no follow-up studies to confirm these observations. These topics for future study will be discussed further in Chapter 5.

In addition to influencing the stability and/or translational efficiency of a transcript, 3'-UTRs can also regulate the subcellular localization of transcripts (Shi, 2012). Previous work has demonstrated that the rat tau 3'-UTR contains an axonal localization signal (Aronov et al., 2001; Behar et al., 1995). However, this axonal localization signal is not well-conserved in humans (Aronov et al., 2001; Poorkaj et al., 2001). The human tau 3'-UTR may contain a different axonal localization signal, and this should be investigated further. This topic will be discussed further in Chapter 5.

Chapter 3

Identification of *cis*-Elements Involved in the Function of the Human Tau 3'-Untranslated Region

Experimental contributions to this chapter: John Dickson performed the cloning of the tau 3'-UTR deletion constructs, transfection of the tau 3'-UTR deletion constructs into HEK 293 and differentiated SH-SY5Y cells and subsequent luciferase assay, transfection of the tau 3'-UTR fragment constructs into M17D and differentiated SH-SY5Y cells and subsequent luciferase assay. Carla Kruse, a master's degree student from the University of Southern Denmark, Odense, Denmark, cloned the approximately 1,000 bp human tau 3'-UTR fragments into the pmirGLO vector under the supervision of John Dickson. Daniel Montagna, an undergraduate student at the College of Wooster, Wooster, OH, performed the transfection of the approximately 1,000 bp human tau 3'-UTR fragment constructs into HEK 293 cells and subsequent luciferase assay under the supervision of John Dickson.

Introduction

The finding that the expression of the short and long tau 3'-UTR isoforms of humans is differentially regulated suggests that the long isoform contains one or more *cis*-element(s) that are responsible for this differential regulation since the sequence of the short tau 3'-UTR isoform is also in the long isoform. A logical follow-up study to these observations is to identify the regulatory *cis*-element(s).

A number of regulatory sequences have been identified in 3'-UTRs. One of the best-studied *cis*-element of 3'-UTRs is the AU-rich element (ARE), which is generally between 50 to 150 nt long. Several occurrences of the pentanucleotide AUUUA are often found in these regions. The ARE is often involved in regulating the stability of mRNA, though they have been reported to affect translation in some instances also (Barrett et al., 2012). In some cases, AREs decrease gene expression, while in other cases they increase it. The effect of AREs on the expression of a particular gene may depend on which ARE-binding proteins bind that site (Knapinska et al., 2005).

Regulatory *cis*-elements need not have particular motifs in the primary structure of the mRNA. A *cis*-element in the 3'-UTR of IL-2, IL-6, and G-CSF consists of a stem-loop structure that destabilizes the transcript. Mutation of the *cis*-element in a way that preserves the stem-loop allows it to retain its destabilizing activity, whereas mutations that disrupt the stem loop cause it to loose its destabilizing activity. This *cis*-element is known as a stem-loop destabilizing element (SLDE) (Brown et al., 1996).

While some *cis*-elements have been identified in the rodent tau 3'-UTR (Aronov et al., 1999; Atlas et al., 2007), the findings in the rodent tau 3'-UTR may not be easily applied to the human tau 3'-UTR because it is not well-conserved with rodents (Poorkaj et al., 2001). In this

chapter, an unbiased approach to identifying regulatory *cis*-elements in the human tau 3'-UTR is presented.

Methods

The methods used were generally those described in Chapter 2. The main exceptions are as follows. The human tau 3'-UTR deletions and fragment constructs were cloned into the pmirGLO vector. Primers used in the cloning of the human tau 3'-UTR deletion constructs are presented in Table 3.1, and primers used in the cloning of the human tau 3'-UTR fragment constructs are presented in Table 3.2. For statistical analyses, comparisons were conducted using a one-way ANOVA followed by Dunnett's test to correct for multiple comparisons.

Results

In order to identify regulatory *cis*-elements in the human tau 3'-UTR, two unbiased approaches were taken. First, a series of tau 3'-UTR luciferase reporter constructs with sequential deletions, each approximately 500 bp long, along the length of the human tau 3'-UTR were made. The general approach to making these deletions constructs is outlined in Figure 3.1. These constructs were transfected into HEK 293 and differentiated SH-SY5Y cells. After 48 h, the cells were lysed, and a dual luciferase assay was performed. In both cell lines, deletion constructs Δ986-1479 and Δ3501-4000 consistently showed significantly increased normalized luciferase activity compared with the Tau3UTR_WT construct (Figure 3.2). Additionally, a significantly increased normalized luciferase activity compared with the Tau3UTR_WT construct was seen with construct Δ4001-4465 in HEK 293 cells (Figure 3.2A) and with constructs Δ2588-3000 and Δ3001-3500 in differentiated SH-SY5Y cells (Figure 3.2B). Thus, several regions that may contain regulatory *cis*-elements were identified with these experiments. However, one caveat to this approach is that it may unintentionally create an artificial regulatory

Table 3.1. Primers Used in the Cloning of Human Tau 3'-UTR Deletion Constructs.

Construct	*Tau 3'-UTR Location*	*Orientation*	*Sequence (5' to 3')*
Δ1-480	481-505	Forward	GCTCGCTAGCCTCGAGCGATGTCAACCTTGTGTGA GTGTGA
Δ1-480	4451-4465	Reverse	ATGCCTGCAGGTCGACTGGTGCCGGTCTTGC
Δ481-984	1-15	Forward	GCTCGCTAGCCTCGAGTCAGGCCCCTGGGGC
Δ481-984	466-480/ 985-999	Reverse	AGCCCTAAAGTCCCATCTGCCTGTGGCTCC
Δ481-984	985-1009	Forward	TGGGACTTTAGGGCTAACCAGTTCT
Δ481-984	4451-4465	Reverse	ATGCCTGCAGGTCGACTGGTGCCGGTCTTGC
Δ986-1479	1-15	Forward	GCTCGCTAGCCTCGAGTCAGGCCCCTGGGGC
Δ986-1479	962-985/ 1480-1494	Reverse	TCCATGTCAACAAGGAGGTCTGCAAAGTGGCCAAA ATCA
Δ986-1479	1480-1502	Forward	CCTTGTTGACATGGAGAGAGCCC
Δ986-1479	4451-4465	Reverse	ATGCCTGCAGGTCGACTGGTGCCGGTCTTGC
Δ1479-2015	1-15	Forward	GCTCGCTAGCCTCGAGTCAGGCCCCTGGGGC
Δ1479-2015	1458-1479/ 2016-2030	Reverse	ACACAGGCCACACGACAGAAACACCTAGGGTCAC AGC
Δ1479-2015	2016-2035	Forward	TCGTGTGGCCTGTGTGGTGC
Δ1479-2015	4451-4465	Reverse	ATGCCTGCAGGTCGACTGGTGCCGGTCTTGC
Δ2001-2587	1-15	Forward	GCTCGCTAGCCTCGAGTCAGGCCCCTGGGGC
Δ2001-2587	1981-2000/ 2588-2602	Reverse	GTCAGCGGGCTGAGGTGAGAGACACCTCGTGAGGG
Δ2001-2587	2588-2607	Forward	CCTCAGCCCGCTGACCTTGC
Δ2001-2587	4451-4465	Reverse	ATGCCTGCAGGTCGACTGGTGCCGGTCTTGC
Δ2588-3000	1-15	Forward	GCTCGCTAGCCTCGAGTCAGGCCCCTGGGGC
Δ2588-3000	2569-2587/ 3001-3015	Reverse	CAAGAACTTCAGGAATGCTCTGGTCAAGGCTTTG
Δ2588-3000	3001-3020	Forward	TTCCTGAAGTTCTTGTGCCC
Δ2588-3000	4451-4465	Reverse	ATGCCTGCAGGTCGACTGGTGCCGGTCTTGC
Δ3001-3500	1-15	Forward	GCTCGCTAGCCTCGAGTCAGGCCCCTGGGGC
Δ3001-3500	2984-3000/ 3501-3515	Reverse	AGGGCCTCTAACTCCGAGGAACCGAGGTGCGT
Δ3001-3500	3501-3519	Forward	GGAGTTAGAGGCCCTTGGG
Δ3001-3500	4451-4465	Reverse	ATGCCTGCAGGTCGACTGGTGCCGGTCTTGC
Δ3501-4000	1-15	Forward	GCTCGCTAGCCTCGAGTCAGGCCCCTGGGGC
Δ3501-4000	3485-3500/ 4001-4015	Reverse	ATTACCGAAGAAATCGTGGCTGCTCCCTCCC
Δ3501-4000	4001-4023	Forward	GATTTCTTCGGTAATTCTGAGGG
Δ3501-4000	4451-4465	Reverse	ATGCCTGCAGGTCGACTGGTGCCGGTCTTGC
Δ4001-4465	1-15	Forward	GCTCGCTAGCCTCGAGTCAGGCCCCTGGGGC
Δ4001-4465	3983-4000	Reverse	ATGCCTGCAGGTCGACATGGGACTTGCAAGTGCC

Table 3.2. Primers Used in the Cloning of Human Tau 3'-UTR Fragment Inserts.

Construct	*Tau 3'-UTR Location*	*Orientation*	*Sequence (5' to 3')*
1-960	1-15	Forward	GCTCGCTAGCCTCGAGTCAGGCCCCTGGGGC
1-960	939-960	Reverse	ATGCCTGCAGGTCGACGGCAGCAGTTCCAACCTC AGA
954-1869	954-975	Forward	GCTCGCTAGCCTCGAGTGCTGCCATGATTTTGGC CACT
954-1869	1846-1869	Reverse	ATGCCTGCAGGTCGACTCCAACTACAACTCAACA GGGTGC
1845-2793	1845-1868	Forward	GCTCGCTAGCCTCGAGTGCACCCTGTTGAGTTGT AGTTGG
1845-2793	2774-2793	Reverse	ATGCCTGCAGGTCGACAGCTGCACACGAAGCTG CCA
2770-3729	2770-2798	Forward	GCTCGCTAGCCTCGAGGGGCTGGCAGCTTCGTGT GC
2770-3729	3709-3729	Reverse	ATGCCTGCAGGTCGACGGAGCCAGTGTGAGAGG TGGC
3730-4163	3730-3747	Forward	GCTCGCTAGCCTCGAGAGACACACAGCCTGTGCT
3730-4163	4133-4163	Reverse	ATGCCTGCAGGTCGACTAATCAGAGTAATAACTT TATTTCCAAATTC
954-1136	954-975	Forward	ATGCCTGCAGGTCGACTCCAACTACAACTCAACA GGGTGC
954-1136	1117-1136	Reverse	ATGCCTGCAGGTCGACGCAGTGGCCGTGGGAAG GAC
1114-1279	1114-1133	Forward	GCTCGCTAGCCTCGAGCCTGTCCTTCCCACGGCC AC
1114-1279	1259-1279	Reverse	ATGCCTGCAGGTCGACACCTCCTGCAACCAACCA GGG
1259-1869	1259-1279	Forward	GCTCGCTAGCCTCGAGCCCTGGTTGGTTGCAGGA GG
1259-1869	1846-1869	Reverse	ATGCCTGCAGGTCGACTCCAACTACAACTCAACA GGGTGC
2770-3259	2770-2798	Forward	GCTCGCTAGCCTCGAGGGGCTGGCAGCTTCGTGT GC
2770-3259	3237-3259	Reverse	ATGCCTGCAGGTCGACCCTATCTAGCCCACCCAA GGACA
3232-3501	3232-3251	Forward	GCTCGCTAGCCTCGAGGCCAGTGTCCTTGGGTGG GC
3232-3501	3482-3501	Reverse	ATGCCTGCAGGTCGACCGTGGCTGCTCCCTCCCT CT
3499-3729	3499-3520	Forward	GCTCGCTAGCCTCGAGACGGAGTTAGAGGCCCTT GGGG
3499-3729	3709-3729	Reverse	ATGCCTGCAGGTCGACGGAGCCAGTGTGAGAGG TGGC

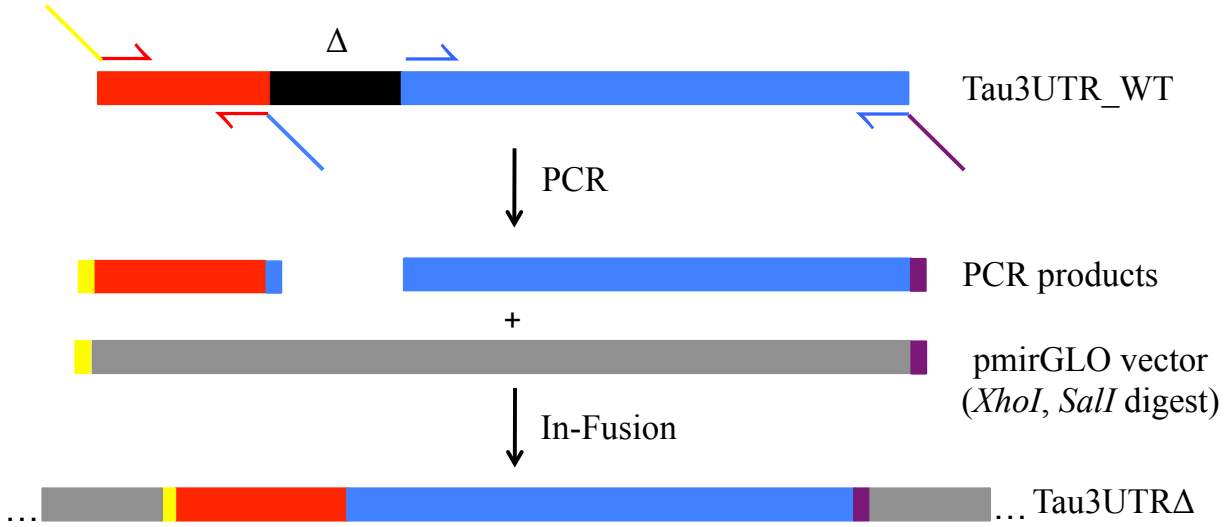

Figure 3.1. Construction of Tau 3'-UTR Deletion Mutants Using In-Fusion. PCR was performed on regions of the Tau3UTR_WT construct, excluding the sequence to be deleted. Primers were constructed to contain 15 bp of homology between the fragments to be cloned using the In-Fusion kit.

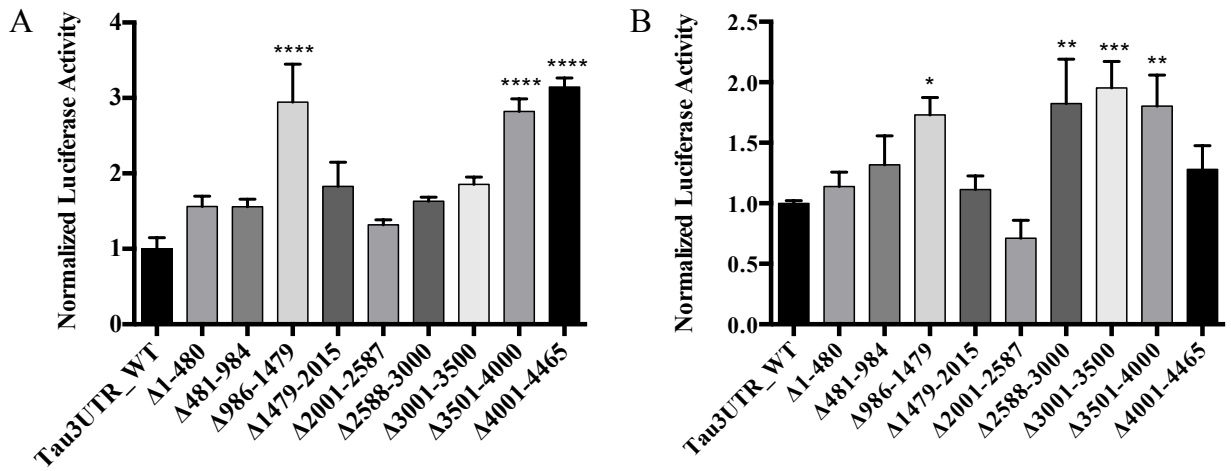

Figure 3.2. Identification of Regulatory *cis*-Elements in the Human Tau 3'-UTR Using Deletion Constructs. The indicated constructs were transfected into (A) HEK 293 cells or (B) differentiated SH-SY5Y cells, and after 48 h, a dual luciferase assay was performed. For each experiment, $n = 3$ biological replicates. The error bars indicate SEM. Data were analyzed by a one-way ANOVA followed by Dunnett's test, compared with Tau3UTR_WT. *,**,***,**** adjusted $p < 0.05$, 0.01, 0.001, and 0.0001, respectively.

cis-element by joining together sequences adjacent to either end of the deleted region. In order to circumvent this potential confounder, a complementary approach of inserting sequential fragments of approximately 1,000 bp of the human tau 3'-UTR into the pmirGLO vector was used for future studies.

Once the human tau 3'-UTR fragments were cloned into the pmirGLO vector, these constructs were initially tested by transfecting them into HEK 293 cells. After 48 h, the cells were lysed, and a dual luciferase assay was performed. A statistically significant reduction in normalized luciferase expression compared with the empty pmirGLO vector was seen for constructs 954-1869 and 2770-3729 (Figure 3.3). These results are consistent with those seen using the deletion fragments in HEK 293 cells (Figure 3.2A), as overlapping regions were identified in these complementary experiments.

The human tau 3'-UTR fragment constructs were then transfected into M17D cells and differentiated SH-SY5Y cells. After 48 h, the cells were lysed, and a dual luciferase assay was performed. In both cases, a statistically significant reduction in normalized luciferase expression compared with the empty pmirGLO vector was seen for constructs 954-1869 and 2770-3729 (Figure 3.4), consistent with those results seen in HEK 293 cells (Figure 3.3). Additionally, a statistically significant increase in normalized luciferase expression compared with the empty pmirGLO vector was seen for construct 3730-4163 in both cell lines (Figure 3.4). For M17D cells, a moderate but statistically significant decrease in normalized luciferase expression compared with the empty pmirGLO vector was seen for construct 1-960 (Figure 3.4A).

For follow-up experiments to further localize the regulatory *cis*-elements of the human tau 3'-UTR, regions 954-1869 and 2770-3729 were selected since they were identified in all three cell lines used for the previous experiments. Smaller sub-fragments from these regions

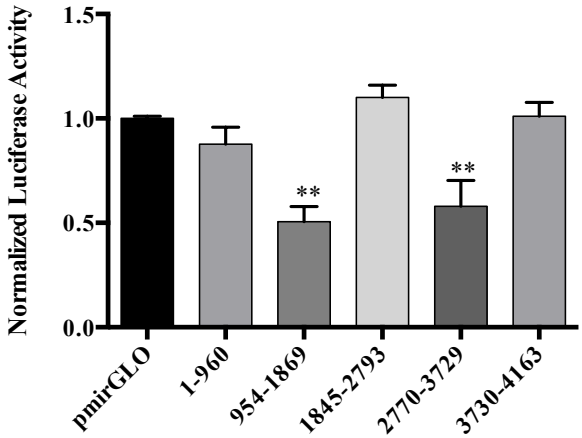

Figure 3.3. Identification of Regulatory *cis*-Elements in the Human Tau 3'-UTR Using HEK Cells. The indicated constructs were transfected into HEK 293 cells, and after 48 h, a dual luciferase assay was performed. For each experiment, $n = 3$ biological replicates. The error bars indicate SEM. Data were analyzed by a one-way ANOVA followed by Dunnett's test, compared with pmirGLO. **, adjusted $p < 0.01$.

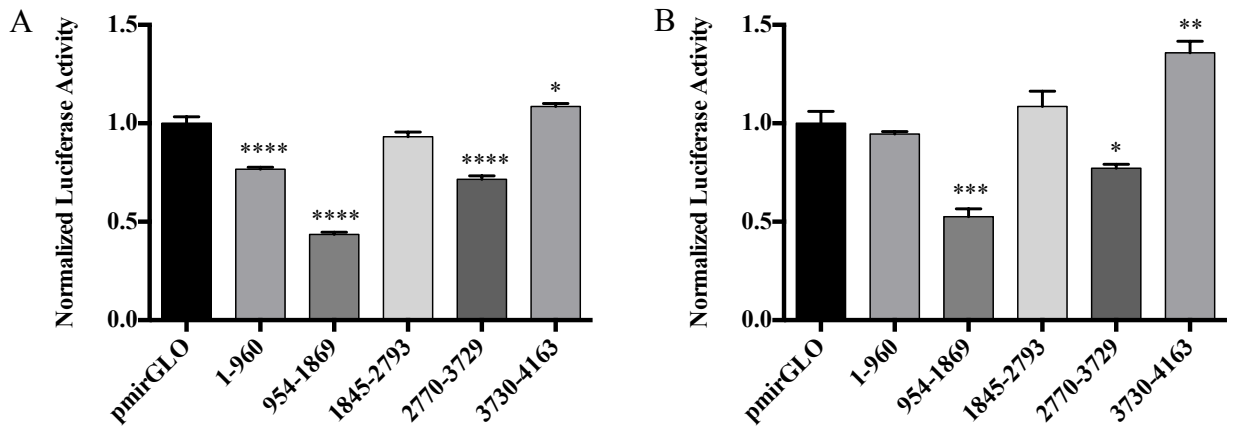

Figure 3.4. Identification of Regulatory *cis*-Elements in the Human Tau 3'-UTR Using Neuroblastoma Cells. The indicated constructs were transfected into (A) M17D cells or (B) differentiated SH-SY5Y cells, and after 48 h, a dual luciferase assay was performed. For each experiment, $n = 3$ biological replicates. The error bars indicate SEM. Data were analyzed by a one-way ANOVA followed by Dunnett's test, compared with pmirGLO. *,**,***,****, adjusted $p < 0.05$, 0.01, 0.001, and 0.0001, respectively.

were inserted into the pmirGLO vector, and these constructs were transfected into M17D cells. After 48 h, the cells were lysed, and a dual luciferase assay was performed. For sub-fragments of the 954-1869 region, a statistically significant reduction in normalized luciferase expression compared with the empty pmirGLO vector was seen for constructs 1114-1279 and 1259-1869 (Figure 3.5A). For the sub-fragments of the 2770-3729 region, the normalized luciferase activity of sub-fragments 2770-3259 and 3499-3729 was significantly decreased compared to empty pmirGLO vector, whereas the normalized luciferase activity of sub-fragment 3232-3501 was significantly increased (Figure 3.5B).

Discussion

The experiments presented here are the first reported to systematically search for regulatory *cis*-elements in the human tau 3'-UTR. A 91 nt fragment from the rat tau 3'-UTR has been identified (Behar et al., 1995), and it has been found to play a role in regulating the stability (Aranda-Abreu et al., 1999; Aronov et al., 1999), translational efficiency (Atlas et al., 2004; 2007), and axonal localization (Aronov et al., 2001; Behar et al., 1995). The embryonic lethal abnormal vision (ELAV)-like protein HuD binds a 21 nt uridine rich region within the larger 91 nt fragment (Aranda-Abreu et al., 1999). The 91 nt region is not well-conserved between rats and humans (Poorkaj et al., 2001). A 600 nt fragment of the rat tau 3'-UTR has been found to contain a binding site for the insulin-like growth factor mRNA binding protein 1 (IMP1); however, since the binding site could not be further localized, Atlas and colleagues concluded that the binding of IMP1 to the rat tau 3'-UTR may be conformation-specific rather than sequence-specific (Atlas et al., 2007). It is currently not possible to determine how conserved this putative IMP1 binding structure is between rats and humans because the binding site of IMP1 has not been further characterized. Since previous studies of the rat tau 3'-UTR cannot

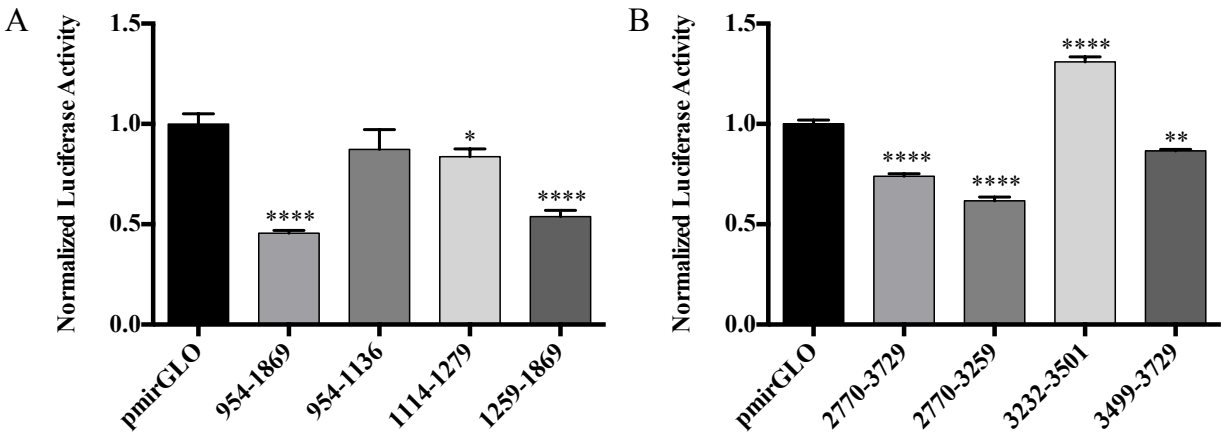

Figure 3.5. Further Localization of Regulatory *cis*-Elements in the Human Tau 3'-UTR. The indicated constructs were transfected into M17D cells, and after 48 h, a dual luciferase assay was performed. For each experiment, $n = 3$ biological replicates. The error bars indicate SEM. Data were analyzed by a one-way ANOVA followed by Dunnett's test, compared with pmirGLO. *,**,****, adjusted $p < 0.05$, 0.01, and 0.0001, respectively. A. Sub-fragments of 954-1869. B. Sub-fragments of 2770-3729.

necessarily be used to predict the regulatory *cis*-elements in the human tau 3'-UTR, a systematic approach to identifying regulatory *cis*-elements in the human tau 3'-UTR is a worthwhile endeavor.

Through the use of two complementary approaches and multiple cell lines, several regions of the human tau 3'-UTR containing putative regulatory *cis*-elements have been identified. Each cell type studied had a specific expression pattern of the luciferase reporter constructs tested. This may be due to the cell type-specific presence or absence of *trans*-factors that bind the *cis*-elements. Despite the differences among the expression patterns of the cells, there were some commonalities among them. The data from the various approaches and cell lines are consistent with the presence of repressive *cis*-elements in the regions of 954-1869 and 2770-3729. Therefore, these regions were chosen for further study. Several luciferase reporter constructs containing sub-fragments of these regions were found to contain regulatory *cis*-elements, most of which are repressive (Figure 3.5). The presence of several repressive *cis*-elements in the long tau 3'-UTR isoform is consistent with the observations from Chapter 2 that the expression of the long tau 3'-UTR is repressed compared to the short tau 3'-UTR. While the studies with the sub-fragment constructs were informative in further localizing the regulatory *cis*-elements, they do not sufficiently identify the exact *cis*-elements or the *trans*-factors that bind them. Additional studies have identified one of the *cis*-elements and its corresponding *trans*-factor, and these studies are discussed in Chapter 4. Future experiments are required to further characterize the other *cis*-elements in the human tau 3'-UTR, which will be discussed in Chapter 5.

While the use of luciferase reporter constructs to identify regulatory *cis*-elements in the human tau 3'-UTR provides for an easily manipulated and analyzed experimental system, it also

comes with limitations. As discussed in Chapter 2, overexpression from the constructs may produce transcripts in excess of the *trans*-factors present in the cell types used. In cases where this occurs, it may not be possible to detect the presence of regulatory *cis*-elements that bind to *trans*-factors that are limiting. In experiments performed with fragment insert constructs (Figures 3.3, 3.4, and 3.5), they are compared with the empty pmirGLO construct in statistical analyses. The empty pmirGLO construct would produce a firefly luciferase transcript with a very short 3'-UTR, consisting primarily of the multiple cloning site. In contrast, the fragment constructs contain inserts in the multiple cloning site from the human tau 3'-UTR that produce firefly luciferase transcripts with 3'-UTRs that can be several hundred nucleotides long. Thus, if the length of the 3'-UTR alters expression of the transcripts in a sequence-independent manner, this could confound the results. In the case of the experiments presented here, this does not appear to be a factor, as inserts with similar lengths can have different expression patterns compared with the empty pmirGLO vector. Another limitation is that the approach of using successively smaller fragments to localize *cis*-elements does not identify the type of *cis*-element *per se* or suggest possible *trans*-factors that bind it. Additional studies are needed in order to accomplish this, and these are discussed further in Chapter 5.

Chapter 4

miR-34 Family Members Regulate Tau Expression via a Binding Site in the Tau 3'-Untranslated Region

Experimental contributions to this chapter: John Dickson performed co-transfections in M17D cells followed by luciferase assay and qPCR, performed the transfection of Pre-miRs and LNAs into M17D cells followed by Western blot and qPCR, and performed the alignment and DIANA-microT analysis of miR-34 family members. Carla Kruse, a master's degree student from the University of Southern Denmark, Odense, Denmark, working under the supervision of John Dickson, identified candidate miRNAs for this study, performed the initial screen of the candidate miRNAs in HEK 293 cells followed by luciferase assay, performed site-directed mutagenesis of miR-34a and miR-132 seed regions, and tested the sensitivity of the wild-type and mutant constructs to the miRNAs of interest in HEK 293 cells followed by luciferase assay.

Introduction

miRNAs are short endogenous RNAs that regulate gene expression, typically by binding the 3'-UTR of the genes (Bartel, 2004). When the miRNA and target mRNA have extensive complementarity, binding of the miRNA may cause cleavage of the target mRNA. When there is less complementarity, binding of the miRNA tends to result in translational repression of the target mRNA. The former scenario is more common in plants, whereas the latter is more common in metazoans (He and Hannon, 2004). The incomplete complementarity between miRNAs and target mRNAs in metazoans poses a challenge to computationally predicting miRNA binding sites. However, most miRNAs have a region of complete complementarity with the target mRNA called the seed region, and this facilitates prediction of miRNA binding sites. Seed regions are found near the 5'-end of miRNAs, with nucleotides 2-7 of mature miRNAs forming the core of the seed region. Canonical seed regions are 7-mers or 8-mers, formed by the core seed region plus nucleotides 1 and/or 8. Several programs have been developed to computationally predict miRNA binding sites (Bartel, 2009).

Several of these programs were used to identify candidate miRNAs predicted to bind the human tau 3'-UTR. Functional studies were then performed to investigate the effect of these miRNAs. Ultimately, these experiments validated the miR-34a family, and miR-34a in particular, as miRNAs that bind the human tau 3'-UTR and regulate tau expression.

Methods

Prediction of miRNAs Binding the Human Tau 3'-UTR

microrna.org (Betel et al., 2007), PicTar (Krek et al., 2005), TargetScan (Lewis et al., 2005), and DIANA-microT (Maragkakis et al., 2009) were searched for miRNAs predicted to bind the human *MAPT* gene.

Cell Culture

Cell culture was performed as described in Chapter 2.

Site-Directed Mutagenesis

Site-directed mutagenesis was performed using the QuikChange Lightning Site-Directed Mutagenesis Kit (Agilent Technologies) according to the manufacturer's instructions. Primers used for site-directed mutagenesis are listed in Table 4.1.

Table 4.1. Primers for Site-Directed Mutagenesis of miR-34a and miR-132 seed regions.

Construct	*Orientation*	*Sequence (5' to 3')*
954-1869_mut	Forward	GTTGTCTGCCGTGAGAGCCCAATGTGACCCTATACCCCTCATCACA
954-1869_mut	Reverse	TGTGATGAGGGGTATAGGGTCACATTGGGCTCTCACGGCAGACAAC
3730-4163_mut	Forward	GTGTATTGTGTGTTTTAACAAATGATTTACACTCTGACAAGCTGTAAAAGTGAATTTGG
3730-4163_mut	Reverse	CCAAATTCACTTTTACAGCTTGTCAGAGTGTAAATCATTTGTTAAAACACACAATACAC

Transfection of Cultured Cells

Co-transfections were preformed at 70-80% confluency and included 200 ng plasmid and 30 nM Pre-miR miRNA Precursor (Life Technologies) per well of a 24-well plate. Transfection of oligonucleotides alone was performed at 60-70% confluency. Transfection of Pre-miR miRNA Precursors was performed at a concentration of 50 nM. Transfection of miRCURY LNA microRNA Inhibitors (Exiqon) was performed at a concentration of 20, 50, 60, or 100 nM per LNA, as indicated. Sequences of these oligonucleotides are listed in Table 4.2.

Dual Luciferase Assay

The dual luciferase assay was performed as described in Chapter 2.

Western Blot

Cells were lysed in M-PER Mammalian Protein Extraction Reagent (Thermo Scientific) containing Halt Protease Inhibitor Cocktail (Thermo Scientific). The protein in the lysates was

Table 4.2. miRNA-Related Oligonucleotides.

Oligonucleotide	*Sequence (5' to 3')*
Pre-miR Negative Control #1	Proprietary (Life Technologies Catalog # AM17110)
Pre-miR-34a-5p	Proprietary (Life Technologies Catalog # PM11030)
Pre-miR-132-3p	Proprietary (Life Technologies Catalog # PM10166)
Pre-miR-181c-5p	Proprietary (Life Technologies Catalog # PM10181)
Pre-miR-642-5p	Proprietary (Life Technologies Catalog # PM11477)
miRCURY LNA Negative Control A	GTGTAACACGTCTATACGCCCA
miRCURY LNA hsa-miR-34a-5p	ACAACCAGCTAAGACACTGCC
miRCURY LNA hsa-miR-34b-5p	AATCAGCTAATGACACTGCCT
miRCURY LNA hsa-miR-34c-5p	GCAATCAGCTAACTACACTGCC

quantified using the Pierce BCA Protein Assay Kit (Thermo Scientific) according to the manufacturer's instructions. For each lysate, 3 μg total protein, NuPAGE Sample Reducing Agent (Life Technologies), and NuPAGE LDS Sample Buffer (Life Technologies) were combined and heated to 70 ºC for 10 min. The samples were subjected to lithium dodecyl sulfate PAGE (LDS-PAGE) on a NuPAGE Novex 4-12% Bis-Tris Gel (Life Techologies) in XT MES Buffer (Bio-Rad) at 200 V for 35 min. The proteins were transferred to an Immobilon-P membrane (Millipore) in Novex Tris-Glycine Buffer (Life Technologies) with 20% methanol at 180 mA for 75 min. The blots were blocked in 5% milk in TBS with 0.1% Tween-20 (TBST) and probed with primary antibodies (1:12,000 dilution) for total tau (Dako), sirtuin 1 (SIRT1) (abcam), and GAPDH (Novus Biologicals) in 5% milk in TBST for 1 h at room temperature or overnight at 4 ºC. Secondary antibodies conjugated to HRP (GE Healthcare) were used as a dilution of 1:8,000 in 5% milk in TBST for 1 h at room temperature. The HRP activity was visualized using Amersham ECL Prime Western Blotting Detection Reagent (GE Healthcare

Life Sciences), which uses luminol and hydrogen peroxide in a chemiluminescent reaction catalyzed by HRP.

Total RNA Isolation

Total RNA isolation was performed as described in Chapter 2.

Quantitative PCR

Quantitative PCR was performed generally as described in Chapter 2. For investigation of endogenous tau expression, TaqMan assays for total tau and GAPDH were used. Additional information for Taqman assays used in these experiments is listed in Table 4.3. Custom GeneArt Strings DNA Fragments (Life Technologies) were used as standards for tau and GAPDH, and the sequences of these standards are provided in Table 4.4.

Table 4.3. TaqMan Gene Expression Assay Probes.

Target	*Oligonucleotide Type*	*Sequence (5' to 3')*
Tau	TaqMan Assay	Proprietary (Life Technologies Assay ID: Hs00902194_m1)
GAPDH	TaqMan Assay	Proprietary (Life Technologies Assay ID: Hs99999905_m1)

Table 4.4. Custom Standards for Absolute Quantification qPCR.

Gene	*Sequence*
Tau	GTAAAATCTGAGAAGCTTGACTTCAAGGACAGAGTCCAGTCGAAGATTGGGTCCC TGGACAATATCACCCACGTCCCTGGCGGAGGAAATAAAAAGATTGAAACCCACA AGCTGACCTTCCGCGAGAACGCCAAAGCCAAGACAGACCACGGGGCGGAGATCG TGTACAAGTCGCCAGTGGTGTCTGGGGACACGTCTCC
GAPDH	AGCCCGCAGCCTCCCGCTTCGCTCTCTGCTCCTCCTGTTCGACAGTCAGCCGCATC TTCTTTTGCGTCGCCAGCCGAGCCACATCGCTCAGACACCATGGGGAAGGTGAAG GTCGGAGTCAACGGATTTGGTCGTATTGGGCGCCTGGTCACCAGGGCTGCTTTTA ACTCTGGTAAAGTGGATATTGTTGCCATCAATGACCCCTTCATTGACCTCAACTAC ATGGTTTACATGTTCCAATATGATTCCACCCATGGCAAATTCCATGGCACCGTCAA GGCTGAGAACGGGAAGCTTGTC

Statistical Analysis

Data are presented as a mean of biological replicates, and variation is indicated as the SEM. Comparisons were conducted using an unpaired Student's *t*-test.

Results

In parallel with the unbiased approach to identify regulatory *cis*-elements in the human tau 3'-UTR, a candidate-based approach to identify *trans*-factors that regulate tau expression via binding to its 3'-UTR was undertaken. In particular, candidate miRNAs that may bind the human tau 3'-UTR were sought because of the availability of several online prediction tools, namely microrna.org (Betel et al., 2007), PicTar (Krek et al., 2005), TargetScan (Lewis et al., 2005), and DIANA-microT (Maragkakis et al., 2009). The initial search identified 17 candidate miRNAs, and the list of candidate miRNAs was narrowed to a manageable number by selecting those with conserved seed regions and/or previous reports of dysregulation in AD (Cogswell et al., 2008; Maes et al., 2009) (Table 4.5).

Table 4.5. Candidate miRNAs Predicted to Target the Human Tau 3'-UTR.

miRNA	*Prediction Program Identifying this miRNA*	*Location of Predicted Binding Site in 3'-UTR*
hsa-miR-34a	microRNA.org, PicTar, TargetScan, DIANA-microT	1172-1194
hsa-miR-132	microRNA.org, DIANA-microT	4104-4121
hsa-miR-181c	microRNA.org, DIANA-microT	4056-4074
hsa-miR-642	DIANA-microT	4019-4036

In order to screen the four final candidate microRNAs for functional effects on constructs expressing the tau 3'-UTR, HEK 293 cells were co-transfected with the Pre-miR precursor miRNA mimic corresponding to the candidate miRNA or a non-targeting negative control Pre-miR and a luciferase reporter vector containing a fragment of the human tau 3'-UTR predicted to contain the miRNA binding site. As a control for specificity, co-transfections of Pre-miRs and the empty pmirGLO vector were also performed. In this screen, a specific reduction in the tau 3'-UTR luciferase reporter activity, which was normalized to the *Renilla* luciferase control, was

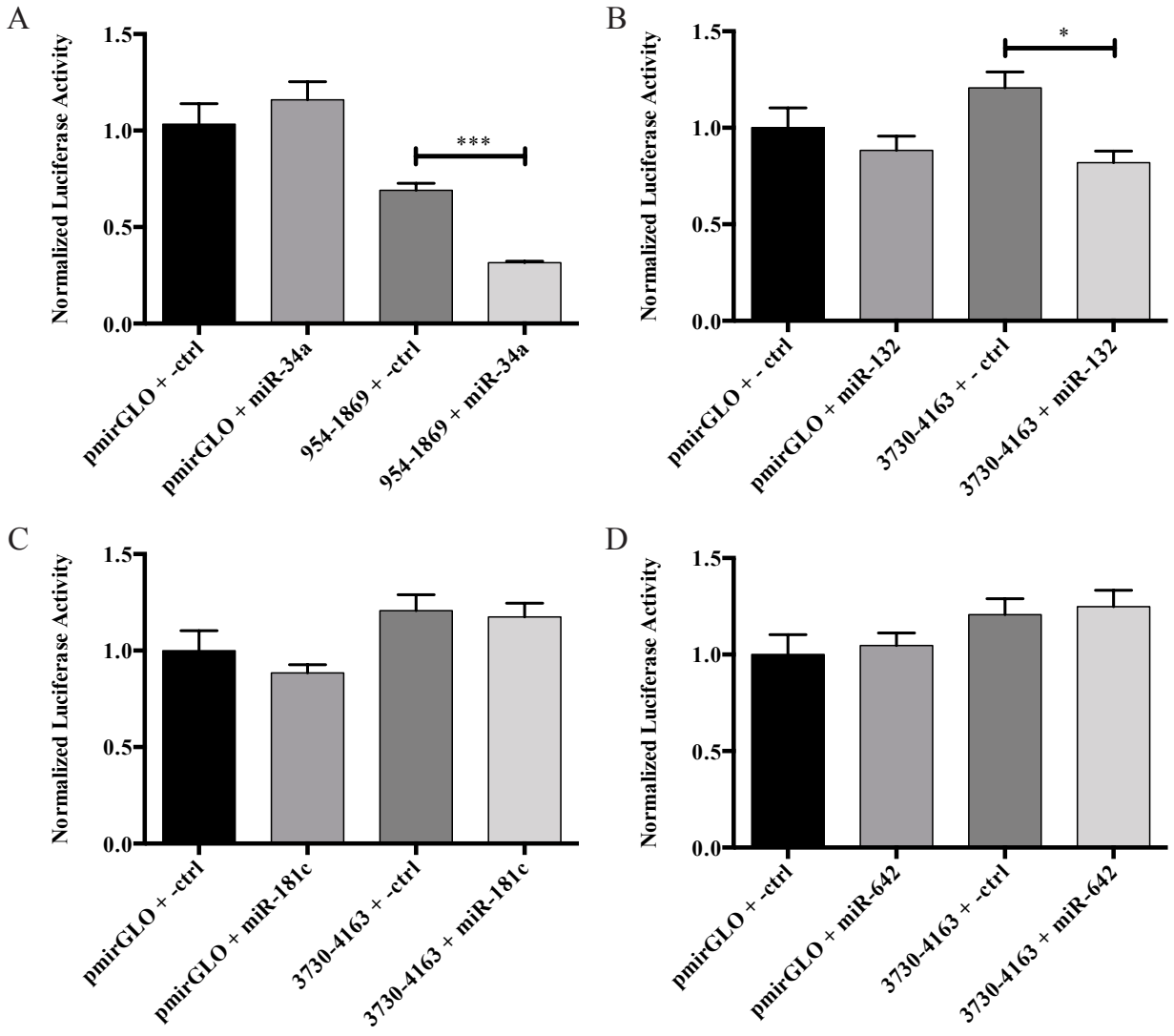

Figure 4.1. Screening Candidate miRNAs for Effects on Luciferase Reporter Activity from Tau 3'-UTR Construct Expression. The indicated luciferase reporter constructs and Pre-miRs were co-transfected into HEK 293 cells. After 48 h, luciferase protein levels were determined by a dual luciferase assay. For each experiment, $n = 3$ biological replicates. The error bars indicate SEM. Data were analyzed by unpaired *t*-test. *,***, $p < 0.05$, 0.001, respectively. Luciferase assays performed on lysates from cells treated with (A) Pre-miR-34a, (B) Pre-miR-132, (C) Pre-miR-181c, and (D) Pre-miR-642.

observed for Pre-miR-34a and Pre-miR-132; however, no effect was seen with Pre-miR-181c or Pre-miR-642 (Figure 4.1).

In a follow-up experiment, the seed regions of miR-34a and miR-132 were mutated in the luciferase reporter constructs by site-directed mutagenesis (Figures 4.2A & B). Co-transfection of Pre-miR-34a with the luciferase reporter construct containing the wild-type miR-34a binding site in HEK 293 cells resulted in lower normalized luciferase reporter expression compared with the non-targeting negative control Pre-miR (Figure 4.2C). In contrast, the miR-34a seed region mutant luciferase reporter vector was insensitive to Pre-miR-34a (Figure 4.2C), demonstrating that miR-34a does indeed interact specifically with this seed region. A similar experiment was performed with Pre-miR-132. In this case, Pre-miR-132 repressed the expression of both the wild-type and mutated miR-132 seed region tau 3'-UTR luciferase reporter constructs (Figure 4.2D), indicating that the observed effect was not due to binding of miR-132 to its predicted binding site in the human tau 3'-UTR. Since these experiments identified the binding site of miR-34a but not miR-132, miR-34a became the focus of additional studies exploring the role of miRNAs in regulating tau expression.

In order to test the effect of miR-34a on the luciferase reporter constructs in a system more relevant to the nervous system, the co-transfections with Pre-miR-34a were repeated in M17D neuroblastoma cells. After 48 h, the cells were lysed and a dual luciferase assay was performed, which yielded the same result in M17D cells (Figure 4.3A) as was seen in HEK293 cells (Figure 4.2C). In order to examine the effect of Pre-miR-34a on the luciferase reporters at the mRNA level, the co-transfections were repeated in M17D cells, and the expression of firefly and *Renilla* luciferase mRNAs was measured by qPCR. Again, the construct with wild-type

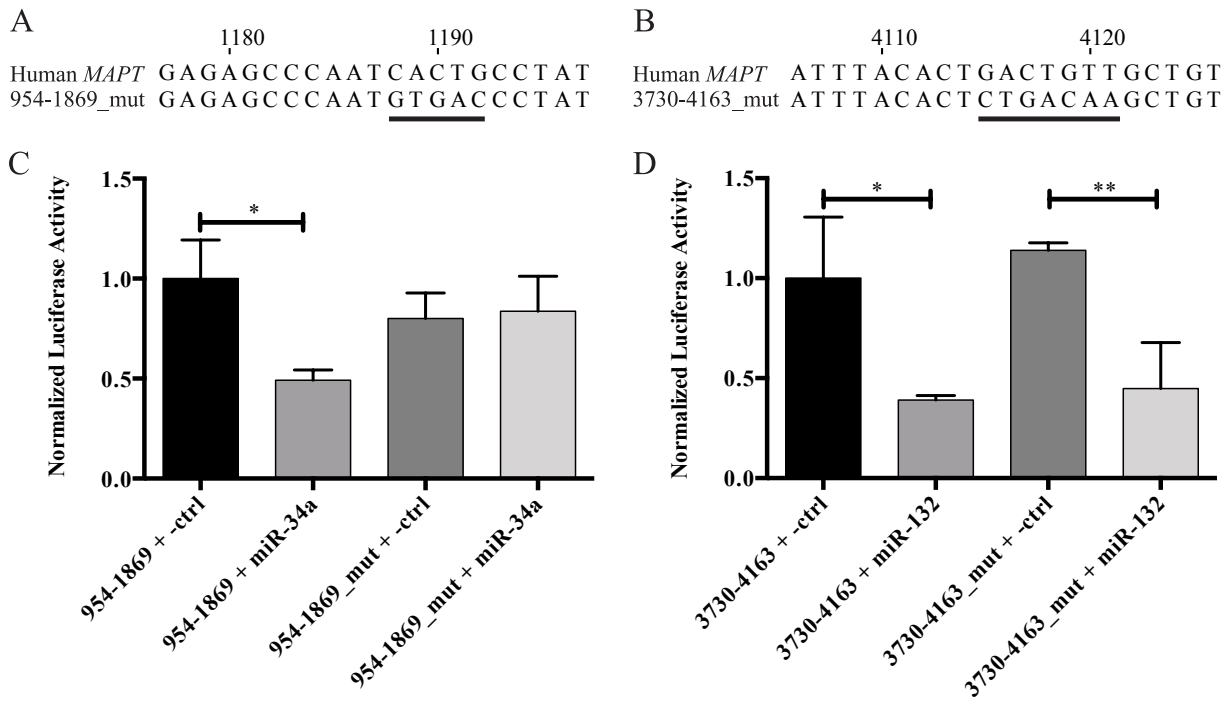

Figure 4.2. Effect of Mutating the miR-34a and miR-132 Seed Regions in Tau 3'-UTR Luciferase Constructs. A and B. Alignment of the mutated (A) miR-34a or (B) miR-132 seed region tau 3'-UTR construct with the wild-type human *MAPT* sequence. The numbering begins at the first nucleotide of the human tau 3'-UTR. The mutated nucleotides of the seed regions are underlined. C and D. The indicated luciferase reporter constructs and Pre-miRs were co-transfected into HEK 293 cells. After 48 h, luciferase expression was determined by a dual luciferase assay. $n = 3$ biological replicates. Error bars indicate SEM. Data analyzed by unpaired *t*-test. *,**, adjusted $p < 0.05$ and 0.01, respectively.

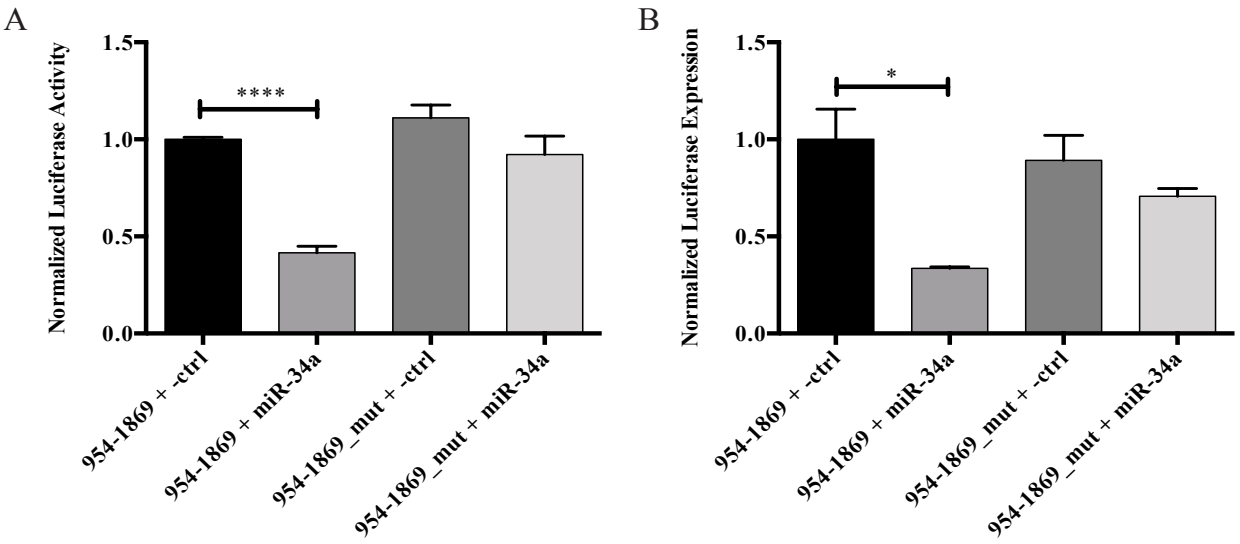

Figure 4.3. The Pre-miR-34a Mediated Repression of Expression from a Tau 3'-UTR Luciferase Reporter Construct is miR-34a Seed region-Dependent in M17D cells. The indicated luciferase reporter constructs and Pre-miRs were co-transfected into M17D cells. After 48 h, luciferase expression was determined at the protein level by (A) dual luciferase assay or at the mRNA level by (B) qPCR. For each experiment, $n = 3$ biological replicates. Error bars indicate SEM. Data analyzed by unpaired *t*-test. *,****, adjusted $p < 0.05$ and 0.0001, respectively.

miR-34a seed region was sensitive to Pre-miR-34a, whereas the miR-34a seed region mutant was not (Figure 4.3B). These results indicate that miR-34a can affect the expression of reporter constructs containing the miR-34a binding site at both the level of protein and mRNA.

In order to investigate the ability of miR-34a to regulate the expression of endogenous tau, Pre-miR-34a or a non-targeting negative control Pre-miR was transfected into M17D cells. After 48 h, the cells were lysed, and a Western blot probing for total tau, SIRT1, and GAPDH was performed. SIRT1 was included as a positive control, as it is a known target of miR-34a (Yamakuchi et al., 2008), and GAPDH was included as a loading control. Cells transfected with Pre-miR-34a had reduced expression of tau and SIRT1 compared to cells transfected with the negative control Pre-miR (Figure 4.4A), demonstrating that miR-34a can control endogenous tau protein expression. To determine the ability of endogenous miRNAs to regulate endogenous tau expression, locked nucleic acid (LNA) microRNA inhibitors of miR-34a, -34b, and -34c were transfected into M17D cells and the Western blot analysis was performed as described above. A combination of LNA inhibitors of all miR-34 family members was used to prevent possible compensation by other family members if an inhibitor of only one family member were used. The Western blot analysis revealed that inhibition of endogenous miR-34 family members led to a moderate increase in endogenous tau protein expression (Figure 4.4B). However, no effect on SIRT1 was detected (Figure 4.4B). The effect of Pre-miR-34a or LNA inhibition of miR-34 family members on the expression of endogenous total tau mRNA in M17D cells was examined using qPCR, with GAPDH mRNA serving as a normalization control. In agreement with the Western blot data, Pre-miR-34a reduced tau mRNA expression (Figure 4.4C), whereas inhibition of miR-34 family members led to an increase in tau mRNA expression (Figure 4.4D). Taken

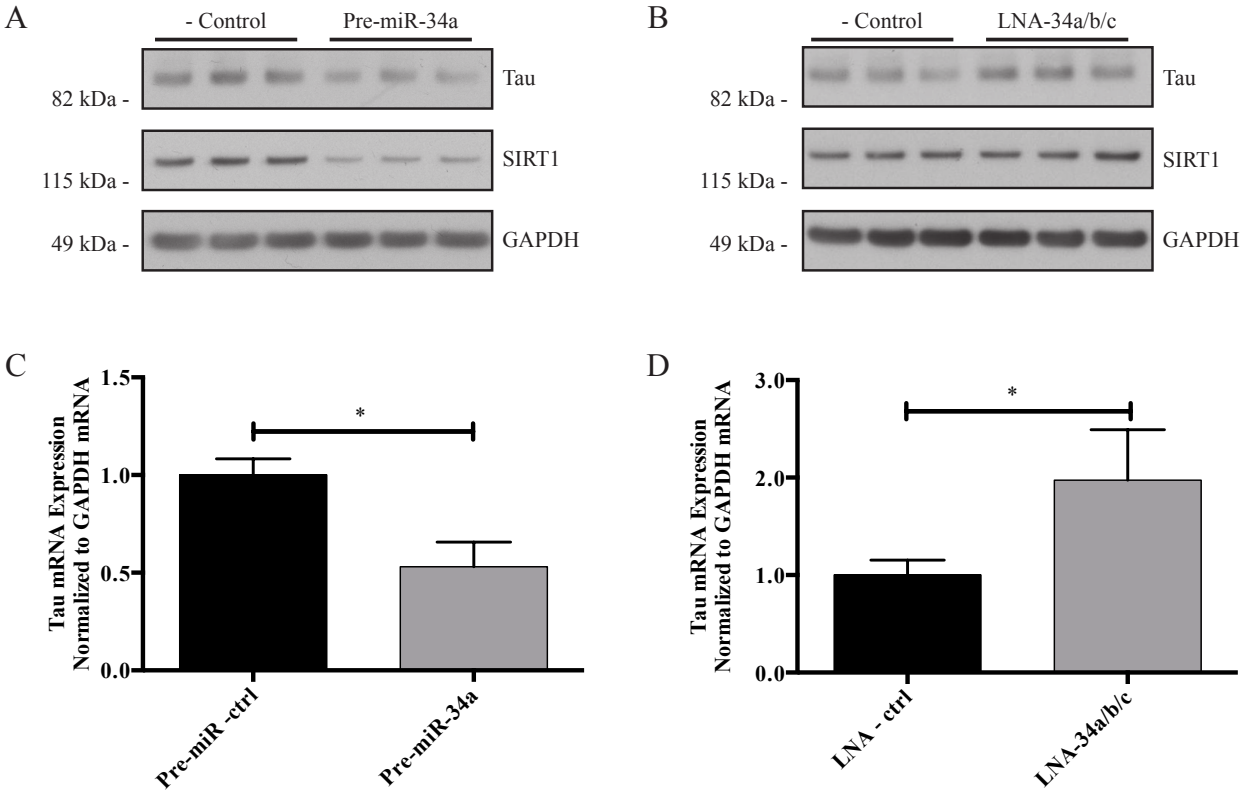

Figure 4.4. miR-34 Family Members Regulate the Expression of Endogenous Tau. The indicated oligonucleotides were transfected into M17D cells. Pre-miRs were used at a concentration of 50 nM. The LNA for each of miR-34 family members had a final concentration of 20 nM, for a final total LNA concentration of 60 nM. The negative control LNA was used at a concentration of 60 nM. After 48 h, the cells were lysed. A and B. Western blot analysis was performed using primary antibodies for tau, SIRT1, and GAPDH. C and D. qPCR was performed using TaqMan probes for tau and GAPDH. For each experiment, $n = 3$ biological replicates. Error bars indicate SEM. Data analyzed by unpaired *t*-test. *, adjusted $p < 0.05$.

together, these data indicate that endogenous miR-34 family members regulate tau expression at both the protein and mRNA levels.

The members of the miR-34 family share a common seed region (Figure 4.5A), and according to the DIANA-microT database (Maragkakis et al., 2009), each member of the family is predicted to bind the human tau 3'-UTR (Figure 4.5B, C, & D). However, for this study, miR-34a is the one of most interest since it is the miR-34 family member with the highest expression in brain tissue (Bommer et al., 2007) and since its expression is upregulated in brain tissue (Cogswell et al., 2008) and blood mononuclear cells (Schipper et al., 2007) from patients with AD. Therefore, the role of endogenous miR-34a in regulating endogenous tau expression was examined by transfecting M17D cells with 50 or 100 nM LNA inhibitor of miR-34a (LNA-34a). The cells were lysed 48 h after transfection, and a luciferase assay was performed as described above. At a concentration of 50 nM, LNA-34a produced a modest increase in tau protein levels (Figure 4.6A), and the effect was more pronounced at a concentration of 100 nM (Figure 4.6B). Again, not effect on SIRT1 was observed (Figure 4.6). These data suggest endogenous miR-34a can regulate the expression of endogenous tau.

Discussion

In the initial screen with commercially available precursor miRNAs (Pre-miRs) of the candidate miRNAs, two were found to affect the expression of a luciferase reporter construct containing a fragment of the human tau 3'-UTR containing the predicted miRNA binding site (Figure 4.1). These two Pre-miRs, Pre-miR-34a and Pre-miR-132, did not alter the expression of the empty luciferase reporter vector (Figure 4.1), indicating that the observed effect was not due to a general alteration in gene expression. Mutation of the miR-34a seed region in the luciferase reporter vector made it insensitive to Pre-miR-34a (Figure 4.2C), which is consistent with the

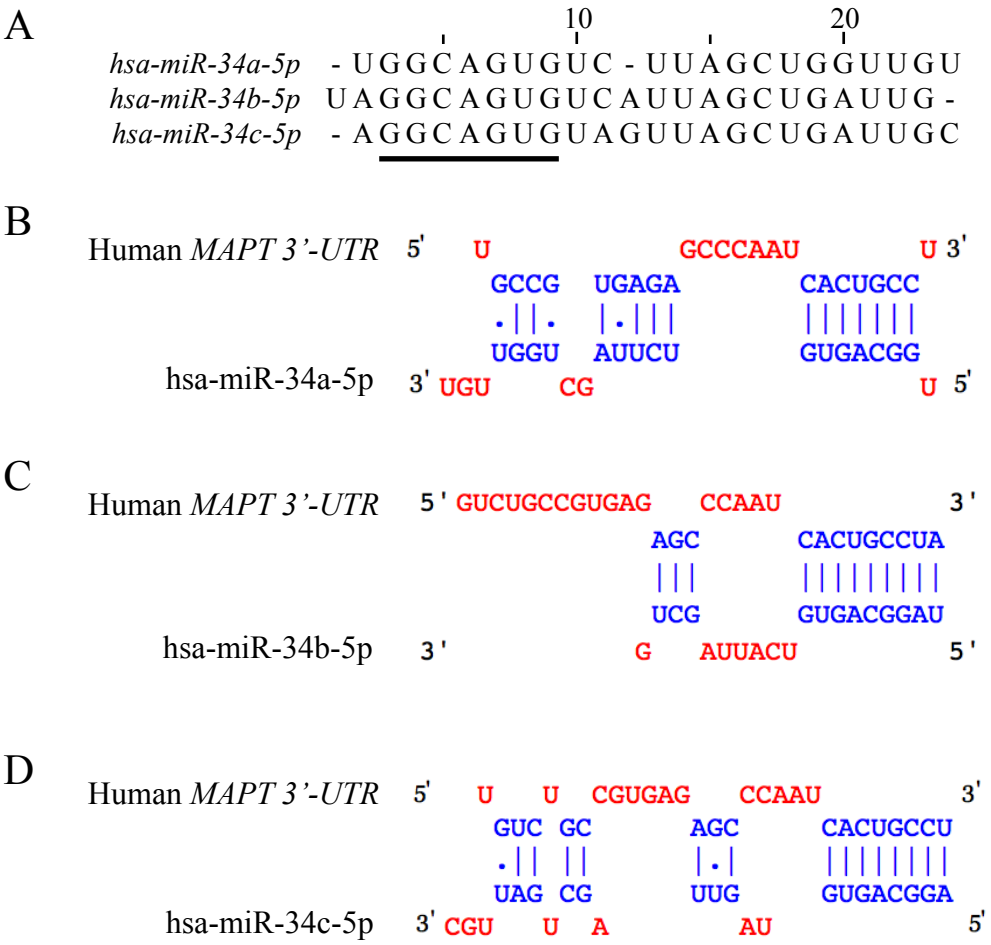

Figure 4.5. hsa-miR-34 Family Members and Their Predicted Binding to the Human Tau 3'-UTR. A. ClustalW alignment of the hsa-miR-34 family members. The common seed region is underlined. The predicted binding of (B) hsa-miR-34a-5p, (C) hsa-miR-34b-5p, and (D) hsa-miR-34c-5p to the human tau 3'-UTR using DIANAmicro-T is shown.

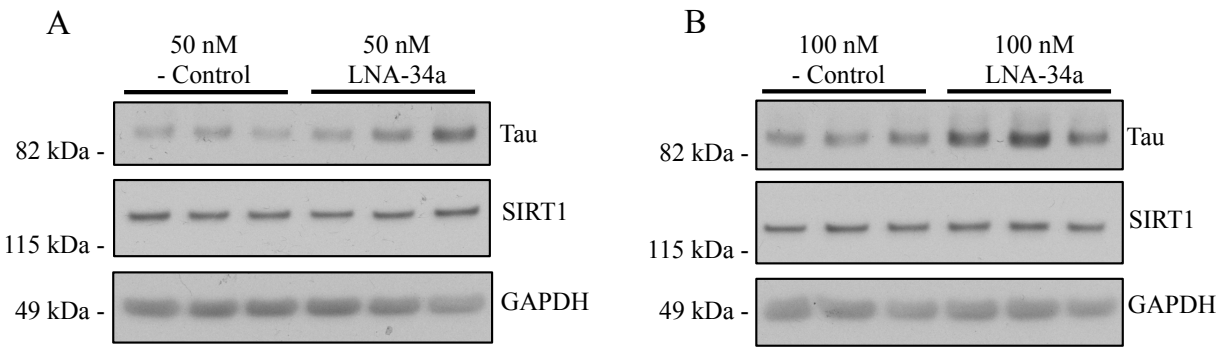

Figure 4.6. miR-34a Regulates the Expression of Endogenous Tau. A non-targeting negative control LNA or LNA-34a was transfected into M17D cells. After 48 h, the cells were lysed. Western blot analysis was performed using primary antibodies for tau, SIRT1, and GAPDH. A. [LNA] = 50 nM. B. [LNA] = 100 nM.

mutated seed region being part of a *bone fide* miR-34a binding site in the tau 3'-UTR. However, the luciferase reporter constructs containing both the wild-type or mutant miR-132 seed region were sensitive to Pre-miR-132 (Figure 4.2D), suggesting Pre-miR-132 is affecting the luciferase reporter via a mechanism that does not involve binding to the predicted miR-132 seed region.

The mechanism by which Pre-miR-132 affects the expression of the 3730-4163 tau 3'-UTR luciferase construct is currently unclear. However, since Pre-miR-132 does not affect the expression of the empty pmirGLO vector (Figure 4.1B), the effect of Pre-miR-132 is most likely mediated by the tau 3'-UTR fragment contained in the 3730-4163 construct. There are a couple of possible mechanisms by which the available data from Pre-miR-132 can be explained. The first possibility is than an additional or alternative miR-132 binding site in the tau 3'-UTR fragment besides the one in which the seed region was mutated (Figure 4.2B). The putative miR-132 binding site in which the seed region was mutated is the only miR-132 binding site in the human tau 3'-UTR predicted by both microRNA.org and DIANA-microT. Thus, if an additional or alternative miR-132 binding site still exists in the human tau 3'-UTR, it must be an unconventional binding site that is not identified by these programs. A second possibility is that miR-132 does not directly bind the human tau 3'-UTR but can indirectly affect the expression of the 3730-4163 construct. For example, miR-132 could regulate the expression of a protein that directly binds the human tau 3'-UTR and regulates its expression. In a search for miRNAs that regulate tau exon 10 splicing, miR-132 was found to cause a significant decrease in the 4R/3R ratio due to the fact that miR-132 regulates the expression of polypyrimidine tract-binding protein 2 (PTBP2), a splicing factor that also regulates the 4R/3R ratio (Smith et al., 2011). Thus, miR-132 has been demonstrated to indirectly regulate tau expression, albeit in regard to exon 10 splicing rather than 3'-UTR function. Interestingly, in the study by Smith and

colleagues, overexpression of miR-132 was found to cause a decrease in total tau levels in addition to the effect on exon 10 splicing (Smith et al., 2011). However, the mechanism by which miR-132 affected total tau levels was not examined. In addition to the role of PTBP2 as a splicing factor, it has been reported to bind the 3'-UTR of the phosphoglycerate kinase 2 transcript in mouse testis and stabilize that mRNA (Xu and Hecht, 2007). Therefore, it is conceivable that miR-132 could indirectly regulate tau expression by repressing the expression of a protein *trans*-factor that binds the human tau 3'-UTR. Further studies are required to fully understand the effect of miR-132 on the 3730-4163 construct.

In order to follow up on the results from co-transfection of wild-type or miR-34a seed region mutant tau 3'-UTR constructs and Pre-miR-34a in HEK 293 cells (Figure 4.2C), the co-transfections were repeated in M17D neuroblastoma cells. The results of the subsequent luciferase assay (Figure 4.3A) were consistent with those observed in HEK 293 cells (Figure 4.2C). Analysis of the same transfection conditions in M17D cells at the mRNA level by qPCR also revealed similar results (Figure 4.3C). Taken together, these data indicate that predicted miR-34a binding site in the human tau 3'-UTR is a *bona fide* miR-34a binding site, and that binding of miR-34a to this site can affect the levels of both protein and mRNA from transcripts containing this miR-34a binding site.

While the use of luciferase reporter constructs in studying miRNAs has utility in screening for miRNA binding sites and in generating seed region mutants to define the miRNA binding site, it is essential to test the effect of the candidate miRNA on the endogenous target gene of interest in order to further validate the miRNA-target mRNA pair. To accomplish this, Pre-miR-34a or negative control Pre-miR was transfected into M17D cells, and tau expression was evaluated at the protein level by Western blot (Figure 4.4A) and at the mRNA level by

qPCR (Figure 4.4C). The results were in agreement with those using the luciferase reporter constructs: Pre-miR-34a causes a decrease in both tau protein and mRNA levels.

Notably, miR-34a expression is upregulated in brain tissue (Cogswell et al., 2008) and blood mononuclear cells (Schipper et al., 2007) from patients with AD. Previous studies have shown additional links between miR-34a and the nervous system. miR-34a is involved in neuronal differentiation (Agostini et al., 2011a; Aranha et al., 2011) and neurite outgrowth (Agostini et al., 2011b). In *Drosophila melanogaster*, deletion of the fly ortholog miR-34 causes accelerated brain aging and neurodegeneration (Liu et al., 2012).

In addition to AD, miR-34a has been implicated in other diseases. In a mouse model of acute myocardial infarction (AMI), miR-34a expression was significantly increased at the border zone of the myocardial infarction. In mice, inhibition of miR-34a resulted in improved cardiac contractile function two weeks after AMI compared with mice treated with a non-targeting control (Boon et al., 2013). miR-34a is a tumor suppressor, and the role of miR-34a in cancer has been extensively studied. Decreased miR-34a expression, either through chromosomal deletion or epigenetic inactivation, has been observed in numerous types of cancer, including retinoblastoma, breast cancer, lung cancer, and colon cancer (Hermeking, 2010). The most well-characterized role of miR-34a in cancer is its involvement in the p53-miR-34a-SIRT1 positive feedback loop (Yamakuchi and Lowenstein, 2009). p53 directly binds the promoter of the primary miR-34a (pri-miR-34a) transcript and induces its expression (He et al., 2007). miR-34a directly binds the 3'-UTR of the deacetylase SIRT1 and decreases its expression (Yamakuchi et al., 2008). Deacetylation of p53 by SIRT1 reduces its activity as a transcription factor for target genes involved in cell cycle exit or apoptosis (Vaziri et al., 2001). Integrating these findings,

p53 induces miR-34a, which inhibits an inhibitor of p53 (SIRT1), thus creating a positive feedback loop (Yamakuchi and Lowenstein, 2009).

In addition to miR-34a, there are two other miR-34 family members in humans: miR-34b and -34c (He et al., 2007). miR-34a is processed from a primary transcript encoded on human chromosome 1p36. The other two members of the miR-34 family, miR-34b and -34c are co-transcribed from the same locus on human chromosome 11q23 (Yang, 2011). Because they are transcribed from different loci, the miR-34 family members can have different expression profiles, with the expression of miR-34a being highest in the brain and the expression of miR-34b and -34c being highest in the lungs (Bommer et al., 2007). Although miR-34b and -34c have been studied somewhat less extensively than miR-34a, it is known that their expression is reduced in several types of cancer (Hermeking, 2010).

Shortly before the preparation of this dissertation, Wu and colleagues published a study focused on understanding mechanisms underlying paclitaxel resistance in gastric cancers. They found that miR-34c expression was significantly reduced in paclitaxel-resistant gastric cancer, and in a search for a possible mechanism underlying this observation, they found that miR-34c regulates tau expression (Wu et al., 2013). The miR-34c binding site in the tau 3'-UTR identified by Wu and colleagues (Wu et al., 2013) corresponds to the miR-34a binding site identified in the studies presented here (Figure 4.2A&C). This is not surprising, given that members of the miR-34 family share the same seed region sequence (Figure 4.5).

In examining the effect of inhibiting endogenous miR-34 family members on endogenous tau, LNA inhibitors of each miR-34 family member were included in the transfection mixture in order to prevent compensation for inhibition of one family member by other family members. Inhibition of miR-34 family members resulted in increased tau protein and mRNA levels

(Figures 4.4B&D). These data, especially in conjunction with the observation by Wu and colleagues that treatment with Pre-miR-34c lowers tau expression(Wu et al., 2013), suggest that endogenous miR-34 family members regulate endogenous tau. Since miR-34a is of particular interest in these studies due to its dysregulation in AD (Cogswell et al., 2008; Schipper et al., 2007), the specific effect of inhibiting endogenous miR-34a on endogenous tau expression was examined. Inhibition of miR-34a resulted in an increase in tau protein expression, with a more pronounced effect at an LNA concentration 100 nM compared to 50 nM (Figure 4.6). This result is consistent with the hypothesis that miR-34a directly binding the tau 3'-UTR and regulates tau expression.

While the data presented here strongly suggest miR-34 family members, and miR-34a in particular, directly bind the human tau 3'-UTR and regulate tau expression, there are some limitations to these studies. Two human cell lines, including a neuroblastoma cell line, were used in these experiments; however, similar experiments have not been conducted in primary neurons, which would be a particularly relevant cell type for these studies. In theory, primary neurons from rat or mouse could be used in follow-up studies since the miR-34 family binding site in the human tau 3'-UTR is conserved in these species. Since the goal of the research presented in this dissertation is directed toward understanding the role of the human tau 3'-UTR in regulating tau expression, using rodent primary neurons would carry their own limitations in achieving this goal. An approach that would circumvent the caveats associated with both using transformed or cancerous human cell lines and using rodent primary neurons would be to use human neurons. Several sources of human neurons exist, including fetal human primary neurons, adult human primary neurons, differentiation of human embryonic stem cells, differentiation of human induced pluripotent stem cells, and differentiation of adult neural stem

cells. The use of these human neuronal cells come with their own challenges, depending of the cell type, including limited tissue available, difficulty obtaining a pure neuronal culture, the need to transform or differentiate cells, difficulty with reproducibility given the inherent variability in the human population, and ethical concerns over the use of fetal or embryonic human tissue (Gibbons and Dragunow, 2010).

Another limitation comes from the use of LNAs to inhibit the endogenous miRNAs. A successful experiment of that type depends on a number of factors. The miRNA(s) of interest must be expressed to a sufficient levels in the cell type used in order for inhibition of the miRNA(s) to have an effect on the expression of the target mRNA. The target mRNA containing the miRNA binding site(s) must be expressed at level such that changes in expression of target will be detectable by the assay method. Additionally, the cell type used must have a transfection efficiency high enough for an appreciable effect of the LNA to be observed. These factors all seem to have allowed for a successful experiment with regard to tau in M17D cells since an effect was observed (Figures 4.4 and 4.6), but the challenges associated with this method may explain why no effect was seen on SIRT1. Another limitation of using LNAs, specifically in the case of inhibiting miR-34a alone, is that an LNA inhibitor could inhibit miRNAs besides the intended target. This is particularly true if the miRNA of interest shares substantial sequence similarity with other miRNAs, as is the case with miR-34a and the other miR-34 family members (Figure 4.5A). Thus, in the experiment with miR-34a inhibition only (Figure 4.6), it is not possible to unequivocally conclude that the effect observed is due only to inhibition of miR-34a. An alternative approach that would more definitively address the role of a specific miRNA in regulating a target gene would be to delete the miRNA of interest from the genome entirely. While not a human system, mice in which miR-34a, miR-34b/c, and miR-34a/b/c have been

knocked out have been reported (Concepcion et al., 2012). These would be interesting system for the future study of the effect of the miR-34 family on tau expression.

Despite the limitations discussed above, the results presented in this chapter indicate the miR-34 family, and miR-34a specifically, play a role in regulating tau expression. This is particularly interesting given that miR-34a expression is increased in AD (Cogswell et al., 2008; Schipper et al., 2007) and that decreased tau expression prevents the development of an AD-like phenotype in transgenic mouse models of AD (Ittner and Götz, 2010; Roberson et al., 2007). These observations raise the questions of if and how the changes in miR-34a expression relate to the pathophysiology of AD. One possibility is that the upregulation of miR-34a may act as a compensatory mechanism to decrease the expression of tau as tau protein accumulates and aggregates during disease progression. Further studies are needed to explore these questions.

Chapter 5

Summary and Future Directions

Summary

The human tau 3'-UTR has not previously been studied in much detail. Discovering the role the human tau 3'-UTR plays in regulating tau expression will increase the understanding of the basic biology of tau. Additionally, it may eventually allow the development of novel strategies to modulate tau expression in humans, which may be therapeutic in Alzheimer's disease. Therefore, the studies presented here aimed to investigate the function of the human tau 3'-UTR.

For the first time, the 3'-ends of the two human tau 3'-UTR isoforms were defined using 3'-RACE, allowing the identification of the PAS and cleavage and polyadenylation site used for each isoform. The studies presented here are the first to show that the expression of the tau 3'-UTR isoforms is differentially regulated (Figures 2.3 and 2.4). The process of APA, which produces the tau 3'-UTR isoforms, is a mechanism by which gene expression is temporally and spatially regulated (Shi, 2012). Thus, APA may allow for the expression of appropriate levels of tau specific to different cell types and developmental stages.

Since the sequence of the short tau 3'-UTR is common to both isoforms, it is logical to assume that any *cis*-elements responsible for the differential regulation of tau expression must be present only in the long tau 3'-UTR isoform. In order to identify such regulatory *cis*-elements, an unbiased search for these was undertaken, and several regions containing *cis*-elements were identified. One of those, fragment 1114-1279 (Figure 3.5), contains the seed region for miR-34 family members, which were subsequently shown to bind that region (Figures 4.2 and 4.3). Additional fragments containing *cis*-elements were identified, but further research is necessary in order to determine the minimal *cis*-element in these fragments and to identify the *trans*-factors that bind them.

In an effort to identify a specific type of *trans*-factor that may bind the tau 3'-UTR, miRNAs, a candidate-based approach of screening selected miRNAs was undertaken in parallel with the unbiased screen for *cis*-elements. Through these efforts, miR-34a was found to bind the tau 3'-UTR and regulate tau expression. These results complement the recently published finding that miR-34c regulates tau expression in gastric cancer cells (Wu et al., 2013). The miR-34 family members have the same seed region sequence and are predicted to bind the human tau 3'-UTR (Figure 4.5). Wu and colleagues only examined the effect of increased miR-34c (Wu et al., 2013), and work present here adds to their findings by demonstrating that the inhibition of endogenous miR-34 family members increases endogenous tau expression (Figure 4.4). In the studies presented in this dissertation, miR-34a instead of miR-34c was of particular interest because miR-34a is more highly expressed in the brain (Bommer et al., 2007) and because miR-34a is upregulated in AD (Cogswell et al., 2008; Schipper et al., 2007). The studies presented here are the first to show that miR-34a can regulate the expression of endogenous tau.

Overall, these findings suggest a model in which the miR-34 family binding site, along with additional regulatory *cis*-elements present only in the long tau 3'-UTR isoform, decrease the expression of the long tau 3'-UTR relative to the short one (Figure 5.1). These findings provide new insights into the basic biology of tau. They also suggest areas for additional research to better understand the role of APA in regulating tau expression in normal and diseased states, as well as to identify additional *cis*-elements and *trans*-factors involved in regulating tau expression.

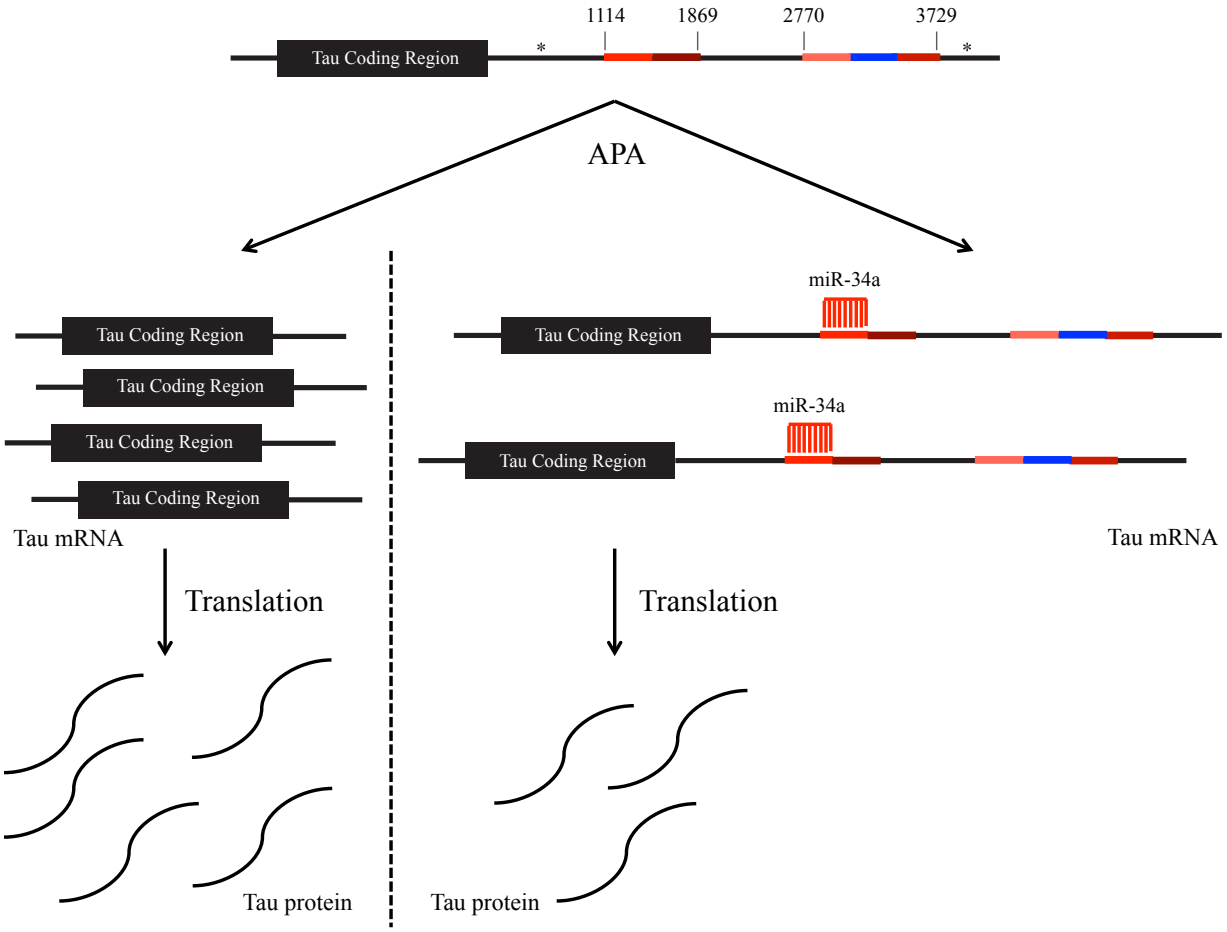

Figure 5.1. Summary of Findings. The human tau 3'-UTR contains several regions that contain regulatory *cis*-elements. Those that decrease expression are shown in shades of red, and the *cis*-element that enhances expression is shown in blue. Nucleotides at the boundaries of regions containing *cis*-elements are indicated. The numbering begins with the first nucleotide following the stop codon. The human tau 3'-UTR contains two PASs (indicated by asterisks), and undergoes APA to produce long and short 3'-UTR isoforms. The long isoform only contains the regulatory *cis*-elements. The miR-34a binding site is indicated. The presence of the regulatory *cis*-elements in the long isoform causes its expression to be reduced at the mRNA and protein levels, relative to the short isoform.

Future Directions

Determining the Half-Lives of the Tau 3'-UTR Isoforms

While the results presented here reveal that the two human tau 3'-UTR isoforms are differentially expressed at the mRNA level (Figure 2.3), they do not specifically examine mRNA stability. As a first step in investigating the possible differences in mRNA stability between the 3'-UTR isoforms, mRNA expression of the tau 3'-UTR isoform constructs can be measured in a time course following inhibition of transcription by actinomycin D treatment. These measurements will allow the determination of the half-lives of the constructs, which can be used to compare the stability of the two tau 3'-UTR isoform constructs.

As a follow up to this experiment, the half-lives of the endogenous tau 3'-UTR isoform transcripts should also be determined in a manner similar to that described above. However, to allow for direct measurement of the tau 3'-UTR isoform levels, the total RNA from the time course should be analyzed by Northern blot.

APA of Tau in Development

Global changes in APA occur during the process of development, with a trend toward expression of longer 3'-UTRs as development progresses (Ji et al., 2009). Changes in alternative splicing of tau occur during brain development (Andreadis, 2005; Andreadis et al., 1992), so it is reasonable to investigate possible changes in the APA of tau during development. Ultimately, definitive examination of APA in human brain development will require assessment of 3'-UTR isoform levels in human embryonic and fetal brain regions over the course of development and correlation of these levels with tau protein levels from the same tissues at the same developmental stages. The expression of the tau 3'-UTR isoform mRNA and tau protein levels can be determined by Northern blot and Western blot, respectively. There are a number of

technical challenges to this approach, including obtaining a sufficient number of samples at various developmental stages and obtaining mRNA of sufficient quality from postmortem human tissue.

Given the challenges associated with this definitive approach, a reasonable first step would be to examine APA of tau in development generally as described above but using rats instead of humans. While there are clearly differences between the human and rat tau 3'-UTR, the rat may be a good model system to explore the role of APA of tau in development prior to beginning those studies in humans. Before examining tau APA in rat development, experiments from Chapter 2 should be repeated using rat instead of human tau 3'-UTR isoform constructs.

Investigating the Possible Dysregulation of the APA of Tau in Alzheimer's Disease

A previously published Northern blot of tau in mRNA from frontal cortex of AD patients and normal controls showed an increase in the short tau 3'-UTR in AD samples (Goedert et al., 1988). At the time, it was not clear what the 2 kb and 6 kb bands, which are now recognized as the tau 3'-UTR isoforms, represented (Goedert et al., 1988; Poorkaj et al., 2001), and the finding was not explored further. This is an interesting and potentially important finding since alterations in the expression levels of 3'-UTR isoforms produced by APA have been observed in some diseases. Global dysregulation of APA has been observed in cancer (Mayr and Bartel, 2009) and cardiac hypertrophy (Park et al., 2011). While other explanations of the finding of tau 3'-UTR isoform level changes are possible, one interesting hypothesis is that the APA of tau is dysregulated in AD.

At the very least, the Northern blot experiment by Goedert and colleagues (Goedert et al., 1988) deserves repeating to determine if the results are reproducible. However, an improved study design would be to globally assess APA states in the frontal cortex of AD and control

subjects using transcriptome-wide RNA sequencing (RNA-seq). Not only would this provide quantitative data on the tau 3'-UTR isoform levels in AD and control frontal cortex, but it would also provide a context for understanding any changes seen specifically seen for tau. That is, if a change in tau 3'-UTR isoform expression is seen when comparing AD and control subjects, is that change specific for tau, or does it occurs in the setting of global changes in APA in AD? Any changes in 3'-UTR isoform expression seen for tau or other key genes as identified by RNA-seq could be confirmed by Northern blot. These studies may provide valuable insights into the possible contribution of a dysregulation of APA to AD pathogenesis.

Investigating the Role of the Human Tau 3'-UTR in the Subcellular Localization of Tau

Tau mRNA is localized to the axon and soma (Litman et al., 1993), and the rat tau 3'-UTR contains an axonal localization signal (Aronov et al., 2001). However, the sequence of this axonal localization signal is not well conserved in human (Poorkaj et al., 2001). Therefore, it is not currently known if the human tau 3'-UTR contains an axonal localization signal. If it does, and it is found in the long 3'-UTR isoform only, the two tau 3'-UTR isoforms should show a different pattern of subcellular localization.

In order to examine this, the tau 3'-UTR isoform constructs can be transfected into differentiated SH-SY5Y cells, which have distinct axon-like neurites and dendrite-like neurites (see Appendix 1). The subcellular localization of the firefly luciferase reporter constructs can then be determined by fluorescence *in situ* hybridization (FISH) with an antisense probe for the firefly luciferase coding region. The use of the tau 3'-UTR isoform luciferase reporter constructs would allow the detection of transcripts containing only the 3'-UTR isoform expressed by the construct by allowing a probe for firefly luciferase, rather than tau, to be used. If a difference in localization between the two tau 3'-UTR isoform constructs is observed, it will indicate that

APA is a mechanism of regulating the subcellular localization of tau, presumably via the inclusion or exclusion of an axonal localization signal.

Identification of Regulatory cis-*Elements in the Human Tau 3'-UTR*

The unbiased search for regulatory *cis*-elements in the human tau 3'-UTR in Chapter 3 allowed for the identification of several regions that likely contain regulatory *cis*-elements. However, with the exception of the miR-34 family member binding site, the exact locations of these regulatory *cis*-elements remain to be determined. In order to fully identify the regulatory *cis*-elements in the human tau 3'-UTR, the process of iteratively making smaller fragments of regions that influence expression of the tau 3'-UTR fragment luciferase reporter constructs and then testing those smaller fragments to determine which one(s) contain regulatory *cis*-elements can be used. Once the minimal *cis*-elements have been defined, the effect of the sequence on the expression of the luciferase reporter construct containing it can be determined at the mRNA level by qPCR. Additionally, the *cis*-elements identified can be examined to determine if they match known binding motifs for RNA-binding proteins. If the human tau 3'-UTR is found to contain an axonal localization signal, the exact location of that *cis*-element can be determined using the iterative process described above except transfecting the constructs into differentiated SH-SY5Y cells and analyzing by FISH rather than luciferase assay.

Identification of Regulatory trans-*Factors in the Human Tau 3'-UTR*

In order to identify the *trans*-factors that bind the *cis*-elements determined above, a biotinylated RNA containing a regulatory *cis*-element can be used to pulldown its binding protein(s) from cell lysate. The protein(s) can then be separated by LDS-PAGE and ultimately identified by mass spectrometry. The ability of candidate *trans*-factors identified in this way to regulate tau expression can be tested using RNA interference (RNAi).

Examining the Effect of Additional miRNAs on the Human Tau 3'-UTR

In the screen of the candidate miRNAs, Pre-miR-132 was found to have an effect on the 3730-4163 tau 3'-UTR fragment construct without affecting the pmirGLO construct (Figure 4.1). However, mutation of the predicted miR-132 seed region (which produced the 3730-4163_mut construct) did not change the sensitivity of the construct to Pre-miR-132 (Figure 4.2), suggesting that the affect is mediated through a site other than the mutated seed region. In order to investigate this further, luciferase reporter constructs containing smaller subfragments of the tau 3'-UTR from the 3730-4163_mut construct should be cloned and tested for sensitivity to Pre-miR-132 to further localize the sequence responsible for the effect of Pre-miR-132. The smaller subfragment that is sensitive to Pre-miR-132 should be examined for a non-canonical miR-132 binding site. If one is found, it could be mutated to determine if that is the site Pre-miR-132 binds. If no obvious miR-132 binding site is found, protein *trans*-factors that may bind this region could be identified using the methods described above. Any *trans*-factors identified could then be assessed for regulation by miR-132.

Additionally, other candidate miRNAs predicted to bind the human tau 3'-UTR that were not examined in the initial round of screening can be studied with the experiments discussed in Chapter 4.

Examining the Effect of the miR-34 Family on Tau Expression in miR-34 Knockout Mice

In order to study the effect of miR-34 family members on tau *in vivo*, tau expression in the cortex and hippocampus of miR-34a, miR-34b/c, and miR-34a/b/c knockout mice (Concepcion et al., 2012) can be compared with that of wild-type littermates using Western blot and qPCR. These experiments may provide valuable insights into the effect of miR-34 family members on tau in the intact brain.

Correlation of miR-34a and Tau mRNA Levels in AD and Control Brains

Since miR-34a can repress tau expression (Figures 4.4 and 4.6) and since miR-34a levels are upregulated in AD (Cogswell et al., 2008), it is possible that increased miR-34a in AD could lead to lower tau expression in the disease. If this were the case, upregulation of miR-34a in AD may have a protective effect since reduced tau expression has been shown to ameliorate the AD phenotype in mouse models of AD (Ittner et al., 2010; Leroy et al., 2012; Roberson et al., 2007). In order to begin to investigate this possibility, miR-34a and tau mRNA expression can quantified and correlated in the medial frontal gyrus, hippocampus, and cerebellum, the regions in which miR-34a expression was found to be upregulated in AD (Cogswell et al., 2008). Measuring tau mRNA expression, rather than tau protein expression, in these studies is a reasonable choice since tau accumulates in NFTs in AD, which could confound the results. Additionally, correlating miR-34a and tau mRNA expression is reasonable since miR-34a affects tau expression at the mRNA level (Figure 4.4). Based on the currently available evidence, which is described above, one would expect miR-34a expression to be higher and tau mRNA expression to be lower in AD brain regions compared with control brain regions. This correlative study will would not provide a causal link between miR-34a and tau mRNA levels in AD, but it could be an informative study, especially in the context of the knowledge that miR-34a regulates tau expression in cell culture (Figures 4.4 and 4.6).

Conclusion

The studies presented here provide new insights into the biology of human tau, particularly the regulation of its expression by APA and miR-34a. However, these finding also bring to light new questions remain to be answered. Hopefully, continued research on this topic will advance our understanding of the basic biology tau, clarify the possible contributions of the

tau 3'-UTR and/or miR-34a to AD, and allow the development of novel therapeutic strategies for treating AD and possibly other tauopathies.

Appendix

Characterization of Differentiated SH-SY5Y Cells

Experimental contributions to the appendix: John Dickson performed all of the experiments presented in the appendix.

Introduction

In theory, the best cell culture model system to study a human gene involved in the function of neurons would be a primary culture of human neurons. However, in practice, there are a number of challenges that make the system less than ideal. New samples of human brain tissue containing viable neurons are required to initiate each new culture. Because of the inherent genetic variability in the human population, each culture will have its own unique genetic background, which can be a confounder in experiments. Additionally, the ability to perform experiments in primary human neurons is limited by the availability of suitable brain tissue from which to obtain cultures.

One alternative to using primary human neurons is to use human cancerous or transformed cells of neuronal origin, which can be maintained in culture. This allows for a ready supply of cells in the lab for experiments and provides consistency among experiments, as the same cell line can be used for all of the experiments. A disadvantage of this system is that the cancerous or transformed cells are genetically abnormal and are not fully differentiated neurons. Another possible alternative, which could in some ways be considered to be a compromise between human primary neurons and cultured cancerous or transformed human cells, is to use primary neurons from rat or mouse brains. These neurons can be readily obtained from rodents kept for research purposes, and the use of inbred laboratory strains allows the rodent primary neurons to have a more homogenous genetic background than is possible with human primary neurons. A disadvantage of using rodent primary neurons to study human genes is that these neurons are not derived from humans. In many cases, this is not a major problem due to conservation of genes between rodents and humans.

In the case of studying the human tau 3'-UTR, rodent primary neurons are not an ideal model system because the rodent and human tau 3'-UTRs are not well conserved (Poorkaj et al., 2001). Additionally, human primary neurons are not ideal for these studies for the reasons discussed above. Therefore, cultured human cells were chosen as model system for studying the human tau 3'-UTR. One of the cell lines chosen for these studies was the SH-SY5Y human neuroblastoma cell line, which grows neurites when differentiated by sequential treatment with retinoic acid and BDNF (Encinas et al., 2000). Having axon-like neurites is particularly important for cells used to study the possible function of the human tau 3'-UTR in directing the subcellular localization of tau mRNA. In order to determine the suitability of differentiated SH-SY5Y cells for studies involving the function of the human tau 3'-UTR, the cells were characterized in with regard to their expression of the tau 3'-UTR, their ability to form axon-like and dendrite-like neurites, and their pattern of tau mRNA localization.

Methods

Cell Culture

The culture and differentiation of SH-SY5Y cells were performed as described in Chapter 2. For cells to be imaged by microscopy, cells were cultured on fibronectin-coated coverslips placed in the wells of a 24-well plate. For the coating of sterile glass coverslips with fibronectin, 2 μg fibronectin from human plasma (Sigma-Aldrich) were diluted in 100 μL Dulbecco's phosphate-buffered saline (DPBS) (Life Technologies) per well. The coverslip was placed in a well, and the diluted fibronectin solution was added to the well and allowed to incubate at room temperature for 45 minutes.

Preparation of Human Frontal Cortex cDNA

Human frontal cortex total RNA (Agilent Technologies) was reverse transcribed to cDNA using Double Primed RNA to cDNA EcoDry Premix (Clontech) according to the manufacturer's instructions.

Polymerase Chain Reaction (PCR)

Sequences spanning human tau exon 13 to 3'-UTR (TauEx13-3UTR), human long tau 3'-UTR only (Tau_long3UTR), and GAPDH were amplified from human frontal cortex cDNA by PCR using KAPA HiFi HotStart ReadyMix (Kapa Biosystems) according to the manufacturer's instructions, with an annealing temperature of 65ºC. The primers used for PCR are listed in Table A.1.

Table A.1. Primers Used in the Cloning of Tau and GAPDH Probes.

Construct	*Location*	*Orientation*	*Sequence (5' to 3')*
TauEx13-3UTR	Ex13 65-88	Forward	CTAGCCTCGAGAATTCTCGTGTACAAGTCGCCAG TGGTGT
TauEx13-3UTR	3UTR 112-138	Reverse	GGGAAGCGGCCGCCCGGGGCCGGGTCATTATTC CCAATTAACCGA
Tau_long3UTR	3UTR 2847-2866	Forward	CTAGCCTCGAGAATTCCCCTGCCGTTCGCTGAGT CC
Tau_long3UTR	3UTR 3115-3136	Reverse	GGGAAGCGGCCGCCCGGGATCTGCCAGCACTGA TCACCCT
GAPDH	Ex8 95-116	Forward	CTAGCCTCGAGAATTCCCTGCCTCTACTGGCGCT GC
GAPDH	Ex8 368-387	Reverse	GGGAAGCGGCCGCCCGGGGTTGAGGGCAATGCC AGCCC

Restriction Digest of pCI-neo Vectors

The pCI-neo Mammalian Expression Vector (Promega) contains a T7 RNA polymerase promoter 5' to the multiple cloning site and a T3 RNA polymerase promoter 3' to the multiple cloning site. Additionally, it contains an ampicillin resistance gene to allow for selection in bacteria. The pCI-neo vector and constructs based on the pCI-neo vector were subjected to restriction digests in 1X Buffer 4 (New England Biolabs), 1X bovine serum albumin (New

England Biolabs), and 0.5 µL the desired restriction enzyme (New England Biolabs) in a total reaction volume of 50 µL. *SmaI* digests were performed at 25 ºC for 30 min. *EcoRI* digests were performed at 37 ºC for 30 min. Double digests were performed sequentially, with the *SmaI* digest followed by the *EcoRI* digest. Restriction enzymes were inactivated by incubation at 65 ºC for 20 min. *NotI*-HF digests were performed at 37 ºC for 1 h.

Agarose Gel Electrophoresis

Agarose gel electrophoresis was performed as described in Chapter 2.

Gel Extraction of DNA

Gel extraction of DNA was performed as described in Chapter 2.

Cloning

Cloning was performed as described in Chapter 2.

Transformation of Bacteria

Transformation of bacteria was performed as described in Chapter 2.

Plasmid Preparation

Plasmid preparation was performed as described in Chapter 2.

Preparation of Biotinylated dsDNA Northern Blot Probes by PCR

The TauEx13-3UTR, Tau_long3UTR, and GAPDH constructs were used as templates for PCR doped with biotinylated dUTP using the SuperTaq Plus Polymerase (Life Technologies) using the primers in Table A1.1 with the following reaction conditions:

100 ng DNA template

5.0 µl 10X Long PCR Buffer (Life Technologies)

1.0 µL 10 mM dATP (Life Technologies)

1.0 µL 10 mM dCTP (Life Technologies)

1.0 µL 10 mM dGTP (Life Technologies)

0.6 µL 10 mM dTTP (Life Technologies)

4.0 µL 1 mM biotin-16-dUTP (Roche)

0.25 µL 5 U/µL SuperTaq Plus Polymerase (Life Technologies)

2 µL 10 µM Forward Primer

2 µL 10 µM Reverse Primer

The PCR cycles were performed according to protocol provided with SuperTaq Plus Polymerase with an annealing temperature of 62 ºC. The biotinylated dsDNA probes generated by PCR were subjected to agarose gel electrophoresis and gel extraction as described above.

Preparation of Nonisotopically Labeled ssRNA Fluorescence *in situ* Hybridization Probes by *in vitro* Transcription

The TauEx13-3UTR, Tau_long3UTR, and GAPDH constructs were digested with *EcoRI* as described above for preparation as a template for *in vitro* transcription of antisense ssRNA probes or with *NotI*-HF as described above for preparation as a template for *in vitro* transcription of sense ssRNA probes. The *in vitro* transcription was performed with the MAXIscript Kit (Life Technologies) according to the manufacturer's instructions for nonisotopic labeling with digoxigenin-11-UTP (Roche). The T3 RNA polymerase was used for the *in vitro* transcription of antisense probes, while the T7 RNA polymerase was used for the *in vitro* transcription of sense probes. Both of these RNA polymerases are included in the MAXIscript Kit. The labeled ssRNA products of *in vitro* transcription were precipitated with ammonium acetate according to the MAXIscript Kit protocol, and they were resuspended in nuclease-free water (Life Technologies).

PAGE Purification of ssRNA Probes

The biotinylated ssRNA products of *in vitro* transcription were purified by PAGE according to the MAXIscript Kit protocol. The bands were visualized by UV shadowing using a Fluor-Coated TLC Plate (Life Technologies) under short wave UV illumination. The bands were excised from the gel, fragmented, and placed in a probe elution buffer consisting of 0.5 M ammonium acetate, 1 mM EDTA, and 0.2% SDS, and incubated at 37 ºC overnight. The eluted probe was precipitated by the ammonium acetate precipitation protocol provided with the MAXIscript Kit.

Total RNA Isolation

Total RNA isolation was performed as described in Chapter 2.

Northern Blot

Agarose gel electrophoresis of 6 µg total RNA was performed with the NorthernMax-Gly Kit (Life Technologies) according to the manufacturer's protocol. The RNA was transferred to a the BrightStar-Plus Positively Charged Nylon Membrane (Life Technologies) by electroblotting using the Genie Blotter (Idea Scientific) in 1X NorthernMAX MOPS Gel Running Buffer (Life Technologies) at 12 V for 1 h according to the protocol provided with the Genie Blotter. Following the transfer, the RNA was crosslinked to the membrane by baking at 80 ºC for 15 min. During the crosslinking, ULTRAhyb hybridization buffer (Life Technologies) was preheated to 42 ºC. The crosslinked membrane was placed in a hybridization tube, to which 10 mL preheated ULTRAhyb buffer was added. The membrane was prehybridized in the ULTRAhyb buffer for at least 30 min at 42 ºC with rotation in a roller oven. During the prehybridization, the biotinylated dsDNA probe was prepared for hybridization: 37.5 ng of biotinylated dsDNA probe was heat denatured in 50 µL 10 mM EDTA at 90 ºC for 10 min. At the end of the probe

denaturation, 0.5 mL ULTRAhyb buffer used in the prehybridization was removed from the hybridization tube, and the denatured probe was added to it. The ULTRAhyb buffer containing the probe was added back to the hybridization tube containing the membrane and the rest of the ULTRAhyb buffer from the prehybridization. The hybridization tube was placed in the roller oven, and the probe was hybridized to the membrane at 42 ºC overnight with rotation. Following the hybridization, the membrane was subjected to a low stringency wash in a 2X SSC, 0.1% SDS solution for 10 min and room temperature. The membrane was then subjected to two high stringency washes in a 0.1X SSC, 0.1% SDS solution for 15 min each at 42 ºC. The biotinylated probes were visualized using the BrightStar BioDetect Nonisotopic Detection Kit (Life Technologies) according to the manufacturer's instructions with wash times following incubation with the Strep-Alkaline Phosphatase extended to 15 minutes each. The substrate for alkaline phosphatase included with the kit is CDP-*Star*. The probes were stripped from the membrane by pouring 200 mL boiling 0.1% SDS solution over it and allowing the SDS solution to cool to room temperature. The stripping was repeated with another 200 mL of boiling 0.1% SDS solution.

Immunofluorescence (IF)

Cells were washed with phosphate buffered saline (PBS) and fixed in 3.65% formaldehyde (Sigma-Aldrich) in PBS for 15 min at room temperature. The cells were then rinsed twice with ice-cold PBS. Cells were permeablized in 0.25% Triton X-100 in PBS for 10 min at room temperature. Cells were washed three times in PBS for 5 min each. Blocking was performed by incubating cells in 1% bovine serum albumin in PBS containing 0.1% Tween-20 (PBST) containing 0.3M glycine. Mouse anti-tau antibody (AnaSpec) and/or rabbit polyclonal anti-MAP2 antibody (Abcam) were diluted 1:100 in 1% bovine serum albumin in PBST and

incubated with the cells in a humidified chamber for 1 h. Cells were washed three times in PBS for 5 min each. Secondary antibodies were diluted 1:100 in 1% bovine serum albumin in PBST and incubated with the cells in a humidified chamber in the dark for 1 h. For single IF, secondary antibodies Alexa Fluor 488 Goat Anti-Mouse and Alexa Fluor 488 Goat Anti-Rabbit (Life Technologies) were used. For double IF, Alexa Fluor 594 Goat Anti-Mouse and Alexa Fluor 488 Goat Anti-Rabbit (Life Technologies) were used. Cells were washed in the dark three times in PBS for 5 min each. The nuclear counterstain TO-PRO-3 (Life Technologies) was diluted 1:2,000 in PBS and incubated with the cells for 5 min in the dark. Cells were washed once in PBS for 5 min and then dipped in purified water. A drop of VECTASHIELD Mounting Medium with DAPI (Vector Laboratories) was placed on a glass microscope slide, and the coverslip was placed cell side down on the drop. Any air bubbles were pressed out with gentle pressure on the coverslip. The edges were sealed using clear SALON Nail Lacquer (Sally Hansen), which was allowed to air dry. The cells were imaged using a Zeiss LSM 510 confocal microscope.

Fluorescence *in situ* Hybridization (FISH)

Hybridization solution was prepared according to the following recipe, aliquoted, and stored at -20 ºC until needed. Hybridization solution recipe:

10 mM Tris HCl, pH 7.5 (Life Technologies)

600 mM NaCl (Life Technologies)

1 mM EDTA (Life Technologies)

0.25% SDS (Life Technologies)

10% (w/v) dextran sulfate (Sigma-Aldrich)

1X Denhardt's solution (Sigma-Aldrich)

200 µg/mL yeast tRNA (Life Technologies)

50% formamide (Life Technologies)

Cells were washed with phosphate buffered saline (PBS) and fixed in 3.65% formaldehyde (Sigma-Aldrich) in PBS for 10 min at room temperature. Cells were washed three times in PBS for 3 min each. Endogenous peroxidase activity was blocked by treat with 0.2 N HCl (Sigma-Aldrich) for 20 min at room temperature. Cells were washed twice in PBS for 3 min each. Acetylation to prevent endogenous RNase activity was performed by incubating cells in 0.1 M triethanolamine (Sigma-Aldrich) containing 2.5 µL/mL acetic anhydride (Sigma-Aldrich). Cells were permeablized by incubating with 0.1% Triton X-100 in PBS for 30 min. Cells were washed three times in PBS for 5 min each. Cells were incubated in 500 µL hybridization solution for 1 h. The hybridization oven was preheated to 65 ºC for during this incubation. The digoxigenin-labeled ssRNA probes were prepared for hybridization by adding 10 ng of the probe to 30 µL of the hybridization solution and heating to 80 ºC for 5 min. The probe was then immediately placed on ice following denaturation. The denatured probe was place on the upside down lid of the 24-well plate the cells were cultured in. The coverslip was placed cell side down on the drop of the denatured probe. The probe and cells were incubated overnight in the hybridization oven at 65 ºC in a humidified container containing 50% formamide (Life Technologies) in 5X SSC (Life Technologies). The coverslips were briefly rinsed in 5X SSC. The coverslips were then washed twice in 0.2X SSC at 65 ºC for 20 min each. The coverslips were washed in a buffer consisting of 0.1 M Tris HCl, pH 7.5, 0.15 M NaCl, and 0.05% Tween-20 (referred to as TNT wash buffer) for 5 min. The coverslips were blocked in 0.1 M Tris HCl, pH 7.5, 0.15 M NaCl, and 0.5% Blocking Reagent (PerkinElmer) (referred to as TNB buffer) in a humidified chamber at room temperature for 30 min. Anti-digoxigenin

antibody conjugated to HRP (Abcam) was diluted 1:500 in TNB buffer and incubated with the coverslip at 4 ºC overnight. The coverslips were washed three times in TNT wash buffer at room temperature for 5 min. Tyramide Signal Amplification (TSA) was performed using the TSA PLUS Fluorescence Kit (PerkinElmer). The fluorescein dye was reconstituted in 150 µL DMSO. The stock dye was diluted 1:50 in 1X Plus Amplification Diluent provided with the kit. The diluted dye (300 µL/coverslip) was added to the coverslip and incubated in the dark at room temperature for 10 min. The coverslips were washed three times in TNT wash buffer in the dark at room temperature for 5 min. The nuclear counterstain TO-PRO-3 was diluted 1:2,000 in PBS and incubated with the cells for 5 minutes in the dark. Cells were washed once in PBS for 5 min and then dipped in purified water. A drop of VECTASHIELD Mounting Medium with DAPI was placed on a glass microscope slide, and the coverslip was placed cell side down on the drop. Any air bubbles were pressed out with gentle pressure on the coverslip. The edges were sealed using clear SALON Nail Lacquer, which was allowed to air dry. The cells were imaged using a Zeiss LSM 510 confocal microscope.

Results

In order to determine if differentiated SH-SY5Y cells express both isoforms of the human tau 3'-UTR, total RNA from differentiated SH-SY5Y cells was subjected to Northern blot, and the tau mRNA bands were visualized using a probe for total tau. GAPDH was probed as a loading control. Total RNA from human frontal cortex was included in the Northern blot analysis for comparison. The postmortem frontal cortex RNA sample is somewhat degraded, but the full-length 6 kb transcript, which corresponds to the long tau 3'-UTR isoform is prominent. The two transcripts corresponding to the tau 3'-UTR isoforms are visible at approximately 6 kb and 2 kb in the differentiated SH-SY5Y cells (Figure A.1). Thus, differentiated SH-SY5Y cells

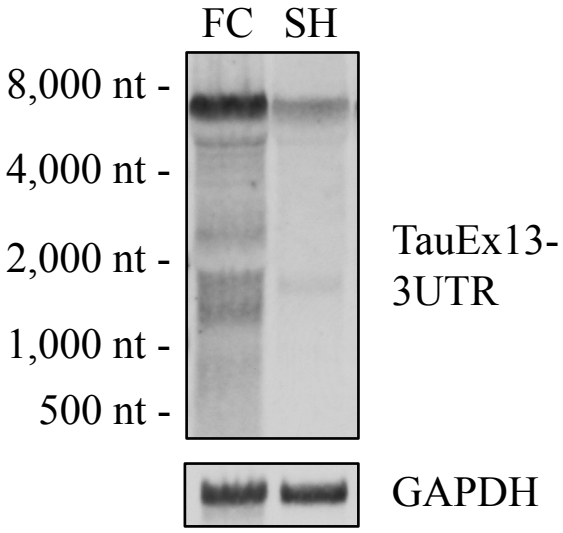

Figure A.1. Northern Blot of Tau mRNA in Differentiated SH-SY5Y Cells. Total RNA from human frontal cortex (FC) and differentiated SH-SY5Y (SH) was analyzed by Northern blot. A probe for total tau (TauEx13-3UTR) was used. GAPDH included as a loading control.

are a good model system for studying the human tau 3'-UTR in that they express both isoforms endogenously.

The neurites of differentiated SH-SY5Y cells were characterized by immunofluorescence (IF), with staining for tau, which is an axonal marker, and the dendritic marker MAP2 (Goedert et al., 1991). In single IF experiments, tau and MAP2 stained the neurites, as well as the soma (Figure A.2). In order to determine if tau and MAP2 stain distinct neurites, double IF was performed, with simultaneous staining for tau and MAP2. Two distinct types of neurites were seen: one that is predominantly stained by tau and another that is predominantly stained by MAP2 (Figure A.3). This indicates that differentiated SH-SY5Y cells have distinct axon-like tau-positive neurites and dendrite-like MAP2-positive neurites.

The subcellular localization of tau mRNA in differentiated SH-SY5Y cells was visualized using fluorescence *in situ* hybridization (FISH). Total tau mRNA was visualized with biotinylated antisense probe (TauEx13-3UTR_A). This revealed staining of tau mRNA in the soma and neurites (Figure A.4A). As a control, the sense probe was used, and it revealed less intense staining, primarily in the soma (Figure A.4B), which may represent non-specific signal. No background autofluorescence was detected (Figure A.4C).

Discussion

These findings presented here suggest differentiated SH-SY5Y cells may be a good model for studying the functions of the human tau 3'-UTR. Given the presence of distinct axon-like tau-positive neurites and dendrite-like MAP2-positive neurites in differentiated SH-SY5Y cells, they are a particularly attractive model for studying the subcellular localization of tau mRNA. However, further optimization of the hybridization conditions in the FISH experiment should be attempted to eliminate any non-specific signal. Additionally, combined FISH for tau

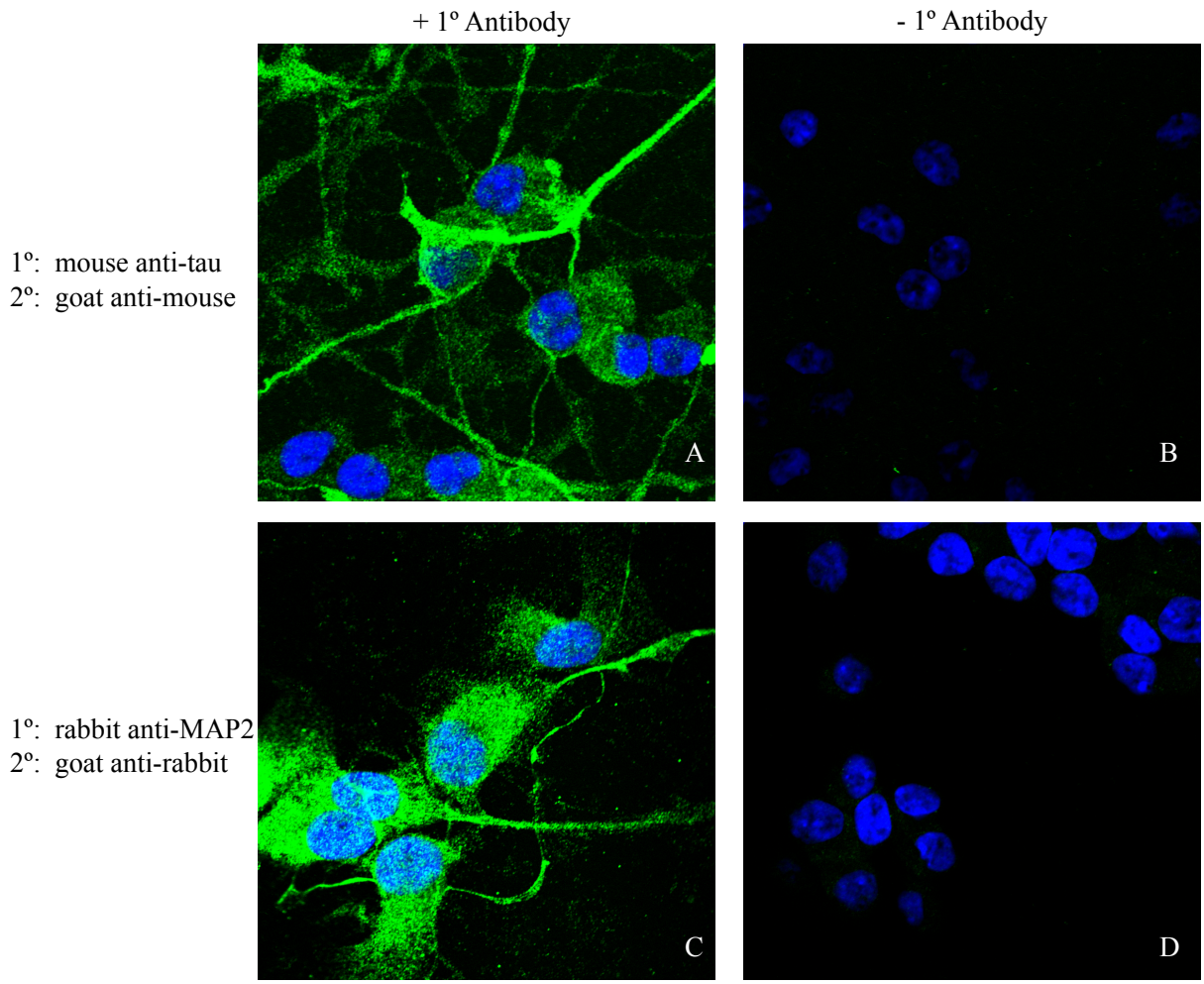

Figure A.2. Tau and MAP2 Proteins are Present in the Neurites of Differentiated SH-SY5Y Cells. Tau (A) and MAP2 (C) proteins (green) were visualized in differentiated SH-SY5Y cells by immunofluorescence. No signal was seen with AlexaFluor 488-conjugated secondary antibodies only (primary antibody omitted) (B and D). Nuclei were counterstained

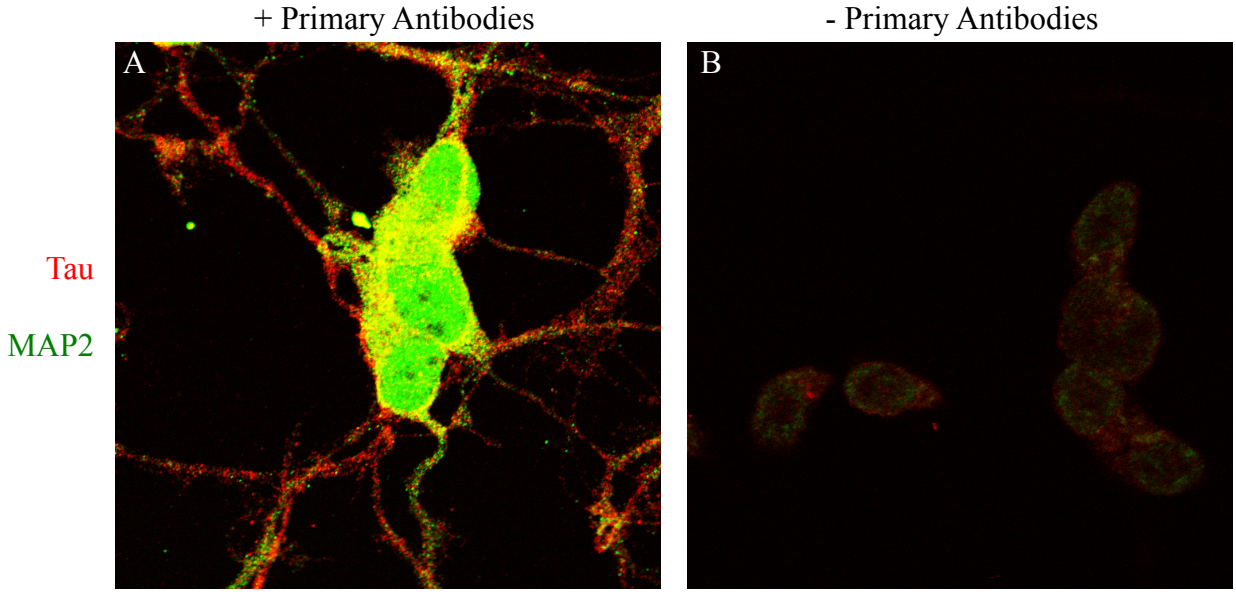

Figure A.3. Tau and MAP2 Proteins Label Distinct Neurites in Differentiated SH-SY5Y Cells. Differentiated SH-SY5Y cells were fixed and double immunofluorescence was performed using anti-tau and anti-MAP2 primary antibodies (A). Minimal staining by secondary antibodies alone was seen in a control in which primary antibodies were omitted. Cells were visualized by confocal microscopy.

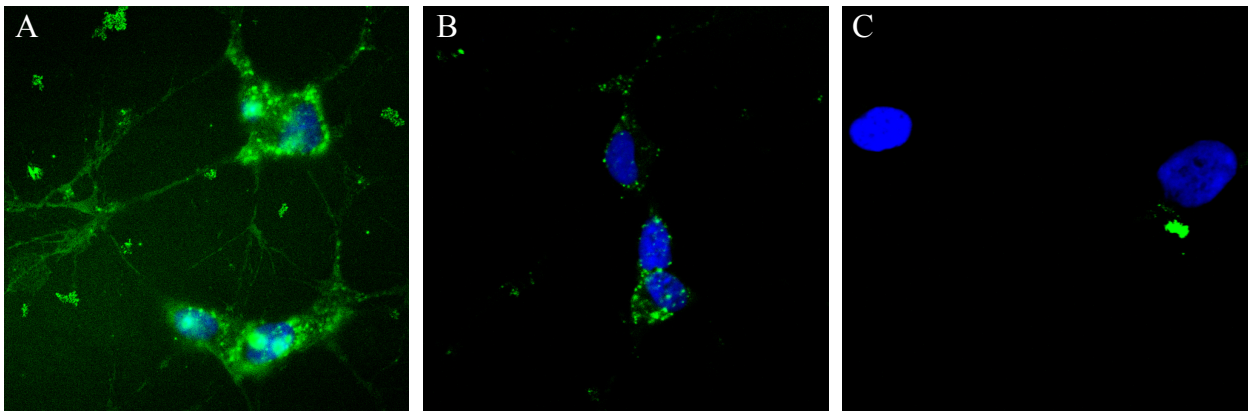

Figure A.4. Localization of Tau mRNA in Differentiated SH-SY5Y Cells. Fluorescent *in situ* hybridization (FISH) was performed on differentiated SH-SY5Y cells using tyramide signal amplification with fluorescein dye (green). Nuclei were counterstained with TO-PRO-3 (blue). (A) Antisense TauEx13-3UTR_A probe. (B) Sense TauEx13-3UTR_S probe. (C) no probe, no anti-DIG-HRP.

mRNA and double IF for tau and MAP2 proteins should be performed to determine the extent to which tau mRNA localizes in tau-positive axon-like neurites.

References

Agostini, M., Tucci, P., Killick, R., Candi, E., Sayan, B.S., Rivetti di Val Cervo, P., Nicotera, P., McKeon, F., Knight, R.A., Mak, T.W., et al. (2011a). Neuronal differentiation by TAp73 is mediated by microRNA-34a regulation of synaptic protein targets. Proceedings of the National Academy of Sciences *108*, 21093–21098.

Agostini, M., Tucci, P., Steinert, J.R., Shalom-Feuerstein, R., Rouleau, M., Aberdam, D., Forsythe, I.D., Young, K.W., Ventura, A., Concepcion, C.P., et al. (2011b). microRNA-34a regulates neurite outgrowth, spinal morphology, and function. Proceedings of the National Academy of Sciences *108*, 21099–21104.

Andreadis, A., Wagner, B.K., Broderick, J.A., and Kosik, K.S. (1996). A tau promoter region without neuronal specificity. J Neurochem *66*, 2257–2263.

Andreadis, A. (2005). Tau gene alternative splicing: expression patterns, regulation and modulation of function in normal brain and neurodegenerative diseases. Biochimica Et Biophysica Acta (BBA) - Molecular Basis of Disease *1739*, 91–103.

Andreadis, A., Brown, W.M., and Kosik, K.S. (1992). Structure and novel exons of the human .tau. gene. Biochemistry *31*, 10626–10633.

Arai, T., Hasegawa, M., Akiyama, H., Ikeda, K., Nonaka, T., Mori, H., Mann, D., Tsuchiya, K., Yoshida, M., Hashizume, Y., et al. (2006). TDP-43 is a component of ubiquitin-positive tau-negative inclusions in frontotemporal lobar degeneration and amyotrophic lateral sclerosis. Biochemical and Biophysical Research Communications *351*, 602–611.

Aranda-Abreu, G.E., Behar, L., Chung, S., Furneaux, H., and Ginzburg, I. (1999). Embryonic lethal abnormal vision-like RNA-binding proteins regulate neurite outgrowth and tau expression in PC12 cells. Journal of Neuroscience *19*, 6907–6917.

Aranha, M.M., Santos, D.M., Solá, S., Steer, C.J., and Rodrigues, C.M.P. (2011). miR-34a Regulates Mouse Neural Stem Cell Differentiation. PLoS ONE *6*, e21396.

Armstrong, M.J.M., Litvan, I.I., Lang, A.E.A., Bak, T.H.T., Bhatia, K.P.K., Borroni, B.B., Boxer, A.L.A., Dickson, D.W.D., Grossman, M.M., Hallett, M.M., et al. (2013). Criteria for the diagnosis of corticobasal degeneration. Neurology *80*, 496–503.

Aronov, S., Aranda, G., Behar, L., and Ginzburg, I. (2001). Axonal tau mRNA localization coincides with tau protein in living neuronal cells and depends on axonal targeting signal. Journal of Neuroscience *21*, 6577–6587.

Aronov, S., Marx, R., and Ginzburg, I. (1999). Identification of 3'UTR region implicated in tau mRNA stabilization in neuronal cells. J Mol Neurosci *12*, 131–145.

Aronov, S., Aranda, G., Behar, L., and Ginzburg, I. (2002). Visualization of translated tau protein in the axons of neuronal P19 cells and characterization of tau RNP granules. J. Cell. Sci. *115*, 3817–3827.

Association, A. (2013). 2013 Alzheimer's disease facts and figures. Alzheimer's & Dementia *9*, 208–245.

Atlas, R., Behar, L., Elliott, E., and Ginzburg, I. (2004). The insulin-like growth factor mRNA binding-protein IMP-1 and the Ras-regulatory protein G3BP associate with tau mRNA and HuD protein in differentiated P19 neuronal cells. J Neurochem *89*, 613–626.

Atlas, R., Behar, L., Sapoznik, S., and Ginzburg, I. (2007). Dynamic association with polysomes during P19 neuronal differentiation and an untranslated-region-dependent translation regulation of the tau mRNA by the tau mRNA-associated proteins IMP1, HuD, and G3BP1. J. Neurosci. Res. *85*, 173–183.

Baker, M., Litvan, I., Houlden, H., Adamson, J., Dickson, D., Perez-Tur, J., Hardy, J., Lynch, T., Bigio, E., and Hutton, M. (1999). Association of an extended haplotype in the tau gene with progressive supranuclear palsy. Human Molecular Genetics *8*, 711–715.

Baloh, R.H. (2012). How do the RNA-binding proteins TDP-43 and FUS relate to amyotrophic lateral sclerosis and frontotemporal degeneration, and to each other? Current Opinion in Neurology *25*, 701–707.

Barrett, L.W., Fletcher, S., and Wilton, S.D. (2012). Regulation of eukaryotic gene expression by the untranslated gene regions and other non-coding elements. CMLS, Cell. Mol. Life Sci. *69*, 3613–3634.

Bartel, D.P. (2004). MicroRNAs: genomics, biogenesis, mechanism, and function. Cell *116*, 281–297.

Bartel, D.P. (2009). MicroRNAs: Target Recognition and Regulatory Functions. Cell *136*, 215–233.

Behar, L., Marx, R., Sadot, E., Barg, J., and Ginzburg, I. (1995). cis-acting signals and trans-acting proteins are involved in tau mRNA targeting into neurites of differentiating neuronal cells. Int. J. Dev. Neurosci. *13*, 113–127.

Bergen, von, M., Barghorn, S., Biernat, J., Mandelkow, E.-M., and Mandelkow, E. (2005). Tau aggregation is driven by a transition from random coil to beta sheet structure. Biochimica Et Biophysica Acta (BBA) - Molecular Basis of Disease *1739*, 158–166.

Betel, D., Wilson, M., Gabow, A., Marks, D.S., and Sander, C. (2007). The microRNA.org resource: targets and expression. Nucleic Acids Research *36*, D149–D153.

Bierer, L.M., Hof, P.R., Purohit, D.P., Carlin, L., Schmeidler, J., Davis, K.L., and Perl, D.P. (1995). Neocortical neurofibrillary tangles correlate with dementia severity in Alzheimer's disease. Arch. Neurol. *52*, 81–88.

Biernat, J., Gustke, N., Drewes, G., Mandelkow, E.M., and Mandelkow, E. (1993). Phosphorylation of Ser262 strongly reduces binding of tau to microtubules: distinction between PHF-like immunoreactivity and microtubule binding. Neuron *11*, 153–163.

Binder, L.I.L., Frankfurter, A.A., and Rebhun, L.I.L. (1985). The distribution of tau in the mammalian central nervous system. J. Cell Biol. *101*, 1371–1378.

Boeve, B.F. (2012). Progressive supranuclear palsy. Parkinsonism and Realted Disorders *18*, S192–S194.

Bommer, G.T., Gerin, I., Feng, Y., Kaczorowski, A.J., Kuick, R., Love, R.E., Zhai, Y., Giordano, T.J., Qin, Z.S., Moore, B.B., et al. (2007). p53-Mediated Activation of miRNA34 Candidate Tumor-Suppressor Genes. Current Biology *17*, 1298–1307.

Boon, R.A., Iekushi, K., Lechner, S., Seeger, T., Fischer, A., Heydt, S., Kaluza, D., Tréguer, K., Carmona, G., Bonauer, A., et al. (2013). MicroRNA-34a regulates cardiac ageing and function. Nature 1–5.

Braak, H., and Braak, E. (1991). Neuropathological stageing of Alzheimer-related changes. Acta Neuropathol *82*, 239–259.

Brandt, R.R., Léger, J.J., and Lee, G.G. (1995). Interaction of tau with the neural plasma membrane mediated by tau's amino-terminal projection domain. J. Cell Biol. *131*, 1327–1340.

Brown, C.Y., Lagnado, C.A., and Goodall, G.J. (1996). A cytokine mRNA-destabilizing element that is structurally and functionally distinct from A+U-rich elements. Proc. Natl. Acad. Sci. U.S.a. *93*, 13721–13725.

Caffrey, T.M., and Wade-Martins, R. (2007). Functional MAPT haplotypes: Bridging the gap between genotype and neuropathology. Neurobiology of Disease *27*, 1–10.

Cairns, N.J., Bigio, E.H., Mackenzie, I.R.A., Neumann, M., Lee, V.M.-Y., Hatanpaa, K.J., White, C.L., III, Schneider, J.A., Grinberg, L.T., Halliday, G., et al. (2007). Neuropathologic diagnostic and nosologic criteria for frontotemporal lobar degeneration: consensus of the Consortium for Frontotemporal Lobar Degeneration. Acta Neuropathol *114*, 5–22.

Chen, J.-M., Férec, C., and Cooper, D.N. (2006). A systematic analysis of disease-associated variants in the 3′ regulatory regions of human protein-coding genes I: general principles and overview. Hum Genet *120*, 1–21.

Chen, M.M., Martins, R.N.R., and Lardelli, M.M. (2009). Complex splicing and neural expression of duplicated tau genes in zebrafish embryos. J Alzheimers Dis *18*, 305–317.

Chen, W.T.W., Liu, W.K.W., and Yen, S.H.S. (1994). Expression of tau exon 8 in different species. Neurosci Lett *172*, 167–170.

Cleveland, D.W.D., Hwo, S.Y.S., and Kirschner, M.W.M. (1977). Physical and chemical properties of purified tau factor and the role of tau in microtubule assembly. Journal of Molecular Biology *116*, 227–247.

Cogswell, J.P.J., Ward, J.J., Taylor, I.A.I., Waters, M.M., Shi, Y.Y., Cannon, B.B., Kelnar, K.K., Kemppainen, J.J., Brown, D.D., Chen, C.C., et al. (2008). Identification of miRNA changes in

Alzheimer's disease brain and CSF yields putative biomarkers and insights into disease pathways. J Alzheimers Dis *14*, 27–41.

Cohen, T.J., Guo, J.L., Hurtado, D.E., Kwong, L.K., Mills, I.P., Trojanowski, J.Q., and Lee, V.M.-Y. (2011). The acetylation of tau inhibits its function and promotes pathological tau aggregation. Nature Communications *2*, 252–259.

Concepcion, C.P., Han, Y.-C., Mu, P., Bonetti, C., Yao, E., D'Andrea, A., Vidigal, J.A., Maughan, W.P., Ogrodowski, P., and Ventura, A. (2012). Intact p53-Dependent Responses in miR-34–Deficient Mice. PLoS Genet *8*, e1002797.

Conrad, C., Vianna, C., Freeman, M., and Davies, P. (2002). A polymorphic gene nested within an intron of the tau gene: implications for Alzheimer's disease. Proc. Natl. Acad. Sci. U.S.a. *99*, 7751–7756.

Couchie, D., Mavilia, C., Georgieff, I.S., Liem, R.K., Shelanski, M.L., and Nunez, J. (1992). Primary structure of high molecular weight tau present in the peripheral nervous system. Proc. Natl. Acad. Sci. U.S.a. *89*, 4378–4381.

Cummings, J.L. (2004). Alzheimer's disease. N Engl J Med *351*, 56–67.

Delacourte, A.A., Sergeant, N.N., Wattez, A.A., Gauvreau, D.D., and Robitaille, Y.Y. (1998). Vulnerable neuronal subsets in Alzheimer“s and Pick”s disease are distinguished by their tau isoform distribution and phosphorylation. Ann Neurol. *43*, 193–204.

Delacourte, A., and Defossez, A. (1986). Alzheimer's disease: Tau proteins, the promoting factors of microtubule assembly, are major components of paired helical filaments. J. Neurol. Sci. *76*, 173–186.

Dickson, D.W., Bergeron, C., Chin, S.S., Duyckaerts, C., Horoupian, D., Ikeda, K., Jellinger, K., Lantos, P.L., Lippa, C.F., Mirra, S.S., et al. (2002). Office of Rare Diseases neuropathologic criteria for corticobasal degeneration. J. Neuropathol. Exp. Neurol. *61*, 935–946.

Dickson, D.W., Ahmed, Z., Algom, A.A., Tsuboi, Y., and Josephs, K.A. (2010). Neuropathology of variants of progressive supranuclear palsy. Current Opinion in Neurology *23*, 394–400.

Dixit, R., Ross, J.L., Goldman, Y.E., and Holzbaur, E.L.F. (2008). Differential Regulation of Dynein and Kinesin Motor Proteins by Tau. Science *319*, 1086–1089.

Drubin, D.G., and Kirschner, M.W. (1986). Tau protein function in living cells. J. Cell Biol. *103*, 2739–2746.

Drubin, D., Kobayashi, S., and Kirschner, M. (1986). Association of tau protein with microtubules in living cells. Annals of the New York Academy of Sciences *466*, 257–268.

Encinas, M.M., Iglesias, M.M., Liu, Y.Y., Wang, H.H., Muhaisen, A.A., Ceña, V.V., Gallego, C.C., and Comella, J.X.J. (2000). Sequential treatment of SH-SY5Y cells with retinoic acid and brain-derived neurotrophic factor gives rise to fully differentiated, neurotrophic factor-

dependent, human neuron-like cells. J Neurochem *75*, 991–1003.

Flavell, S.W., Kim, T.-K., Gray, J.M., Harmin, D.A., Hemberg, M., Hong, E.J., Markenscoff-Papadimitriou, E., Bear, D.M., and Greenberg, M.E. (2008). Genome-Wide Analysis of MEF2 Transcriptional Program Reveals Synaptic Target Genes and Neuronal Activity-Dependent Polyadenylation Site Selection. Neuron *60*, 1022–1038.

Foster, N.L., Wilhelmsen, K., Sima, A.A., Jones, M.Z., D'Amato, C.J., and Gilman, S. (1997). Frontotemporal dementia and parkinsonism linked to chromosome 17: a consensus conference. Conference Participants. pp. 706–715.

Friedmann, D., Hwang, A.W., Marmorstein, R., Lee, V.M.-Y., and Cohen, T.J. (2013). The microtubule-associated tau protein has intrinsic acetyltransferase activity. Nature Structural & Molecular Biology 1–8.

Fu, Y., Sun, Y., Li, Y., Li, J., Rao, X., Chen, C., and Xu, A. (2011). Differential genome-wide profiling of tandem 3' UTRs among human breast cancer and normal cells by high-throughput sequencing. Genome Research *21*, 741–747.

Gao, L.L., Tse, S.-W.S., Conrad, C.C., and Andreadis, A.A. (2005). Saitohin, which is nested in the tau locus and confers allele-specific susceptibility to several neurodegenerative diseases, interacts with peroxiredoxin 6. J. Biol. Chem. *280*, 39268–39272.

Georgieff, I.S.I., Liem, R.K.R., Couchie, D.D., Mavilia, C.C., Nunez, J.J., and Shelanski, M.L.M. (1993). Expression of high molecular weight tau in the central and peripheral nervous systems. J. Cell. Sci. *105 (Pt 3)*, 729–737.

Gibbons, H.M., and Dragunow, M. (2010). Adult human brain cell culture for neuroscience research. International Journal of Biochemistry and Cell Biology *42*, 844–856.

Goate, A., Chartier-Harlin, M.C., Mullan, M., Brown, J., Crawford, F., Fidani, L., Giuffra, L., Haynes, A., Irving, N., and James, L. (1991). Segregation of a missense mutation in the amyloid precursor protein gene with familial Alzheimer's disease. Nature *349*, 704–706.

Goedert, M.M., Crowther, R.A.R., and Garner, C.C.C. (1991). Molecular characterization of microtubule-associated proteins tau and MAP2. Trends Neurosci *14*, 193–199.

Goedert, M.M., Spillantini, M.G.M., and Crowther, R.A.R. (1992). Cloning of a big tau microtubule-associated protein characteristic of the peripheral nervous system. Proc. Natl. Acad. Sci. U.S.a. *89*, 1983–1987.

Goedert, M., Spillantini, M.G., Jakes, R., Rutherford, D., and Crowther, R.A. (1989a). Multiple isoforms of human microtubule-associated protein tau: sequences and localization in neurofibrillary tangles of Alzheimer's disease. Neuron *3*, 519–526.

Goedert, M., Spillantini, M.G., Potier, M.C., Ulrich, J., and Crowther, R.A. (1989b). Cloning and sequencing of the cDNA encoding an isoform of microtubule-associated protein tau containing four tandem repeats: differential expression of tau protein mRNAs in human brain. The EMBO

Journal *8*, 393–399.

Goedert, M., Wischik, C.M., Crowther, R.A., Walker, J.E., and Klug, A. (1988). Cloning and sequencing of the cDNA encoding a core protein of the paired helical filament of Alzheimer disease: identification as the microtubule-associated protein tau. Proc. Natl. Acad. Sci. U.S.a. *85*, 4051–4055.

Goldgaber, D., Lerman, M.I., McBride, O.W., Saffiotti, U., and Gajdusek, D.C. (1987). Characterization and chromosomal localization of a cDNA encoding brain amyloid of Alzheimer's disease. Science *235*, 877–880.

Goode, B.L. (2000). Structural and Functional Differences between 3-Repeat and 4-Repeat Tau Isoforms. IMPLICATIONS FOR NORMAL TAU FUNCTION AND THE ONSET OF NEURODEGENERATIVE DISEASE. Journal of Biological Chemistry *275*, 38182–38189.

Goode, B.L.B., Denis, P.E.P., Panda, D.D., Radeke, M.J.M., Miller, H.P.H., Wilson, L.L., and Feinstein, S.C.S. (1997). Functional interactions between the proline-rich and repeat regions of tau enhance microtubule binding and assembly. Mol Biol Cell *8*, 353–365.

Grundke-Iqbal, I., Iqbal, K., Quinlan, M., Tung, Y.C., Zaidi, M.S., and Wisniewski, H.M. (1986). Microtubule-associated protein tau. A component of Alzheimer paired helical filaments. J. Biol. Chem. *261*, 6084–6089.

Gu, Y.Y., Oyama, F.F., and Ihara, Y.Y. (1996). Tau is widely expressed in rat tissues. J Neurochem *67*, 1235–1244.

Hardy, J.A., and Higgins, G.A. (1992). Alzheimer's disease: the amyloid cascade hypothesis. Science *256*, 184–185.

He, L., and Hannon, G.J. (2004). MicroRNAs: small RNAs with a big role in gene regulation. Nat Rev Genet *5*, 522–531.

He, L., He, X., Lim, L.P., de Stanchina, E., Xuan, Z., Liang, Y., Xue, W., Zender, L., Magnus, J., Ridzon, D., et al. (2007). A microRNA component of the p53 tumour suppressor network. Nature *447*, 1130–1134.

Heicklen-Klein, A.A., and Ginzburg, I.I. (2000). Tau promoter confers neuronal specificity and binds Sp1 and AP-2. J Neurochem *75*, 1408–1418.

Hendriks, L., van Duijn, C.M., Cras, P., Cruts, M., Van Hul, W., van Harskamp, F., Warren, A., McInnis, M.G., Antonarakis, S.E., and Martin, J.J. (1992). Presenile dementia and cerebral haemorrhage linked to a mutation at codon 692 of the beta-amyloid precursor protein gene. Nature Genetics *1*, 218–221.

Hermeking, H. (2010). The miR-34 family in cancer and apoptosis. Cell Death and Differentiation *17*, 193–199.

Himmler, A.A., Drechsel, D.D., Kirschner, M.W.M., and Martin, D.W.D. (1989). Tau consists of

a set of proteins with repeated C-terminal microtubule-binding domains and variable N-terminal domains. Mol Cell Biol *9*, 1381–1388.

Himmler, A. (1989). Structure of the bovine tau gene: alternatively spliced transcripts generate a protein family. Mol Cell Biol *9*, 1389–1396.

Hirokawa, N.N. (2000). Stirring up development with the heterotrimeric kinesin KIF3. Traffic *1*, 29–34.

Hutton, M., Lendon, C.L., Rizzu, P., Baker, M., Froelich, S., Houlden, H., Pickering-Brown, S., Chakraverty, S., Isaacs, A., Grover, A., et al. (1998). Association of missense and 5'-splice-site mutations in tau with the inherited dementia FTDP-17. Nature *393*, 702–705.

Hyman, B.T., Phelps, C.H., Beach, T.G., Bigio, E.H., Cairns, N.J., Carrillo, M.C., Dickson, D.W., Duyckaerts, C., Frosch, M.P., Masliah, E., et al. (2012). National Institute on Aging-Alzheimer“s Association guidelines for the neuropathologic assessment of Alzheimer”s disease. Alzheimer's & Dementia *8*, 1–13.

Ikegami, S.S., Harada, A.A., and Hirokawa, N.N. (2000). Muscle weakness, hyperactivity, and impairment in fear conditioning in tau-deficient mice. Neurosci Lett *279*, 129–132.

Irwin, C.R., Farmer, A., Willer, D.O., and Evans, D.H. (2012). In-Fusion® Cloning with Vaccinia Virus DNA Polymerase. In Methods in Molecular Biology, (Totowa, NJ: Humana Press), pp. 23–35.

Ittner, L.M., and Götz, J. (2010). Amyloid-β and tau — a toxic pas de deux in Alzheimer's disease. Nature Reviews Neuroscience 1–6.

Ittner, L.M., Ke, Y.D., Delerue, F., Bi, M., Gladbach, A., van Eersel, J., Wölfing, H., Chieng, B.C., Christie, M.J., Napier, I.A., et al. (2010). Dendritic Function of Tau Mediates Amyloid-β Toxicity in Alzheimer's Disease Mouse Models. Cell *142*, 387–397.

Ji, Z., Lee, J.Y., Pan, Z., Jiang, B., and Tian, B. (2009). Progressive lengthening of 3′ untranslated regions of mRNAs by alternative polyadenylation during mouse embryonic development. Proc. Natl. Acad. Sci. U.S.a. *106*, 7028–7033.

Jones, R.W. (2003). The dementias. Clin Med *3*, 404–408.

Kang, J., Lemaire, H.G., Unterbeck, A., Salbaum, J.M., Masters, C.L., Grzeschik, K.H., Multhaup, G., Beyreuther, K., and Müller-Hill, B. (1987). The precursor of Alzheimer's disease amyloid A4 protein resembles a cell-surface receptor. Nature *325*, 733–736.

Ke, Y.D., Suchowerska, A.K., van der Hoven, J., De Silva, D.M., Wu, C.W., van Eersel, J., Ittner, A., and Ittner, L.M. (2012). Lessons from Tau-Deficient Mice. International Journal of Alzheimer's Disease *2012*, 1–8.

Kimberly, W.T., Xia, W., Rahmati, T., Wolfe, M.S., and Selkoe, D.J. (2000). The transmembrane aspartates in presenilin 1 and 2 are obligatory for gamma-secretase activity and

amyloid beta-protein generation. J. Biol. Chem. *275*, 3173–3178.

Klein, C., Kramer, E.-M., Cardine, A.-M., Schraven, B., Brandt, R., and Trotter, J. (2002). Process outgrowth of oligodendrocytes is promoted by interaction of fyn kinase with the cytoskeletal protein tau. J. Neurosci. *22*, 698–707.

Knapinska, A.M., Irizarry-Barreto, P., Adusumalli, S., Androulakis, I., and Brewer, G. (2005). Molecular mechanisms regulating mRNA stability: physiological and pathological significance. Curr. Genomics *6*, 471–486.

Kosik, K.S., Joachim, C.L., and Selkoe, D.J. (1986). Microtubule-associated protein tau (tau) is a major antigenic component of paired helical filaments in Alzheimer disease. Proc. Natl. Acad. Sci. U.S.a. *83*, 4044–4048.

Krek, A., Grün, D., Poy, M.N., Wolf, R., Rosenberg, L., Epstein, E.J., MacMenamin, P., da Piedade, I., Gunsalus, K.C., Stoffel, M., et al. (2005). Combinatorial microRNA target predictions. Nature Genetics *37*, 495–500.

Kwiatkowski, T.J., Bosco, D.A., LeClerc, A.L., Tamrazian, E., Vanderburg, C.R., Russ, C., Davis, A., Gilchrist, J., Kasarskis, E.J., Munsat, T., et al. (2009). Mutations in the FUS/TLS Gene on Chromosome 16 Cause Familial Amyotrophic Lateral Sclerosis. Science *323*, 1205–1208.

LaPointe, N.E., Horowitz, P.M., Guillozet-Bongaarts, A.L., Silva, A., Andreadis, A., and Binder, L.I. (2009). Tau 6D and 6P Isoforms Inhibit Polymerization of Full-Length Tau in Vitro. Biochemistry *48*, 12290–12297.

Larkin, M.A., Blackshields, G., Brown, N.P., Chenna, R., McGettigan, P.A., McWilliam, H., Valentin, F., Wallace, I.M., Wilm, A., Lopez, R., et al. (2007). Clustal W and Clustal X version 2.0. Bioinformatics *23*, 2947–2948.

Lee, E.B., Lee, V.M.-Y., and Trojanowski, J.Q. (2011). Gains or losses: molecular mechanisms of TDP43-mediated neurodegeneration. 1–13.

Lee, G.G., Cowan, N.N., and Kirschner, M.M. (1988). The primary structure and heterogeneity of tau protein from mouse brain. Science *239*, 285–288.

Lee, G., Neve, R.L., and Kosik, K.S. (1989). The microtubule binding domain of tau protein. Neuron *2*, 1615–1624.

Lee, G., Newman, S.T., Gard, D.L., Band, H., and Panchamoorthy, G. (1998). Tau interacts with src-family non-receptor tyrosine kinases. J. Cell. Sci. *111 (Pt 21)*, 3167–3177.

Lee, G.G., Thangavel, R.R., Sharma, V.M.V., Litersky, J.M.J., Bhaskar, K.K., Fang, S.M.S., Do, L.H.L., Andreadis, A.A., Van Hoesen, G.G., and Ksiezak-Reding, H.H. (2004). Phosphorylation of tau by fyn: implications for Alzheimer's disease. Journal of Neuroscience *24*, 2304–2312.

Lee, V.M., Goedert, M., and Trojanowski, J.Q. (2001). Neurodegenerative tauopathies. Annu.

Rev. Neurosci. *24*, 1121–1159.

Leroy, K., Ando, K., Laporte, V., Dedecker, R., Suain, V., Authelet, M., Héraud, C., Pierrot, N., Yilmaz, Z., Octave, J.N., et al. (2012). Lack of Tau Proteins Rescues Neuronal Cell Death and Decreases Amyloidogenic Processing of APP in APP/PS1 Mice. Ajpa *181*, 1928–1940.

Levy-Lahad, E., Wasco, W., Poorkaj, P., Romano, D.M., Oshima, J., Pettingell, W.H., Yu, C.E., Jondro, P.D., Schmidt, S.D., and Wang, K. (1995a). Candidate gene for the chromosome 1 familial Alzheimer's disease locus. Science *269*, 973–977.

Levy-Lahad, E., Wijsman, E.M., Nemens, E., Anderson, L., Goddard, K.A., Weber, J.L., Bird, T.D., and Schellenberg, G.D. (1995b). A familial Alzheimer's disease locus on chromosome 1. Science *269*, 970–973.

Lewis, B.P., Burge, C.B., and Bartel, D.P. (2005). Conserved Seed Pairing, Often Flanked by Adenosines, Indicates that Thousands of Human Genes are MicroRNA Targets. Cell *120*, 15–20.

Lin, Y., Li, Z., Ozsolak, F., Kim, S.W., Arango-Argoty, G., Liu, T.T., Tenenbaum, S.A., Bailey, T., Monaghan, A.P., Milos, P.M., et al. (2012). An in-depth map of polyadenylation sites in cancer. Nucleic Acids Research *40*, 8460–8471.

Lindwall, G., and Cole, R.D. (1984). Phosphorylation affects the ability of tau protein to promote microtubule assembly. J. Biol. Chem. *259*, 5301–5305.

Litman, P., Barg, J., and Ginzburg, I. (1994). Microtubules are involved in the localization of tau mRNA in primary neuronal cell cultures. Neuron *13*, 1463–1474.

Litman, P., Barg, J., Rindzoonski, L., and Ginzburg, I. (1993). Subcellular localization of tau mRNA in differentiating neuronal cell culture: implications for neuronal polarity. Neuron *10*, 627–638.

Liu, N., Landreh, M., Cao, K., Abe, M., Hendriks, G.-J., Kennerdell, J.R., Zhu, Y., Wang, L.-S., and Bonini, N.M. (2012). The microRNA miR-34 modulates ageing and neurodegeneration in Drosophila. Nature 1–7.

Luo, M.-H., Leski, M.L., and Andreadis, A. (2004a). Tau isoforms which contain the domain encoded by exon 6 and their role in neurite elongation. J. Cell. Biochem. *91*, 880–895.

Luo, M.-H., Tse, S.-W., Memmott, J., and Andreadis, A. (2004b). Novel isoforms of tau that lack the microtubule-binding domain. J Neurochem *90*, 340–351.

Mackenzie, I.R.A., Neumann, M., Bigio, E.H., Cairns, N.J., Alafuzoff, I., Kril, J., Kovacs, G.G., Ghetti, B., Halliday, G., Holm, I.E., et al. (2009). Nomenclature for neuropathologic subtypes of frontotemporal lobar degeneration: consensus recommendations. Acta Neuropathol *117*, 15–18.

Maes, O.C., Chertkow, H.M., Wang, E., and Schipper, H.M. (2009). MicroRNA: Implications for Alzheimer Disease and other Human CNS Disorders. Curr. Genomics *10*, 154–168.

Maloney, B., and Lahiri, D.K. (2012). Structural and functional characterization of H2 haplotype MAPT promoter: Unique neurospecific domains and a hypoxia-inducible element would enhance rationally targeted tauopathy research for Alzheimer's disease. Gene *501*, 63–78.

Maragkakis, M., Reczko, M., Simossis, V.A., Alexiou, P., Papadopoulos, G.L., Dalamagas, T., Giannopoulos, G., Goumas, G., Koukis, E., Kourtis, K., et al. (2009). DIANA-microT web server: elucidating microRNA functions through target prediction. Nucleic Acids Research *37*, W273–W276.

Masters, C.L., Simms, G., Weinman, N.A., Multhaup, G., McDonald, B.L., and Beyreuther, K. (1985). Amyloid plaque core protein in Alzheimer disease and Down syndrome. Proc. Natl. Acad. Sci. U.S.a. *82*, 4245–4249.

Mayr, C., and Bartel, D.P. (2009). Widespread Shortening of 3′UTRs by Alternative Cleavage and Polyadenylation Activates Oncogenes in Cancer Cells. Cell *138*, 673–684.

McKhann, G.M., Knopman, D.S., Chertkow, H., Hyman, B.T., Jack, C.R., Jr, Kawas, C.H., Klunk, W.E., Koroshetz, W.J., Manly, J.J., Mayeux, R., et al. (2011). The diagnosis of dementia due to Alzheimer's disease: Recommendations from the National Institute on Aging-Alzheimer‘s Association workgroups on diagnostic guidelines for Alzheimer’s disease. Alzheimer's & Dementia *7*, 263–269.

Morishima-Kawashima, M., Hasegawa, M., Takio, K., Suzuki, M., Yoshida, H., Watanabe, A., Titani, K., and Ihara, Y. (1995). Hyperphosphorylation of tau in PHF. Neurobiology of Aging *16*, 365–71–discussion371–80.

Mullan, M., Crawford, F., Axelman, K., Houlden, H., Lilius, L., Winblad, B., and Lannfelt, L. (1992). A pathogenic mutation for probable Alzheimer's disease in the APP gene at the N-terminus of beta-amyloid. Nature Genetics *1*, 345–347.

Murayama, S.S., Mori, H.H., Ihara, Y.Y., and Tomonaga, M.M. (1990). Immunocytochemical and ultrastructural studies of Pick's disease. Ann Neurol. *27*, 394–405.

Neary, D., Snowden, J.S., Gustafson, L., Passant, U., Stuss, D., Black, S., Freedman, M., Kertesz, A., Robert, P.H., Albert, M., et al. (1998). Frontotemporal lobar degeneration: a consensus on clinical diagnostic criteria. pp. 1546–1554.

Nelson, P.T., Stefansson, K., Gulcher, J., and Saper, C.B. (1996). Molecular evolution of tau protein: implications for Alzheimer's disease. J Neurochem *67*, 1622–1632.

Neumann, M., Rademakers, R., Roeber, S., Baker, M., Kretzschmar, H.A., and Mackenzie, I.R.A. (2009). A new subtype of frontotemporal lobar degeneration with FUS pathology. Brain *132*, 2922–2931.

Neumann, M., Sampathu, D.M., Kwong, L.K., Truax, A.C., Micsenyi, M.C., Chou, T.T., Bruce, J., Schuck, T., Grossman, M., Clark, C.M., et al. (2006). Ubiquitinated TDP-43 in Frontotemporal Lobar Degeneration and Amyotrophic Lateral Sclerosis. Science *314*, 130–133.

Neve, R.L., Harris, P., Kosik, K.S., Kurnit, D.M., and Donlon, T.A. (1986). Identification of cDNA clones for the human microtubule-associated protein tau and chromosomal localization of the genes for tau and microtubule-associated protein 2. Brain Research *387*, 271–280.

Nukina, N., and Ihara, Y. (1986). One of the antigenic determinants of paired helical filaments is related to tau protein. J. Biochem. *99*, 1541–1544.

Park, J.Y., Li, W., Zheng, D., Zhai, P., Zhao, Y., Matsuda, T., Vatner, S.F., Sadoshima, J., and Tian, B. (2011). Comparative Analysis of mRNA Isoform Expression in Cardiac Hypertrophy and Development Reveals Multiple Post-Transcriptional Regulatory Modules. PLoS ONE *6*, e22391.

Peng, I.I., Binder, L.I.L., and Black, M.M.M. (1986). Biochemical and immunological analyses of cytoskeletal domains of neurons. J. Cell Biol. *102*, 252–262.

Pittman, A.M. (2005). Linkage disequilibrium fine mapping and haplotype association analysis of the tau gene in progressive supranuclear palsy and corticobasal degeneration. Journal of Medical Genetics *42*, 837–846.

Poorkaj, P., Bird, T.D., Wijsman, E., Nemens, E., Garruto, R.M., Anderson, L., Andreadis, A., Wiederholt, W.C., Raskind, M., and Schellenberg, G.D. (1998). Tau is a candidate gene for chromosome 17 frontotemporal dementia. Ann Neurol. *43*, 815–825.

Poorkaj, P., Kas, A., D'Souza, I., Zhou, Y., Pham, Q., Stone, M., Olson, M.V., and Schellenberg, G.D. (2001). A genomic sequence analysis of the mouse and human microtubule-associated protein tau. Mammalian Genome *12*, 700–712.

Rapoport, M., Dawson, H.N., Binder, L.I., Vitek, M.P., and Ferreira, A. (2002). Tau is essential to beta -amyloid-induced neurotoxicity. Proc. Natl. Acad. Sci. U.S.a. *99*, 6364–6369.

Robakis, N.K., Ramakrishna, N., Wolfe, G., and Wisniewski, H.M. (1987). Molecular cloning and characterization of a cDNA encoding the cerebrovascular and the neuritic plaque amyloid peptides. Proc. Natl. Acad. Sci. U.S.a. *84*, 4190–4194.

Roberson, E.D., Scearce-Levie, K., Palop, J.J., Yan, F., Cheng, I.H., Wu, T., Gerstein, H., Yu, G.Q., and Mucke, L. (2007). Reducing Endogenous Tau Ameliorates Amyloid -Induced Deficits in an Alzheimer's Disease Mouse Model. Science *316*, 750–754.

Rogaev, E.I., Sherrington, R., Rogaeva, E.A., Levesque, G., Ikeda, M., Liang, Y., Chi, H., Lin, C., Holman, K., and Tsuda, T. (1995). Familial Alzheimer“s disease in kindreds with missense mutations in a gene on chromosome 1 related to the Alzheimer”s disease type 3 gene. Nature *376*, 775–778.

Sadot, E., Heicklen-Klein, A., Barg, J., Lazarovici, P., and Ginzburg, I. (1996). Identification of a tau promoter region mediating tissue-specific-regulated expression in PC12 cells. Journal of Molecular Biology *256*, 805–812.

Saito, Y.D., Jensen, A.R., Salgia, R., and Posadas, E.M. (2010). Fyn. Cancer *116*, 1629–1637.

Sandberg, R., Neilson, J.R., Sarma, A., SHARP, P.A., and Burge, C.B. (2008). Proliferating Cells Express mRNAs with Shortened 3' Untranslated Regions and Fewer MicroRNA Target Sites. Science *320*, 1643–1647.

Saper, C.B., Wainer, B.H., and German, D.C. (1987). Axonal and transneuronal transport in the transmission of neurological disease: potential role in system degenerations, including Alzheimer's disease. Nsc *23*, 389–398.

Schipper, H.M., Maes, O.C., Chertkow, H.M., and Wang, E. (2007). MicroRNA expression in Alzheimer blood mononuclear cells. Gene Regul Syst Bio *1*, 263–274.

Schweers, O., Schönbrunn-Hanebeck, E., Marx, A., and Mandelkow, E. (1994). Structural studies of tau protein and Alzheimer paired helical filaments show no evidence for beta-structure. J. Biol. Chem. *269*, 24290–24297.

Seltman, R.E.R., and Matthews, B.R.B. (2012). Frontotemporal lobar degeneration: epidemiology, pathology, diagnosis and management. CNS Drugs *26*, 841–870.

Sherrington, R., Rogaev, E.I., Liang, Y., Rogaeva, E.A., Levesque, G., Ikeda, M., Chi, H., Lin, C., Li, G., Holman, K., et al. (1995). Cloning of a gene bearing missense mutations in early-onset familial Alzheimer's disease. Nature *375*, 754–760.

Shi, Y. (2012). Alternative polyadenylation: New insights from global analyses. Rna *18*, 2105–2117.

Smith, P.Y., Delay, C., Girard, J., Papon, M.A., Planel, E., Sergeant, N., Buee, L., and Hebert, S.S. (2011). MicroRNA-132 loss is associated with tau exon 10 inclusion in progressive supranuclear palsy. Human Molecular Genetics *20*, 4016–4024.

Spillantini, M.G., Murrell, J.R., Goedert, M., Farlow, M.R., Klug, A., and Ghetti, B. (1998). Mutation in the tau gene in familial multiple system tauopathy with presenile dementia. Proc. Natl. Acad. Sci. U.S.a. *95*, 7737–7741.

Stefansson, H., Helgason, A., Thorleifsson, G., Steinthorsdottir, V., Masson, G., Barnard, J., Baker, A., Jonasdottir, A., Ingason, A., Gudnadottir, V.G., et al. (2005). A common inversion under selection in Europeans. Nature Genetics *37*, 129–137.

Takanashi, M.M., Mori, H.H., Arima, K.K., Mizuno, Y.Y., and Hattori, N.N. (2002). Expression patterns of tau mRNA isoforms correlate with susceptible lesions in progressive supranuclear palsy and corticobasal degeneration. Brain Res Mol Brain Res *104*, 210–219.

Tanzi, R.E., Gusella, J.F., Watkins, P.C., Bruns, G.A., St George-Hyslop, P., Van Keuren, M.L., Patterson, D., Pagan, S., Kurnit, D.M., and Neve, R.L. (1987). Amyloid beta protein gene: cDNA, mRNA distribution, and genetic linkage near the Alzheimer locus. Science *235*, 880–884.

Trepanier, C.H., Jackson, M.F., and MacDonald, J.F. (2012). Regulation of NMDA receptors by the tyrosine kinase Fyn. FEBS Journal *279*, 12–19.

Vaziri, H., Dessain, S.K., Ng Eaton, E., Imai, S.I., Frye, R.A., Pandita, T.K., Guarente, L., and Weinberg, R.A. (2001). hSIR2(SIRT1) functions as an NAD-dependent p53 deacetylase. Cell *107*, 149–159.

Veo, B.L., and Krushel, L.A. (2009). Translation initiation of the human tau mRNA through an internal ribosomal entry site. J Alzheimers Dis *16*, 271–275.

Veo, B.L., and Krushel, L.A. (2012). Secondary RNA structure and nucleotide specificity contribute to internal initiation mediated by the human tau 5′ leader. Rnabiology *9*, 8–7.

Visootsak, J., and Sherman, S. (2007). Neuropsychiatric and behavioral aspects of trisomy 21. Curr Psychiatry Rep *9*, 135–140.

Vossel, K.A., Zhang, K., Brodbeck, J., Daub, A.C., Sharma, P., Finkbeiner, S., Cui, B., and Mucke, L. (2010). Tau reduction prevents Abeta-induced defects in axonal transport. Science *330*, 198.

Wang, Y., Loomis, P.A., Zinkowski, R.P., and Binder, L.I. (1993). A novel tau transcript in cultured human neuroblastoma cells expressing nuclear tau. J. Cell Biol. *121*, 257–267.

Wang, Y., Gao, L., Conrad, C.G., and Andreadis, A. (2011). Saitohin, which is nested within the tau gene, interacts with tau and Abl and its human-specific allele influences Abl phosphorylation. J. Cell. Biochem. *112*, 3482–3488.

Wei, M.L.M., and Andreadis, A.A. (1998). Splicing of a regulated exon reveals additional complexity in the axonal microtubule-associated protein tau. J Neurochem *70*, 1346–1356.

Weingarten, M.D. (1975). A Protein Factor Essential for Microtubule Assembly. Proceedings of the National Academy of Sciences *72*, 1858–1862.

Wolfe, M.S. (2008). Tau Mutations in Neurodegenerative Diseases. Journal of Biological Chemistry *284*, 6021–6025.

Wolfe, M.S., Xia, W., Ostaszewski, B.L., Diehl, T.S., Kimberly, W.T., and Selkoe, D.J. (1999). Two transmembrane aspartates in presenilin-1 required for presenilin endoproteolysis and gamma-secretase activity. Nature *398*, 513–517.

Wolfe, M.S. (2012). The Role of Tau in Neurodegenerative Diseases and Its Potential as a Therapeutic Target. Scientifica *2012*, 1–20.

Wood, J.G., Mirra, S.S., Pollock, N.J., and Binder, L.I. (1986). Neurofibrillary tangles of Alzheimer disease share antigenic determinants with the axonal microtubule-associated protein tau (tau). Proc. Natl. Acad. Sci. U.S.a. *83*, 4040–4043.

Wu, H., Huang, M., Lu, M., Zhu, W., Shu, Y., Cao, P., and Liu, P. (2013). Regulation of microtubule-associated protein tau (MAPT) by miR-34c-5p determines the chemosensitivity of gastric cancer to paclitaxel. Cancer Chemother Pharmacol.

Xu, M., and Hecht, N.B. (2007). Polypyrimidine Tract Binding Protein 2 Stabilizes Phosphoglycerate Kinase 2 mRNA in Murine Male Germ Cells by Binding to Its 3'UTR. Biology of Reproduction *76*, 1025–1033.

Yamakuchi, M., and Lowenstein, C.J. (2009). MiR-34, SIRT1 and p53. Cell Cyle 712–715.

Yamakuchi, M., Ferlito, M., and Lowenstein, C.J. (2008). miR-34a repression of SIRT1 regulates apoptosis. Proceedings of the National Academy of Sciences *105*, 13421–13426.

Yang (2011). microRNA-34 family and treatment of cancers with mutant or wild-type p53 (Review). Int J Oncol *38*.